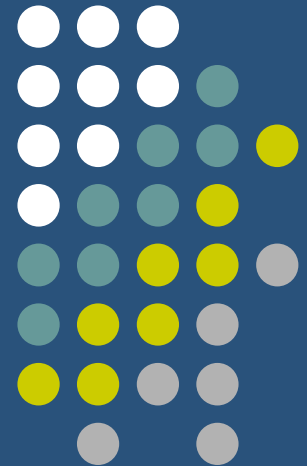


A Fractional Derivative Model of Anomalous Diffusion in White and Gray Matter



Professor Richard L. Magin
Department of Bioengineering
University of Illinois at Chicago

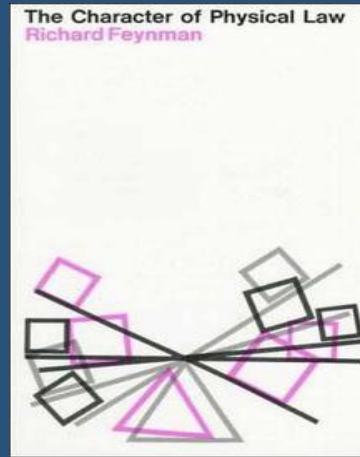
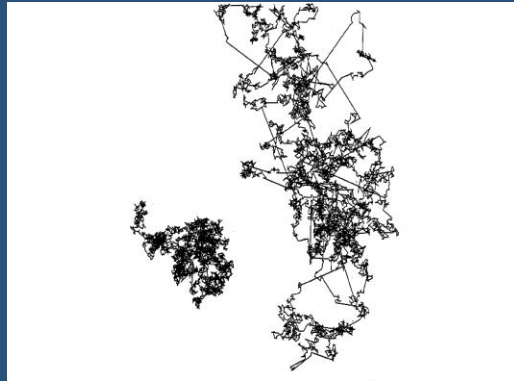
A Workshop on Future Directions in Fractional Calculus
Research and Applications, Oct 17-21, 2016



Department of Statistics and Probability

Michigan State University

The Character of Physical Law

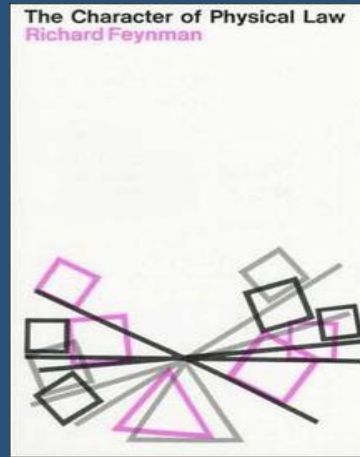
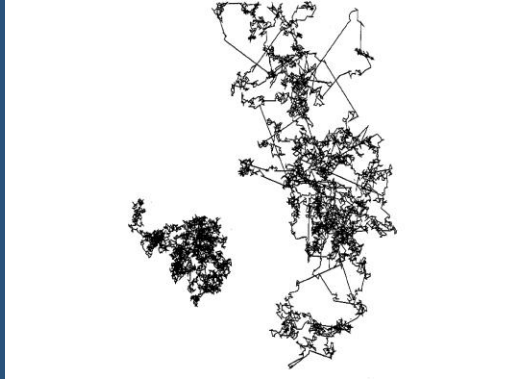


“There is a **rhythm and a pattern** between the phenomena of nature which is not apparent to the eye, but only to the eye of analysis; and it is these **rhythms and patterns** which we call Physical Laws.”



Richard P. Feynman, The Messenger Lectures for 1964 at Cornell University on The Character of Physical Law

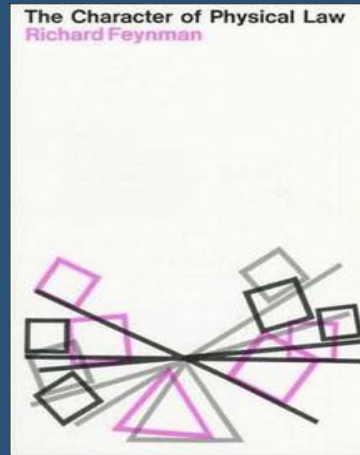
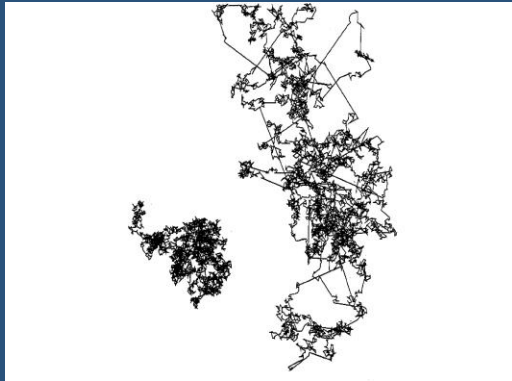
The Character of Physical Law



“There is a **rhythm and a pattern** between the phenomena of nature which is not apparent to the **eye**, but only to the **eye of analysis**; and it is these **rhythms and patterns** which we call Physical Laws.”

Richard P. Feynman, The Messenger Lectures for 1964 at Cornell University on The Character of Physical Law

The Character of Physical Law

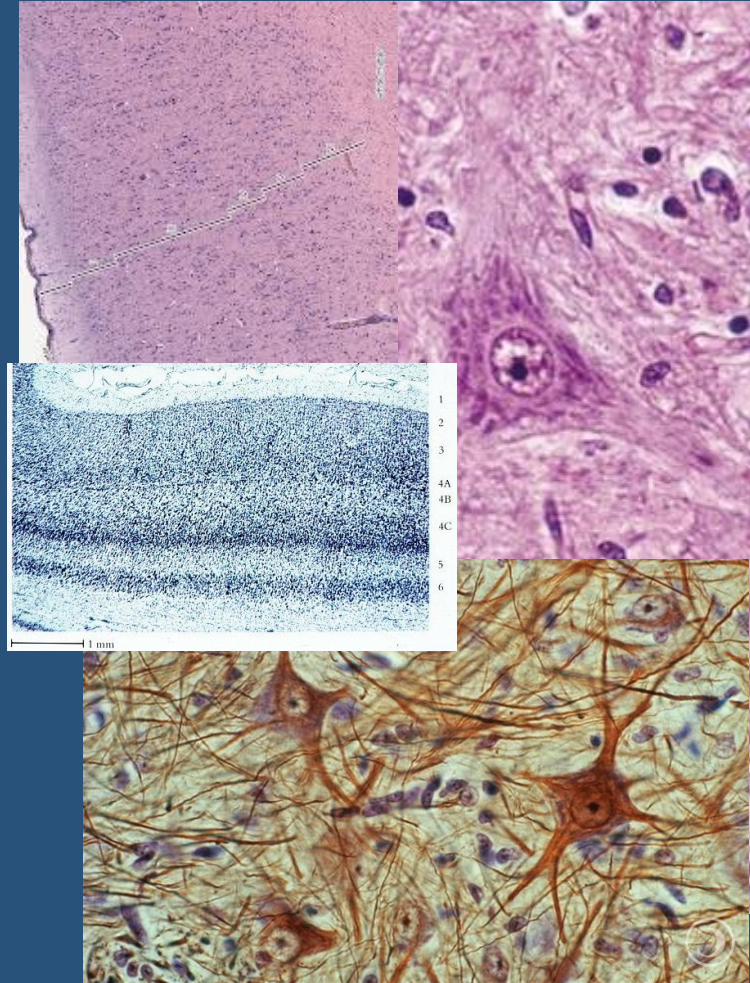


“There is a **rhythm and a pattern** between the phenomena of nature which is not apparent to the **eye**, but only to the **eye of analysis**; and it is these **rhythms and patterns** which we call Physical Laws.”

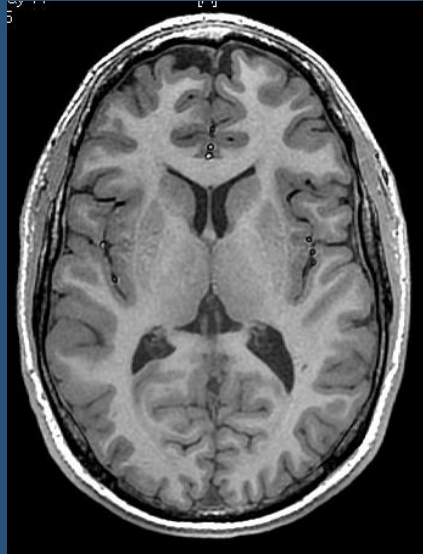
Richard P. Feynman, The Messenger Lectures for 1964 at Cornell University on The Character of Physical Law

By age 15, Feynman had mastered differential and integral calculus, and frequently experimented and re-created mathematical topics such as **the half-derivative** before even entering college.

How Does Microstructure Affect Water Diffusion In Brain Tissue?



Gray Matter

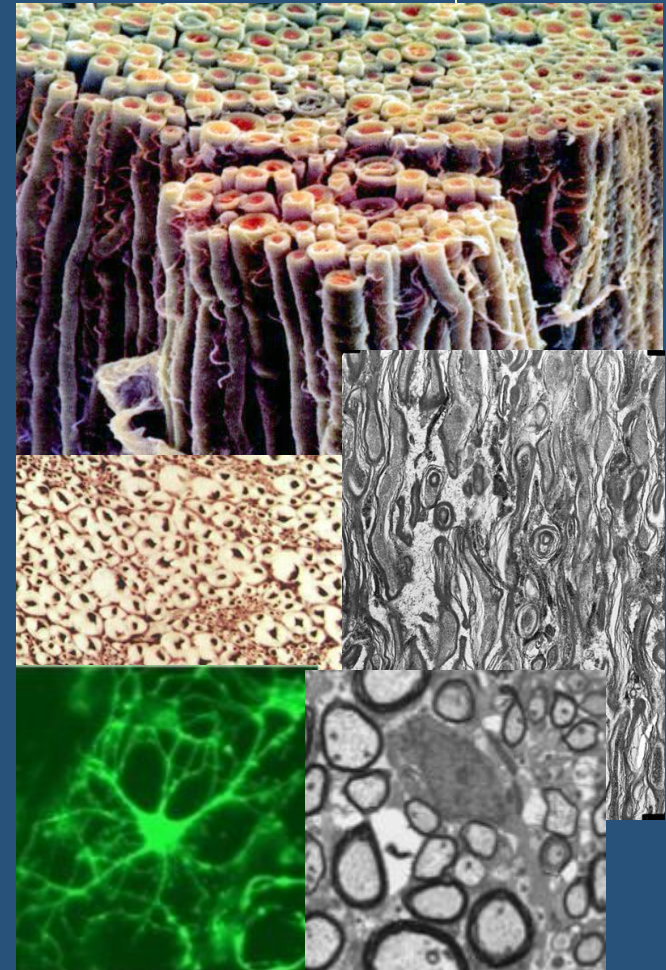


Diffusion Time

$$\langle x^2 \rangle = 2Dt$$

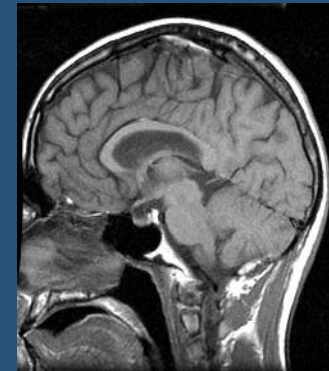
Typical length scale for MRI

1-20 μm

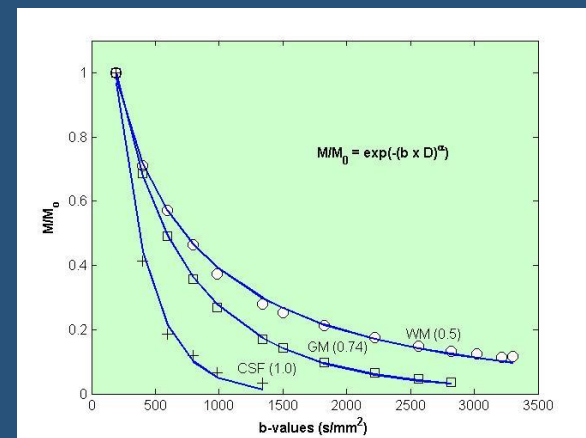
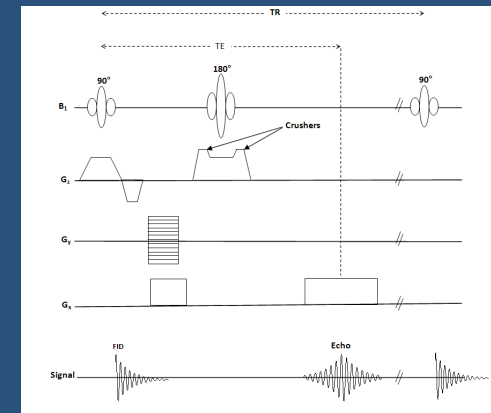


White Matter

Overview



- Diffusion weighted MRI and DTI are used to detect and stage neurodegenerative, malignant and ischemic disease.
- Correlation between pathology and the apparent diffusion coefficient relies on a model to design an efficient phase encoding pulse sequence.
- A common empirical approach to model the data encodes the diffusion coefficient as a stretched exponential, $\exp[-(bD)^\alpha]$ and the Mittag-Leffler, $E_\alpha[-(bD)^\alpha]$ functions.
- Here, we show how this functional behavior is a natural consequence of the Bloch-Torrey equation by using fractional-order calculus.



$${}_0 I_t^a f(t) = \frac{1}{\Gamma(a)} \int_0^t (t - \tau)^{a-1} f(\tau) d\tau$$

Anomalous Behaviour

Why do we expect fractional calculus to be useful in describing relaxation and diffusion in biological tissues?





Universal power-law scaling of water diffusion in human brain defines what we see with MRI

Jelle Veraart, Els Fieremans and Dmitry S. Novikov
 Dept. of Radiology, NYU School of Medicine
<https://arxiv.org/pdf/1609.09145.pdf>

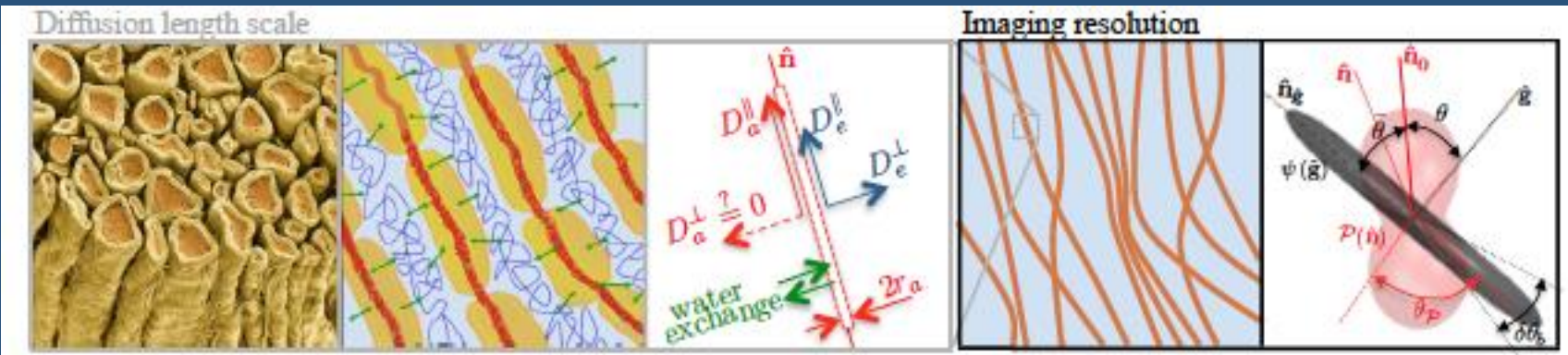
The viability of model-based “super-resolution” MRI rests on validating fundamental model assumptions. In white matter (WM), the most essential assumption underpinning most biophysical models¹⁻¹³ is compartmentalization — i.e. representing the dMRI signal as a sum of independent contributions from separate pools of water, corresponding to locally anisotropic intra- and extra-axonal spaces, Fig. 1.

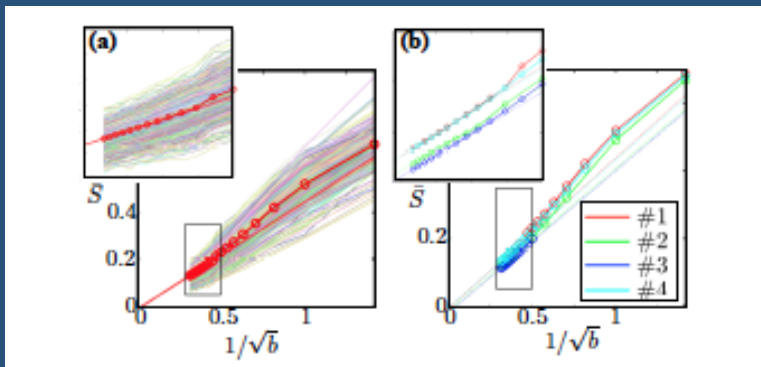
Here we argue that our experimental *in vivo* observation of the universal power-law form (Fig. 2)

$$S(b \rightarrow \infty) \simeq \beta \cdot b^{-\alpha} + \gamma \quad (1)$$

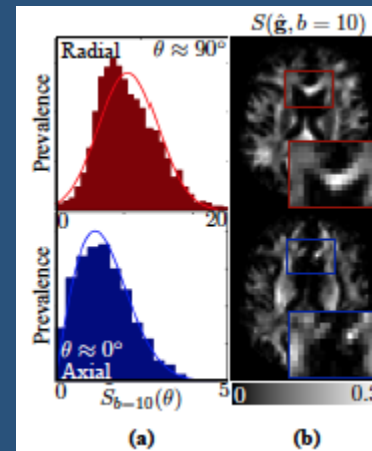
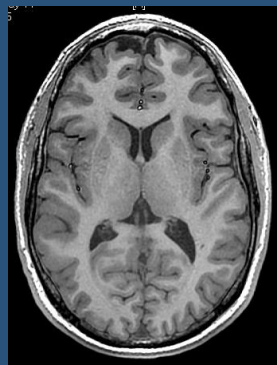
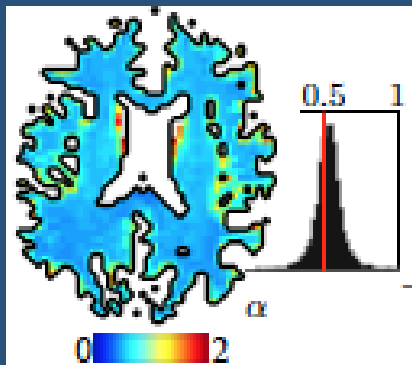
The asymptotic power-law (1) with exponent $\alpha = 1/2$ can only originate from the *intra-axonal water*. Indeed, consider the dMRI signal (henceforth normalized to $S|_{b=0} \equiv 1$)

$$S(\hat{\mathbf{g}}, b) = f \int d\hat{\mathbf{n}} \mathcal{P}(\hat{\mathbf{n}}) \psi_{\hat{\mathbf{n}}}(\hat{\mathbf{g}}, b) + \gamma + S^{\text{eas}}(\hat{\mathbf{g}}, b) \quad (2)$$





Here we argue that our experimental *in vivo* observation of the universal power-law form (Fig. 2)

$$S(b \rightarrow \infty) \simeq \beta \cdot b^{-\alpha} + \gamma \quad (1)$$


“The remarkably slow decay of the signal, retaining much SNR even for very high b , provides an exciting avenue for probing brain tissue microstructure with extremely strong diffusion gradients on clinical systems, such as on Human Connectom scanners, ...

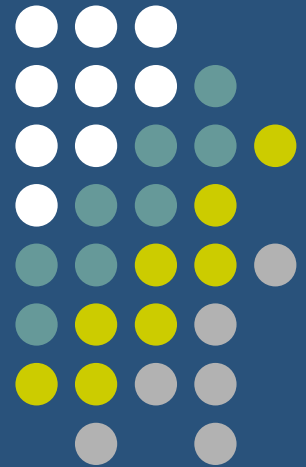
.... thereby fostering the translation of advanced diffusion MRI methods into basic neuroscience research and clinical practice.”

Surprisingly, the above paper does not mention fractional calculus as a potential tool for deriving and expressing their results.

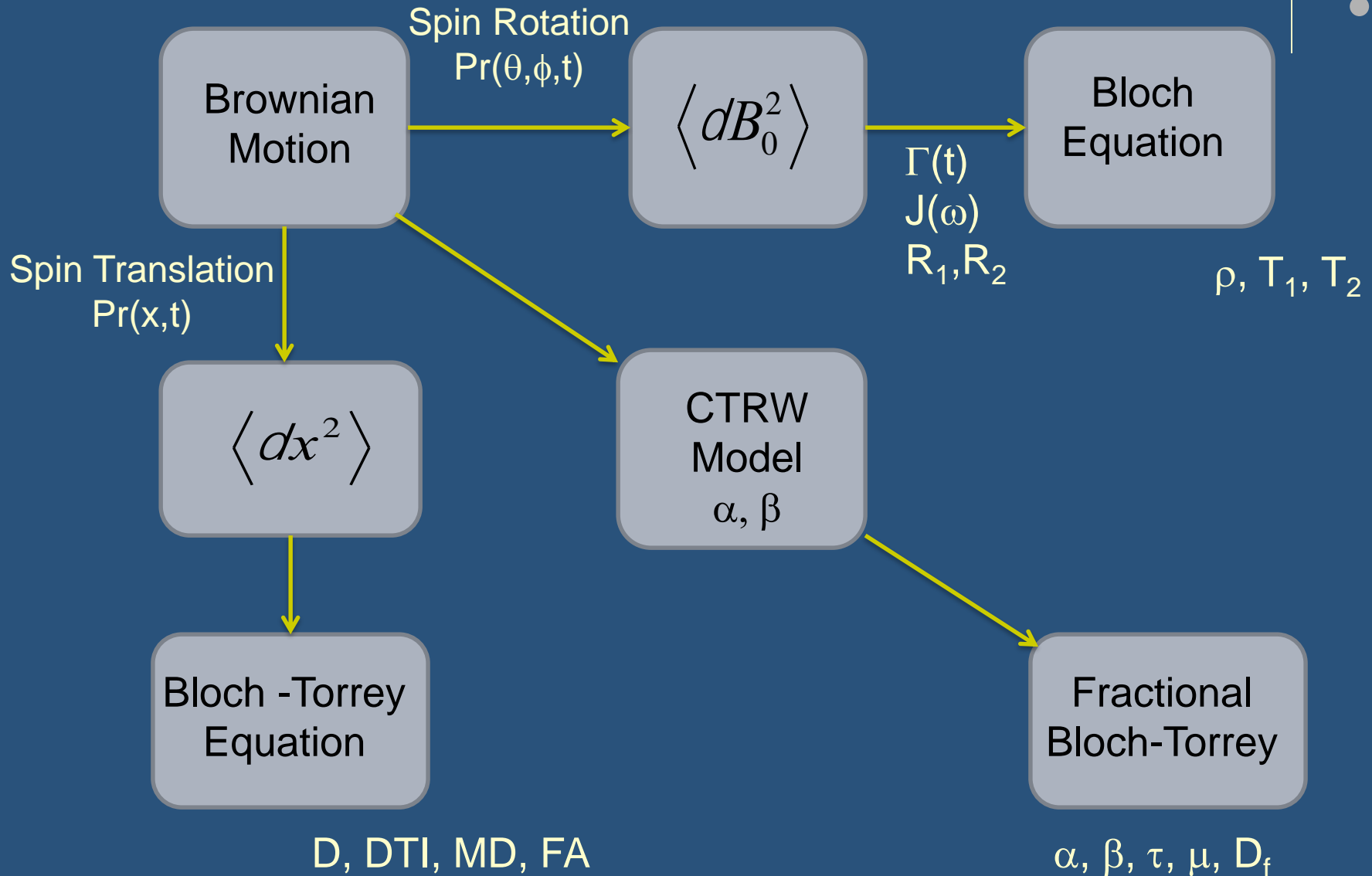
Anomalous Behaviour

“It was ever thus: whenever you introduce a new idea it is discredited. Then after it is accepted it is said to be obvious. And the final stage is that it was their idea all along, so why reference another person’s work?”

Email from Bruce West, 10/13/2016



Development of Fractional Magnetic Resonance Models

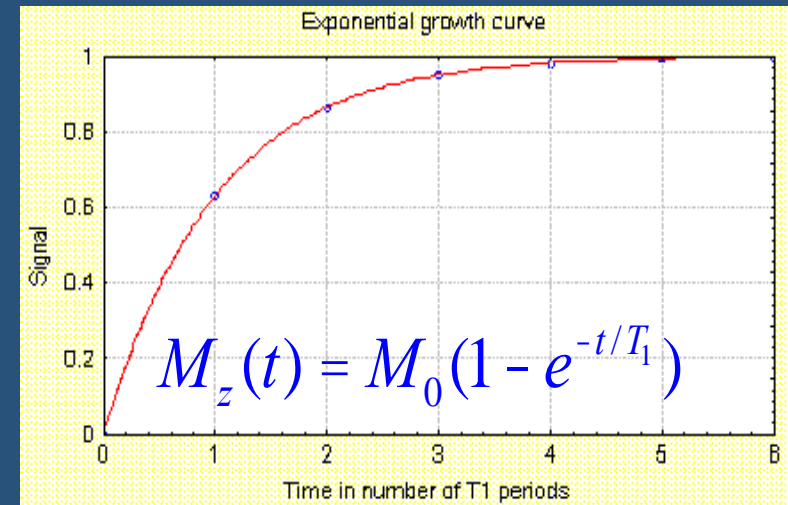
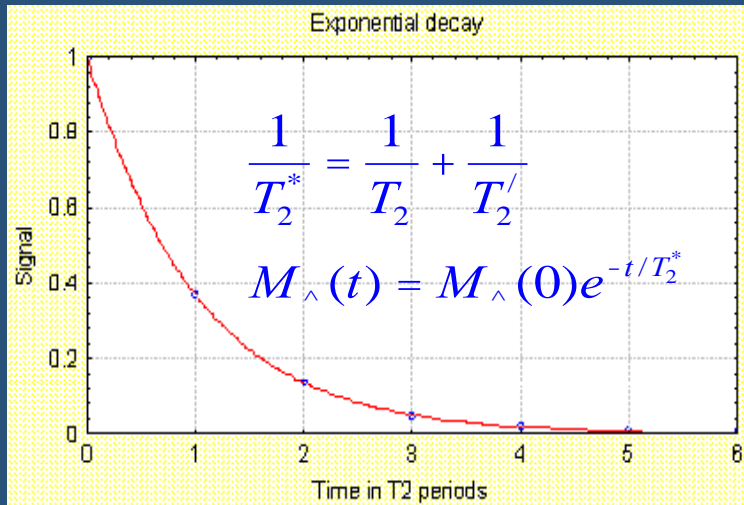




Bloch Equation / Relaxation

Entropy

Energy



$$\frac{\partial \mathbf{M}}{\partial t} = \gamma \mathbf{M} \times \mathbf{B} + \frac{M_0 - M_z}{T_1} \hat{k} - \frac{M_x \hat{i} - M_y \hat{j}}{T_2}$$

Fractional NMR Relaxation



Fractional T_1 Relaxation

$${}_0^C D_t^b M_z(t) = \frac{M_0 - M_z(t)}{T_1^b}$$

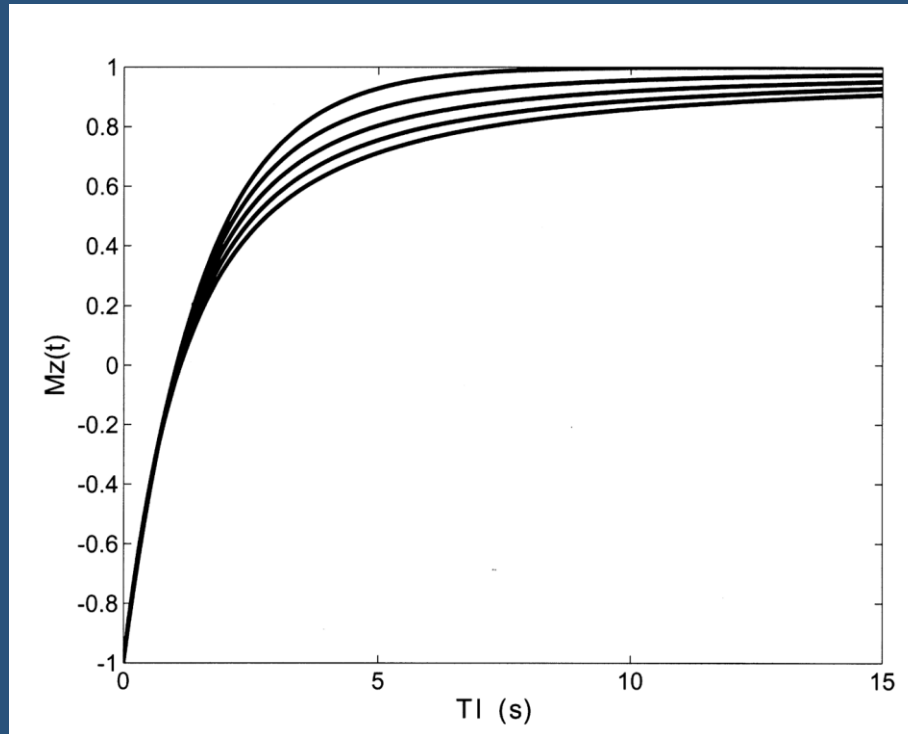
$$M_z(t) = M_z(0) + [M_0 - M_z(0)] [1 - E_b(-(t/T_1)^b)]$$

Fractional T_2 Relaxation

$${}_0^C D_t^a M_{xy}(t) = -i\omega_0 I_t^{1-a} M_{xy}(t) - \frac{1}{T_2^a} M_{xy}(t)$$

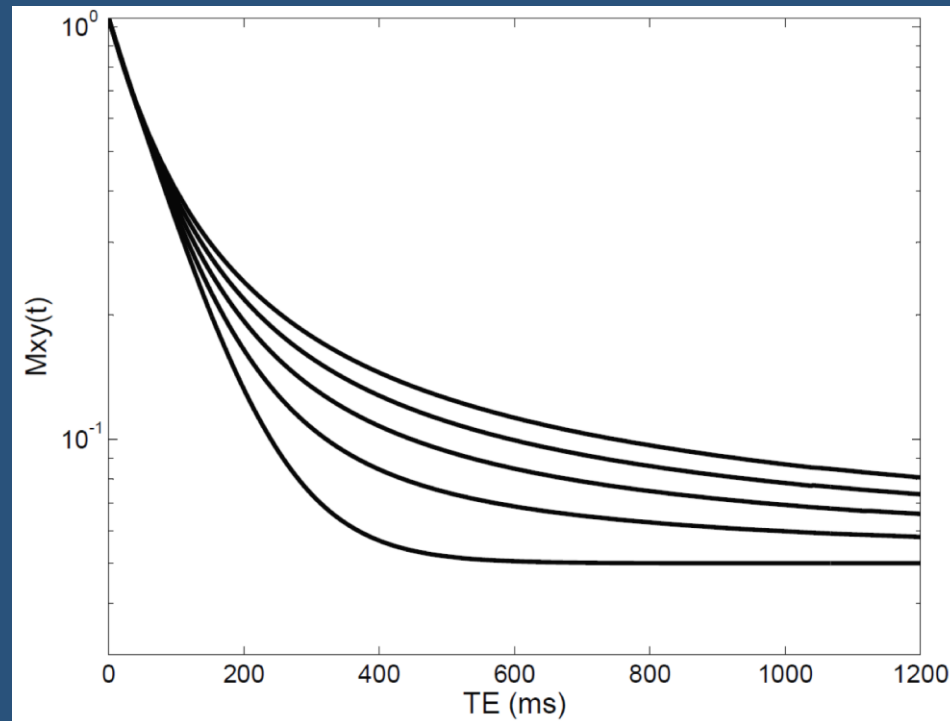
$$M_{xy}(t) = M_{xy}(0) E_a[-(t/T_2)^a] + M_{xy}(\neq)$$

Fractional T_1 Relaxation



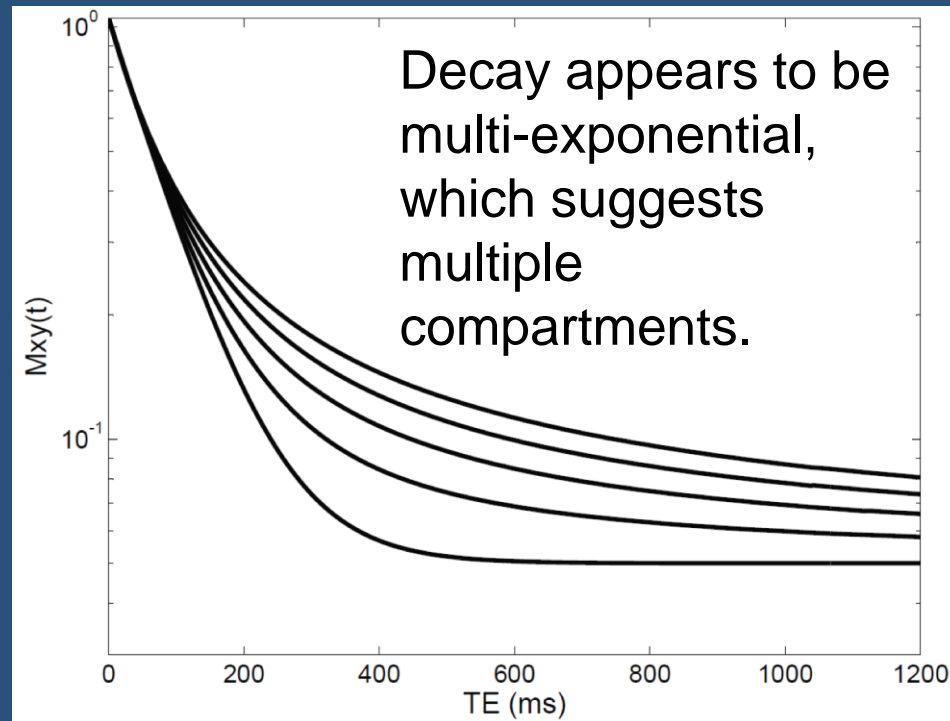
Fractional-order T_1 relaxation curves. Plots of $M_z(TI)$ versus TI (inversion recovery) for different values of β in the range from $\beta = 0.6$ (bottom curve) to $\beta = 1$ in steps of 0.1 ($M_0 = 1$, $T_1 = 1.5$ s, $A = 1$).

Fractional T_2 Relaxation



Fractional-order T_2 relaxation curves. Plots of $M_{xy}(TE)$ versus TE (Spin Echo) for different values of α in the range from $\alpha = 0.6$ (top curve at $TE = 1,200$ ms) to $\alpha = 1$ in steps of 0.1 ($M_{xy}(0) = 1$, $T_2 = 80$ ms).

Fractional T_2 Relaxation



Fractional-order T_2 relaxation curves. Plots of $M_{xy}(TE)$ versus TE (Spin Echo) for different values of α in the range from $\alpha = 0.6$ (top curve at $TE = 1,200$ ms) to $\alpha = 1$ in steps of 0.1 ($M_{xy}(0) = 1$, $T_2 = 80$ ms).

Anomalous Relaxation

Anomalous T2 relaxation in normal and degraded cartilage

David A. Reiter, Richard L. Magin, Weiguo Li, Juan J. Trujillo, M. Pilar Velasco, and Richard G. Spencer

Magnetic Resonance in Medicine. 2016;76:953-962.

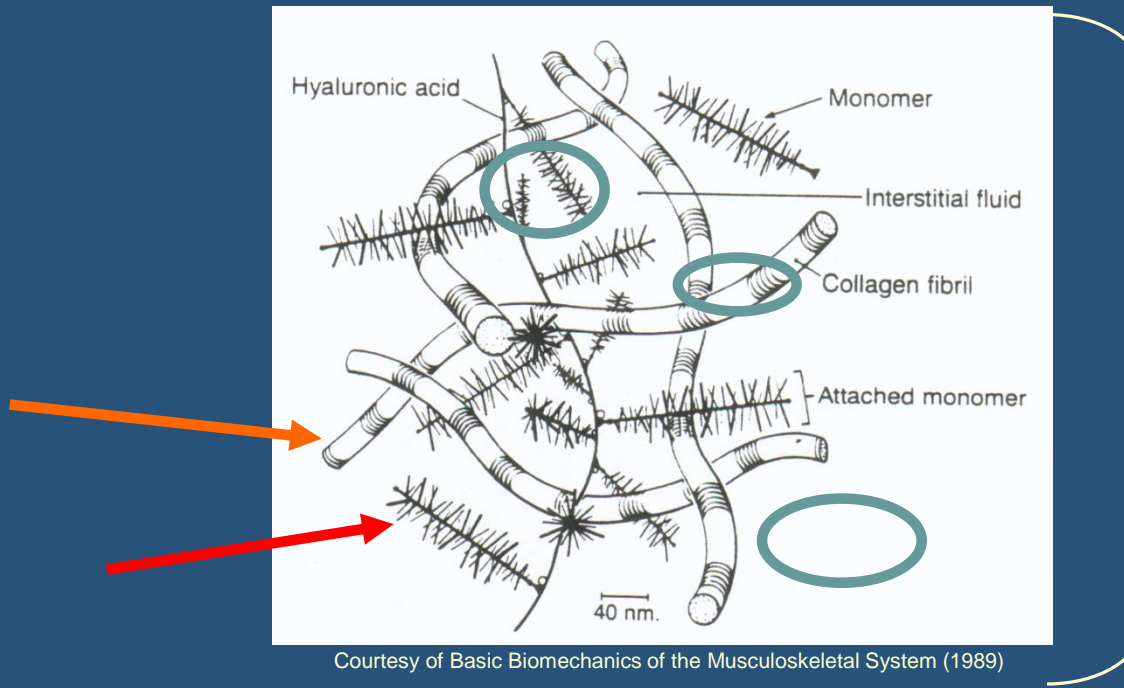
Anomalous NMR relaxation in cartilage matrix components and native cartilage: fractional-order models.

Magin RL, Li W, Pilar Velasco M, Trujillo J, Reiter DA, Morgenstern A, Spencer RG.

J Magn Reson 2011;210:184-191.



Cartilage Ultrastructure



Courtesy of Basic Biomechanics of the Musculoskeletal System (1989)

- **Collagen** provides tissue integrity and tensile strength
- **Proteoglycans (PGs)** provide compressive resistance
- **Water** exists in several compartments of different mobility



T₂ Relaxation Models

Stretched Exponential

$$M_{xy}(TE \cdot n) = b + M_{xy}(0) \cdot \exp\left(\frac{-(TE \cdot n)^{\alpha_{se}}}{T_{2,se}}\right)$$

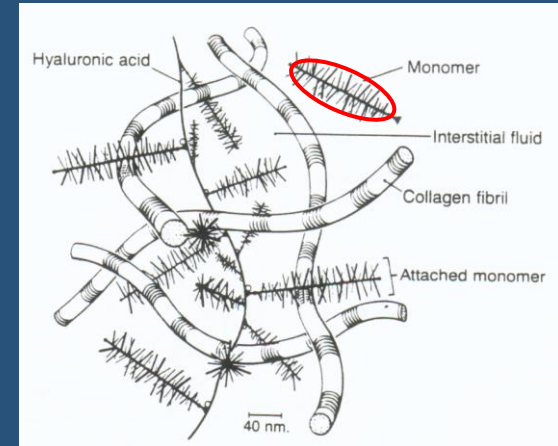
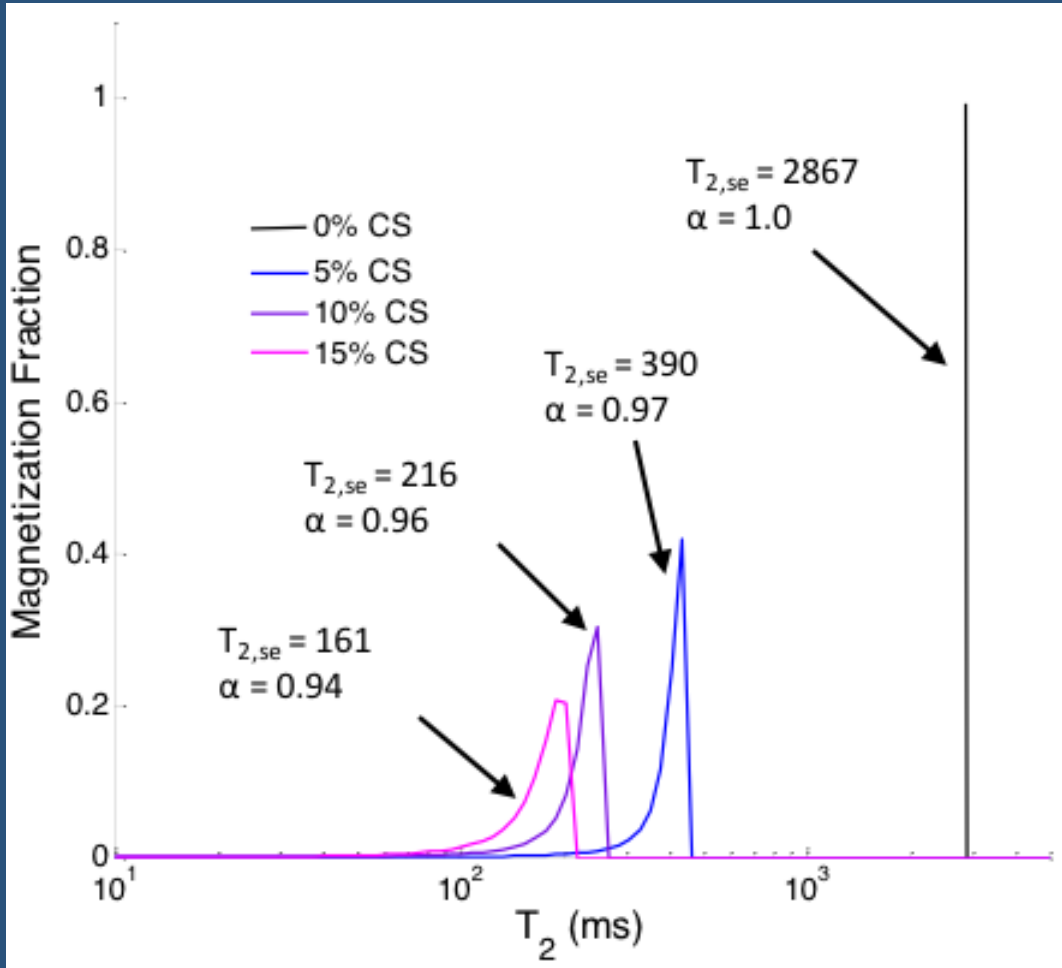
Stretched Mittag-Leffler

$$M_{xy}(TE \cdot n) = b + M_{xy}(0) \cdot E_{\alpha}\left(\frac{-(TE \cdot n)^{\alpha_{sml}}}{T_{2,sml}}\right)$$

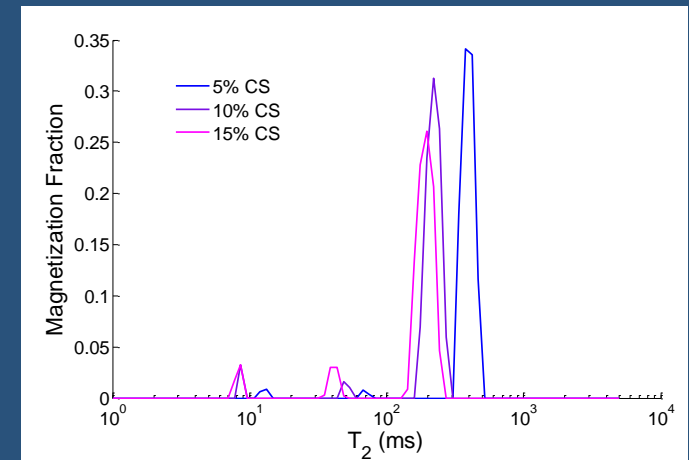
Two Exponential

$$M_{xy}(TE \cdot n) = b + M_{xy}(0) \cdot \left(w_1 \cdot \exp\left(\frac{-TE \cdot n}{T_{2,1}}\right) + (1 - w_1) \cdot \exp\left(\frac{-TE \cdot n}{T_{2,2}}\right) \right)$$

Stretched Exponential T_2 Relaxation Chondroitin Sulfate (CS) Solutions



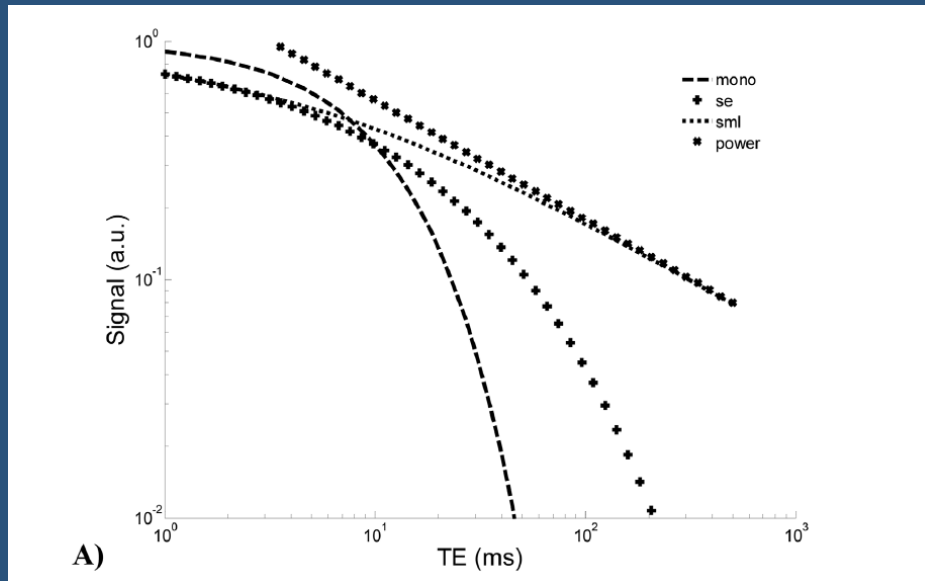
Source: *Basic Biomechanics of the Musculoskeletal System* (1989)



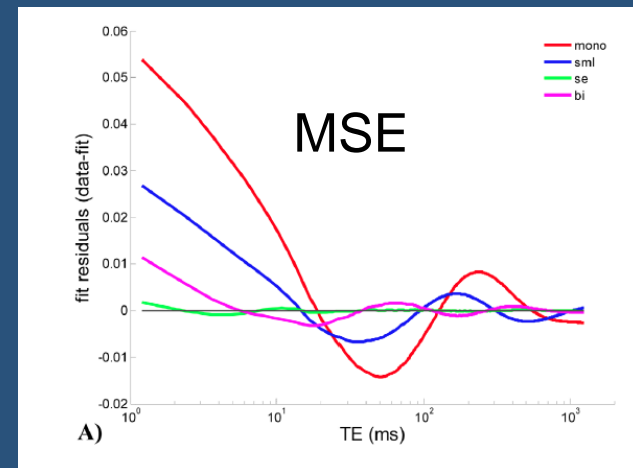
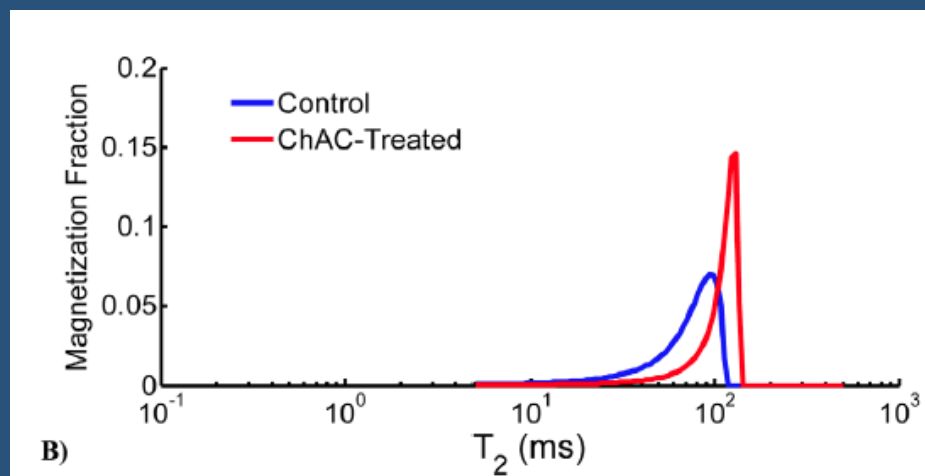
RL Magin et al. *J Magn Reson* 2011;210:184-191

reiterda@nia.nih.gov

Anomalous T2 Relaxation in Normal and Degraded Cartilage



Comparison of different models: i) the exponential function $\exp(-t)$, ii) the stretched exponential function $\exp(-t^{0.5})$, iii) the stretched Mittag-Leffler function $E_{1/2}(-t^{0.5})$, and iv) the power function $t^{-0.5}/\Gamma(1/2)$.



Anomalous Relaxation

Qin, S., Liu, F., Turner, I. W., Yu, Q., Yang, Q., & Vegh, V. (2016). Characterization of anomalous relaxation using the time-fractional Bloch equation and multiple echo T2*-weighted magnetic resonance imaging at 7 T. *Magnetic Resonance in Medicine*. DOI:10.1002/mrm.26222.

Centre for Advanced Imaging, the University of Queensland,
Brisbane, Queensland, Australia





Relaxation models

- Classical monoexponential model for transverse magnetisation

$$|M_+(t)| = |M_+(0)|e^{-t/T_2^*}$$

- Magin's time-fractional model transverse magnetisation

$$|M_+(t)| = |M_+(0)|E_\alpha\left(-\frac{t^\alpha}{T_2^*}\right)$$

- Our extended time-fractional model transverse magnetisation model

$$|M_+(t)| = |M_+(0)| \sqrt{E_\alpha\left(-\frac{t^\alpha}{T_2^*} + i\Delta\omega t^\alpha\right) E_\alpha\left(-\frac{t^\alpha}{T_2^*} - i\Delta\omega t^\alpha\right)}$$

$$= |M_+(0)| \left| E_\alpha\left(-\frac{t^\alpha}{T_2^*} + i\Delta\omega t^\alpha\right) \right|$$

- Fitting equation

$$S(t) = A_0 |M_+(t)| + C$$

Fractional model for T_2^* decay



- We take the frequency shift $\Delta\omega$ into consideration

$$\begin{cases} {}^C_0 D_t^\alpha M_z(t) &= \frac{M_0 - M_z(t)}{T_1}, \\ {}^C_0 D_t^\alpha M_{x'}(t) &= -\frac{1}{T_2^*} M_{x'}(t) + \Delta\omega M_{y'}(t), \\ {}^C_0 D_t^\alpha M_{y'}(t) &= -\frac{1}{T_2^*} M_{y'}(t) + \Delta\omega M_{x'}(t), \end{cases}$$

- By using the matrix method and diagonalising the parameter matrix

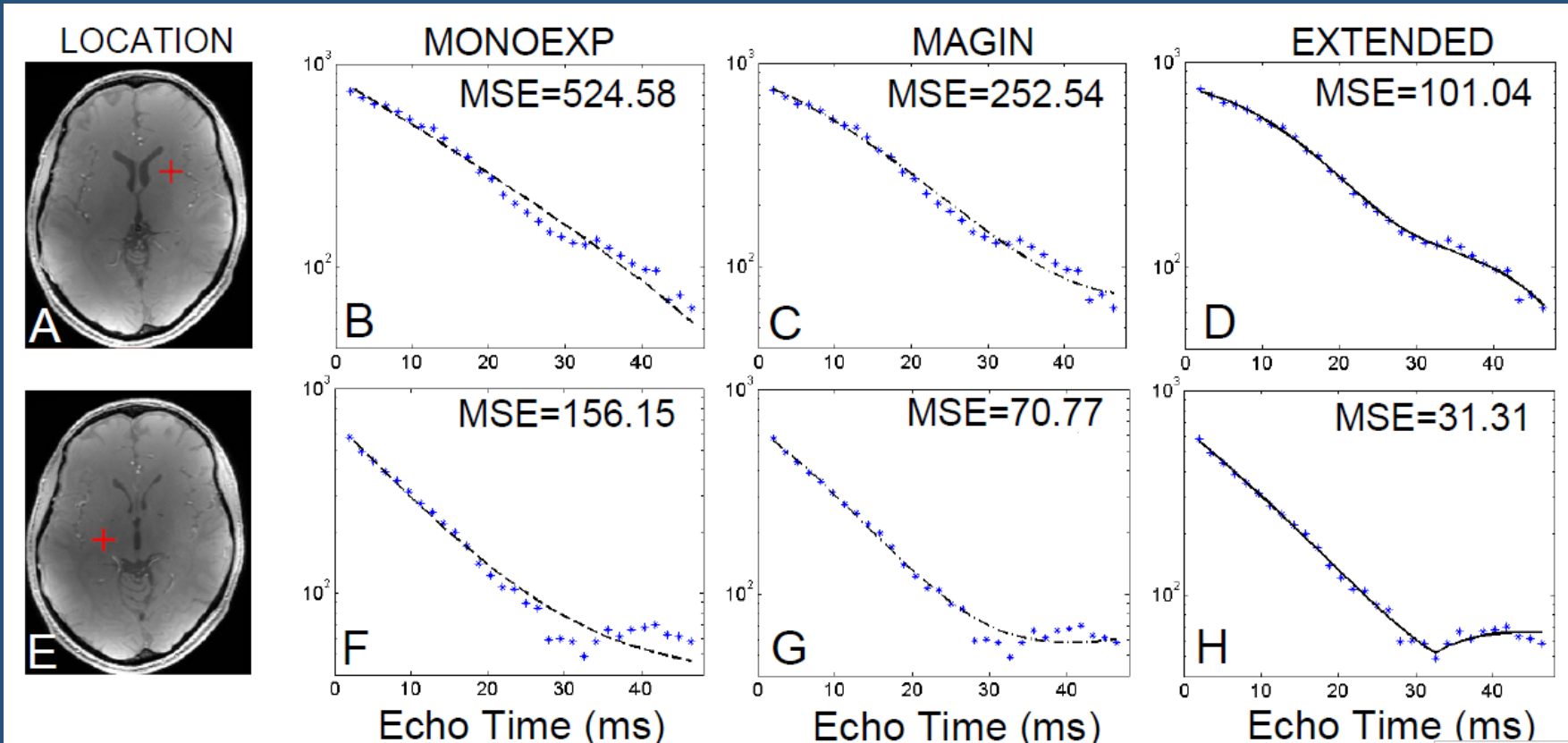
$$\begin{cases} M_{x'}(t) &= \frac{M_x(0) - iM_y(0)}{2} E_\alpha\left(-\frac{t^\alpha}{T_2^*} + i\Delta\omega t^\alpha\right) + \frac{M_x(0) + iM_y(0)}{2} E_\alpha\left(-\frac{t^\alpha}{T_2^*} - i\Delta\omega t^\alpha\right), \\ M_{y'}(t) &= \frac{M_y(0) + iM_x(0)}{2} E_\alpha\left(-\frac{t^\alpha}{T_2^*} + i\Delta\omega t^\alpha\right) + \frac{M_y(0) - iM_x(0)}{2} E_\alpha\left(-\frac{t^\alpha}{T_2^*} - i\Delta\omega t^\alpha\right), \\ M_z(t) &= M_z(0) E_\alpha\left(-\frac{t^\alpha}{T_1}\right) + \frac{M_0}{T_1} t^\alpha E_{\alpha, \alpha+1}\left(-\frac{t^\alpha}{T_1}\right), \end{cases}$$

In vivo experiment

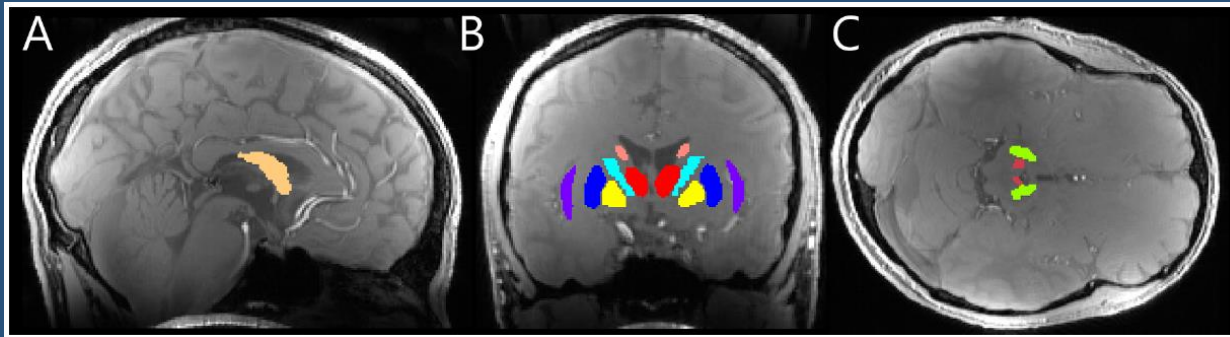


- Subjects: 5 healthy participants (two females and three males) aged 30-41 years were scanned
- MRI data: 7T MRI data collected on the Siemens Magnetom Research scanner with a 32 channel head coil (Nova Medical, Wilmington, USA).
- Data processing: Individual channel data were combined using the sum-of-squares approach in a voxel-by-voxel manner

Voxel-based fitting results






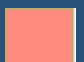





Fitting method: Isqcurvefit (a standard nonlinear fitting function in Matlab)



(A)Sagittal, (B) Coronal and (C) Axial

$$R_2^* = 1/T_2^*$$

$$\Delta f = \Delta\omega / 2\pi$$

fornix  putamen  thalamus  caudate  insula  pallidum 
 internal capsule  red nucleus  substantia nigra 

Fitting Results of the Monoexponential and Time-Fractional Models to Signal Decays in Nine ROIs

ROI	#	TISSUE (%)				MONOEXP			EXTENDED				
		WM	GM	CSF	WM/GM	A_0	R_2^* (Hz)	MSE	A_0	R_2^* (Hz)	$ \Delta f $ (Hz)	α	MSE
CA	419	37	43	20	0.87	691	43.07	9.54	668	34.91	21.76	0.979	1.71
FO	57	42	45	13	0.94	567	39.68	3.21	611	30.31	1.59	0.949	2.35
IN	190	30	61	9	0.49	804	32.19	2.08	855	26.52	2.49	0.964	1.47
IC	235	59	39	2	1.50	619	47.76	2.94	668	36.26	0.02	0.947	1.39
PA	431	56	42	2	1.33	733	93.06	16.11	718	74.17	19.70	0.965	0.21
PU	461	39	59	2	0.67	779	44.73	8.28	743	37.45	17.21	0.972	0.41
RN	142	42	53	5	0.79	636	60.93	8.51	602	38.75	11.76	0.907	3.56
SN	230	50	46	4	1.09	658	73.99	10.92	642	58.11	27.13	0.976	2.17
TH	978	32	51	17	0.63	611	37.50	6.09	663	28.49	0.01	0.951	5.27

Note: Data were averaged across voxels in selected regions of five subjects. “#” denotes the average number of voxels contained in each region. We also computed the tissue parameters, such as white matter (WM), gray matter (GM), and cerebrospinal fluid (CSF) proportions, and WM-GM ratio. The fitted parameters are amplitude A_0 , relaxation rate R_2^* , frequency shift $|\Delta f|$ ($|\Delta f| = |\Delta\omega|/2\pi$), time-fractional order α , and MSE.

Anomalous Diffusion

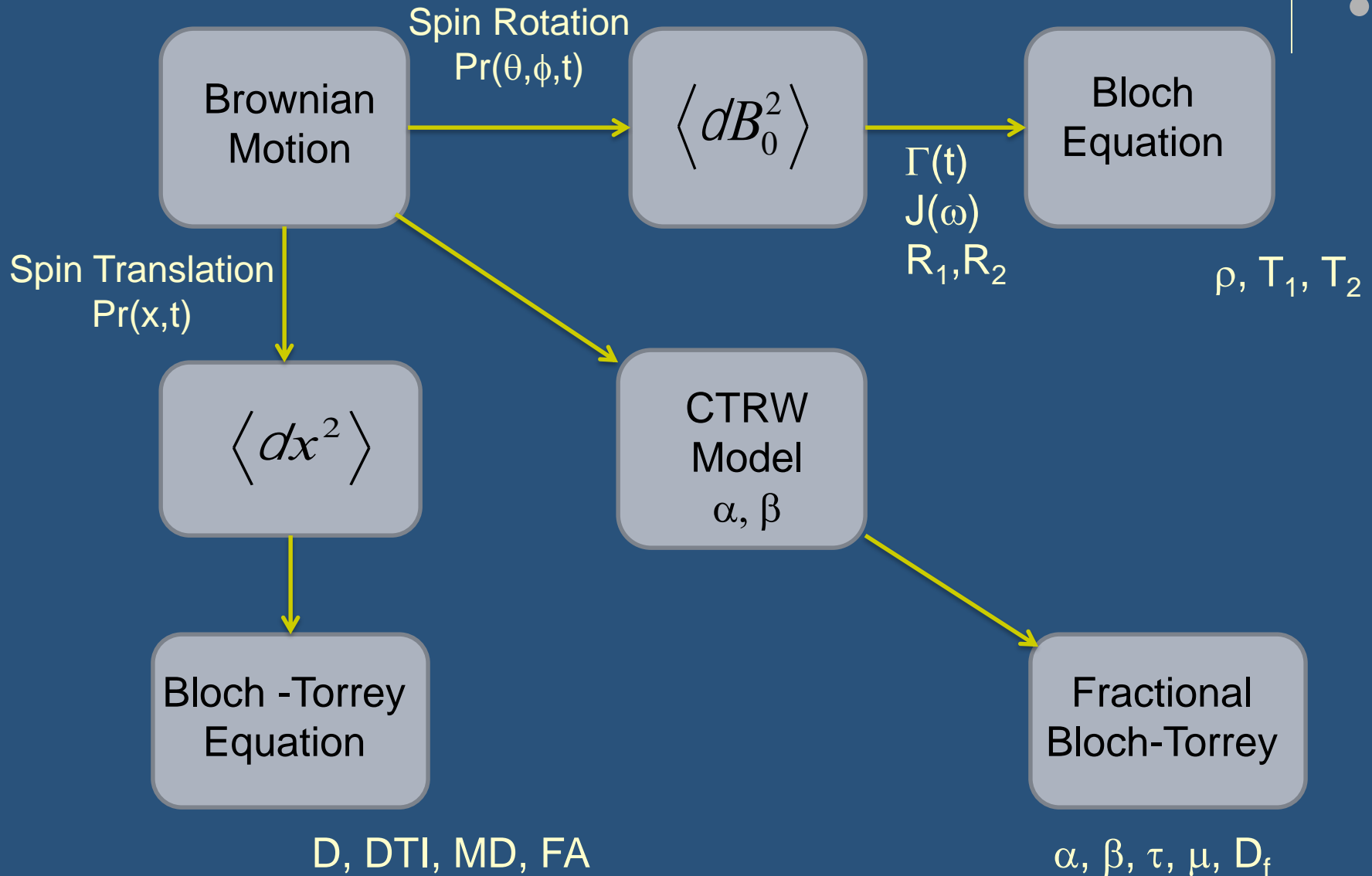
Anomalous diffusion expressed through fractional order differential operators in the Bloch-Torrey equation.

Magin RL, Abdullah O, Baleanu D, and Zhou XJ.

J Magnetic Resonance, 190(2):255-70 (2008).



Development of Fractional Magnetic Resonance Models



Fractional Generalization of Bloch-Torrey Equation



$$t^{a-1} {}_0^C D_t^a M_{xy}(r, t) = l M_{xy}(r, t) + D m^{2(b-1)} D^b M_{xy}(r, t)$$

where $l = -ig(r \times G)$; $0 < a \leq 1$; $0 < b \leq 1$

${}_0^C D_t^a$ - fractional order time derivative

$D^b = (D_x^{2b} + D_y^{2b} + D_z^{2b})$ - fractional order spatial Laplacian

$t^{a-1}, m^{2(b-1)}$ - fractional order time and space constants needed to maintain correct units

Note: for $\alpha = 1, \beta = 1$, we recover the classical Bloch-Torrey equation

Magin et al., JMR, 190: 255-270, 2008

For fixed, bipolar and Stejskal-Tanner gradient pulses we find



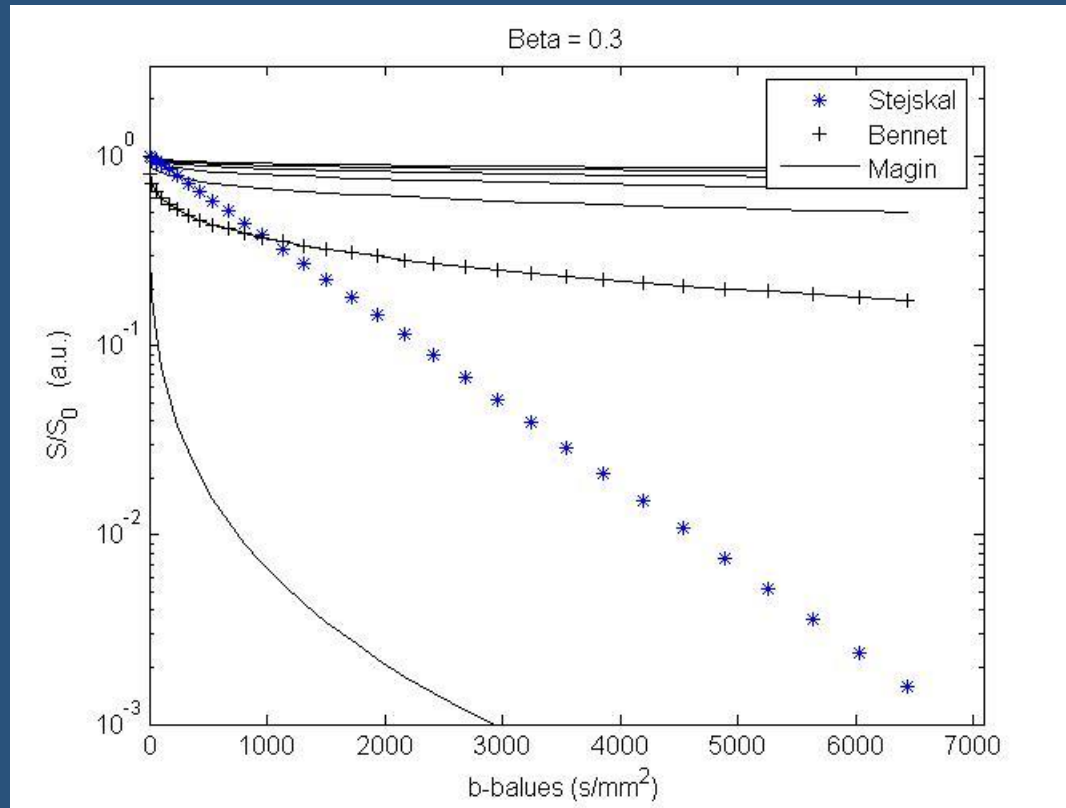
$$M_{xy} = \begin{cases} M_0 \exp(-igG_z zt - Dm^{2(b-1)} g^{2b} G_z^{2b} t^{2b+1} / (2b + 1)) \\ M_0 \exp(-2Dm^{2(b-1)} g^{2b} G_z^{2b} T_b^{2b+1} / (2b + 1)) \\ M_0 \exp[-Dm^{2(b-1)} (gG_z d)^{2b} (D - \frac{2b-1}{2b+1} d)] \end{cases}$$

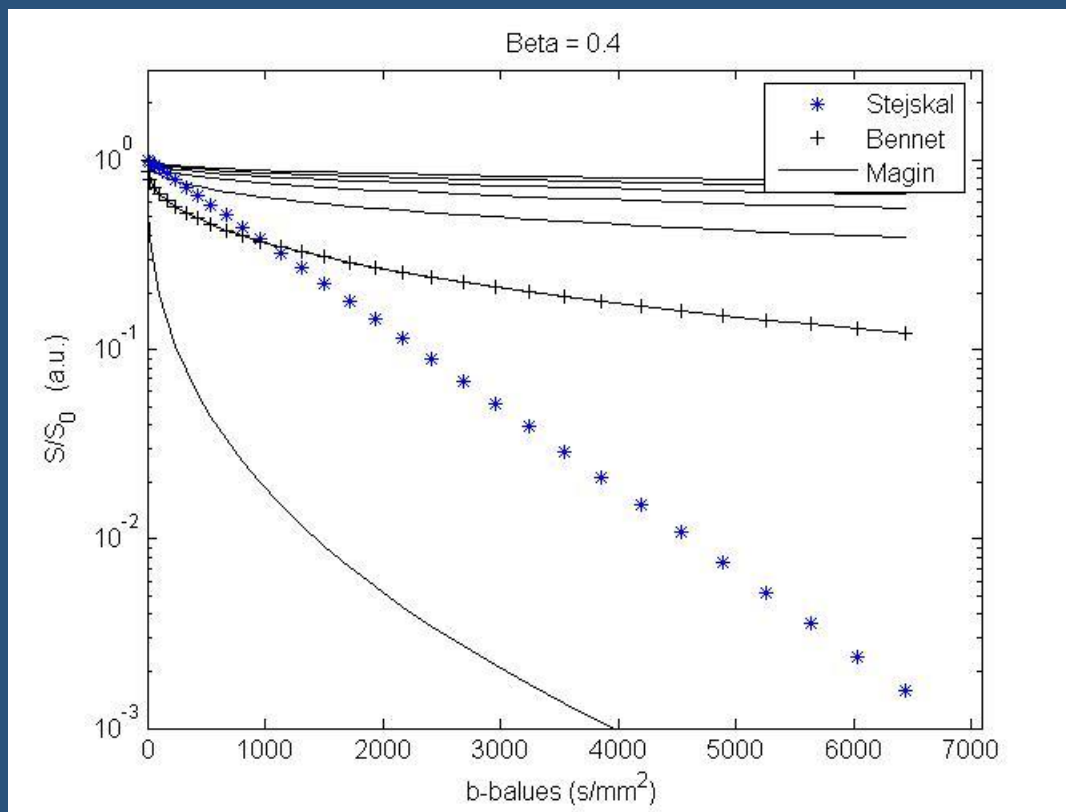
Note that here $0 < \beta < 1$ and that for $\beta = 1$, we recover the classical results.

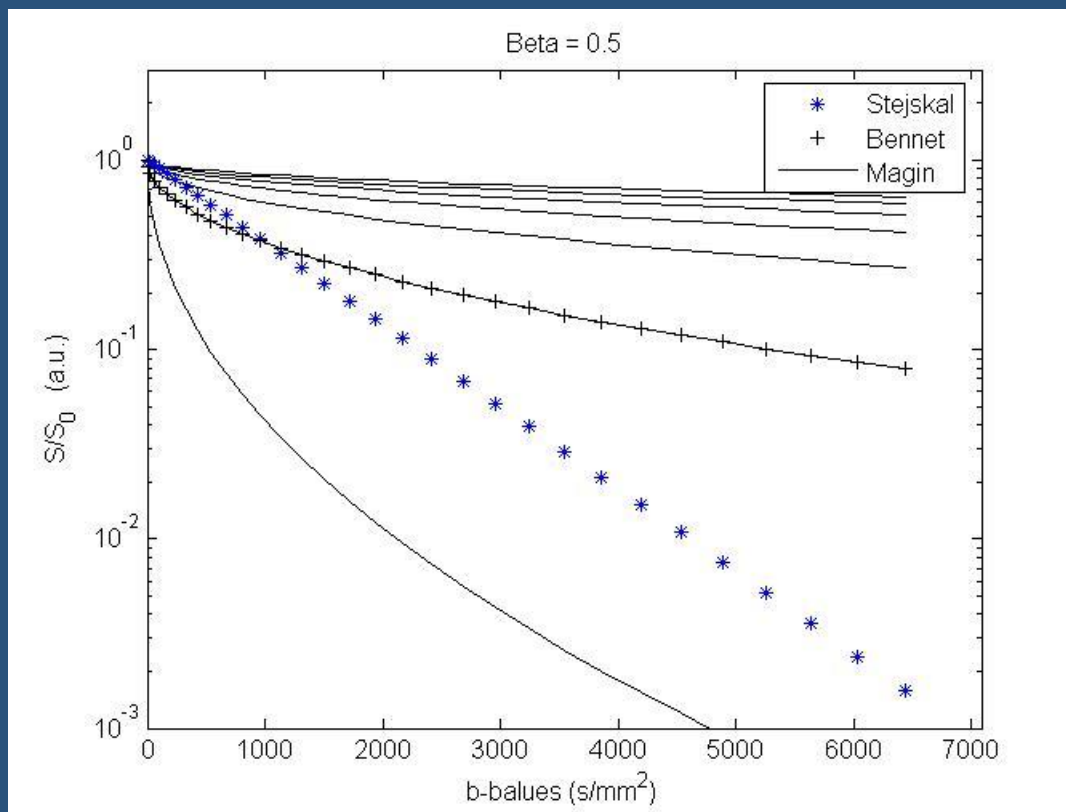
PGSE (Stejskal-Tanner)

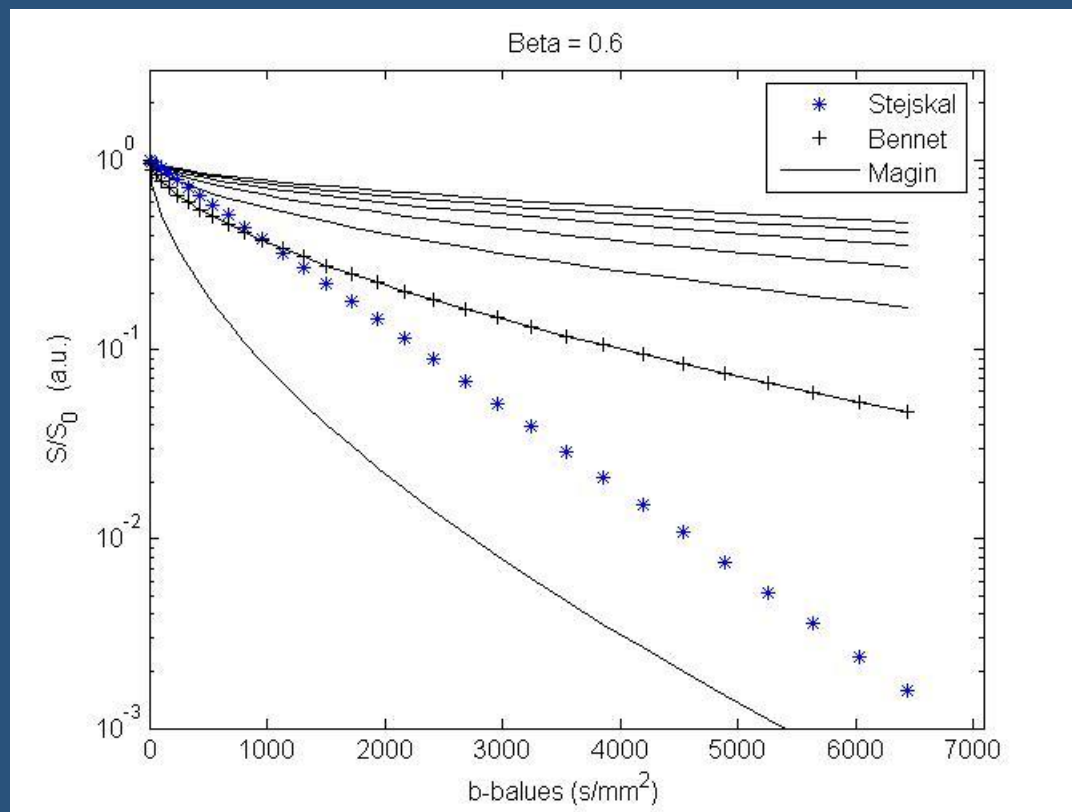


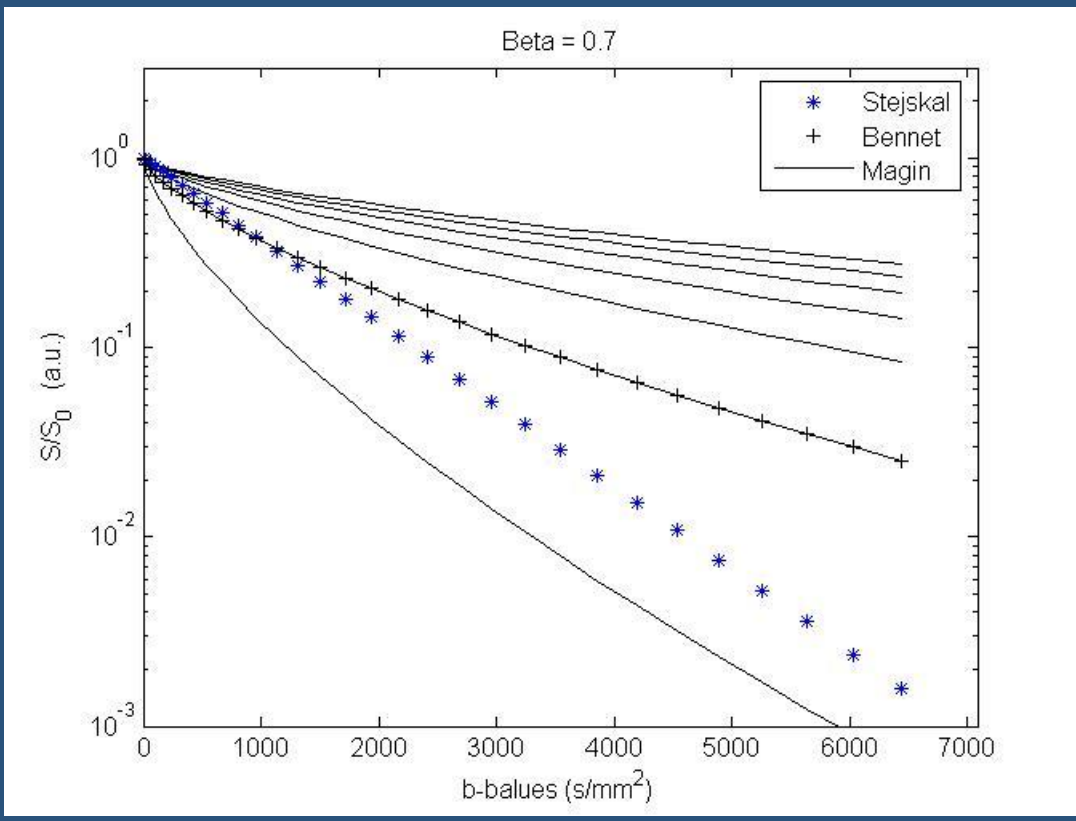
Changing β (0.3 – 1.0) and μ (5–55 μm)

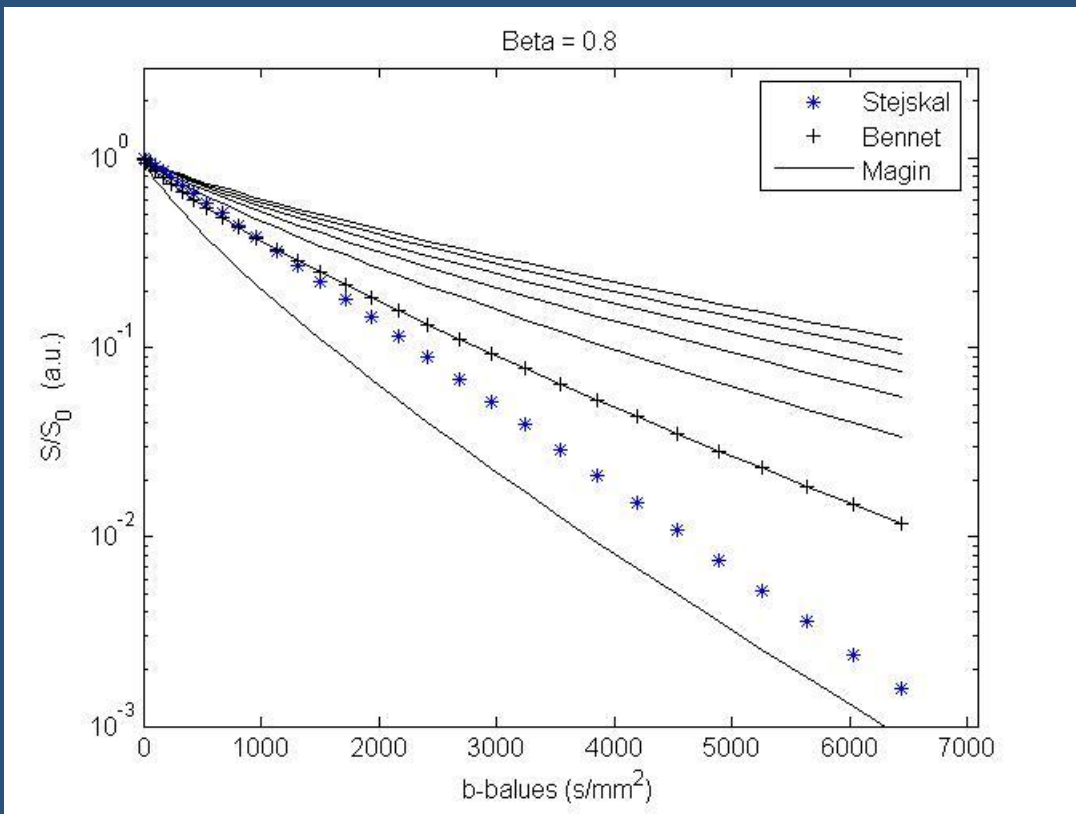


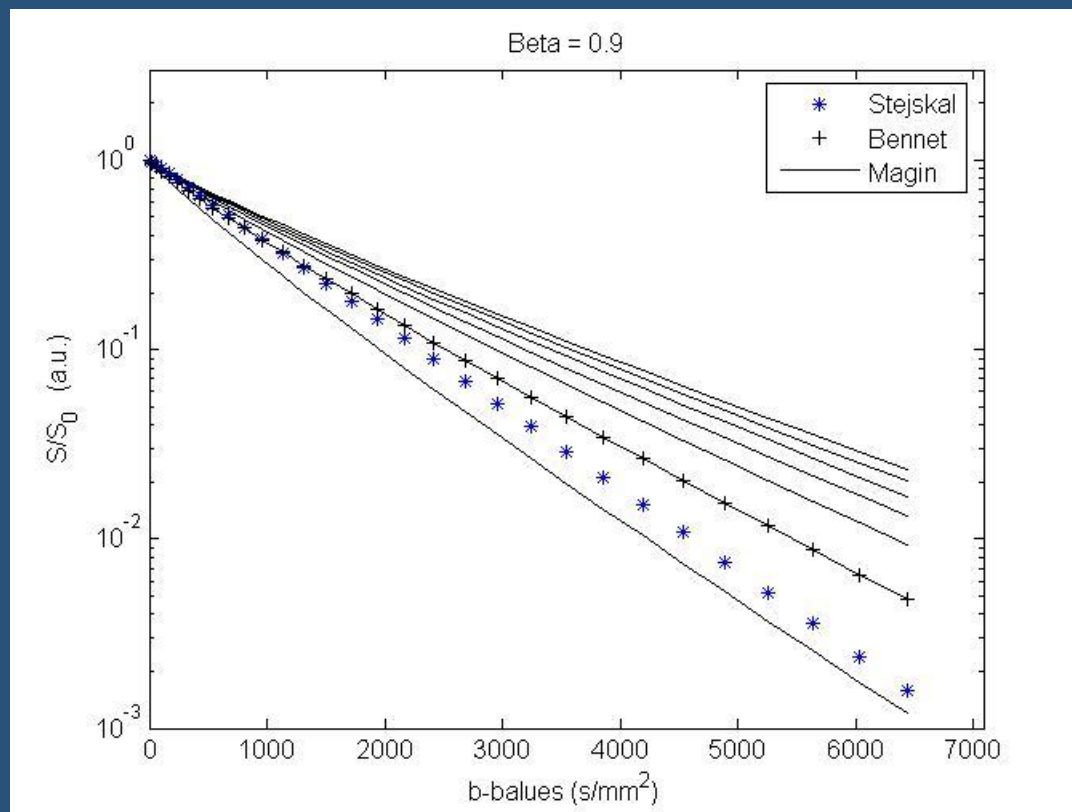


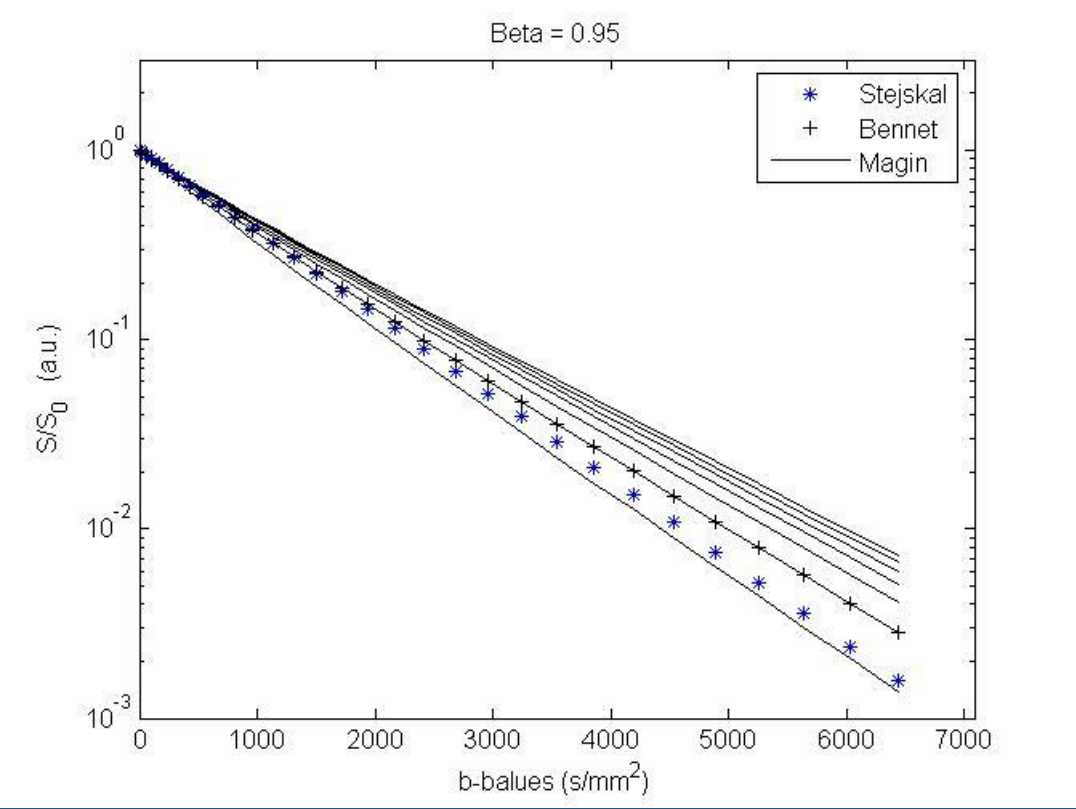


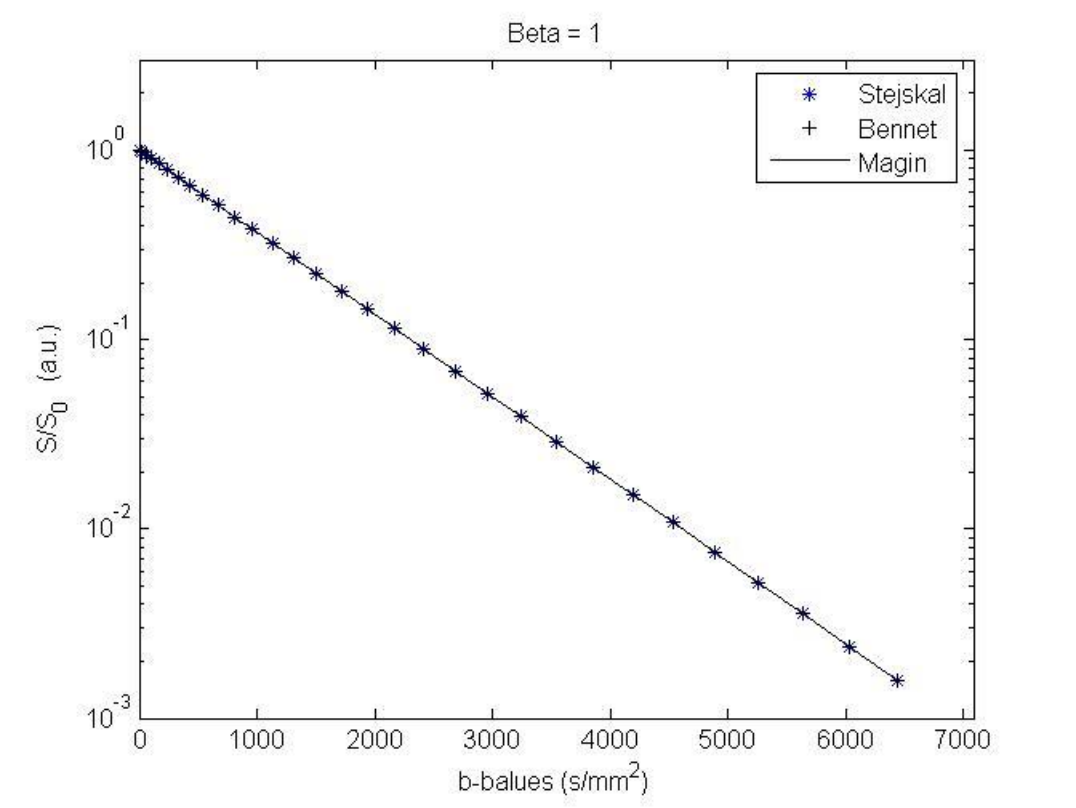








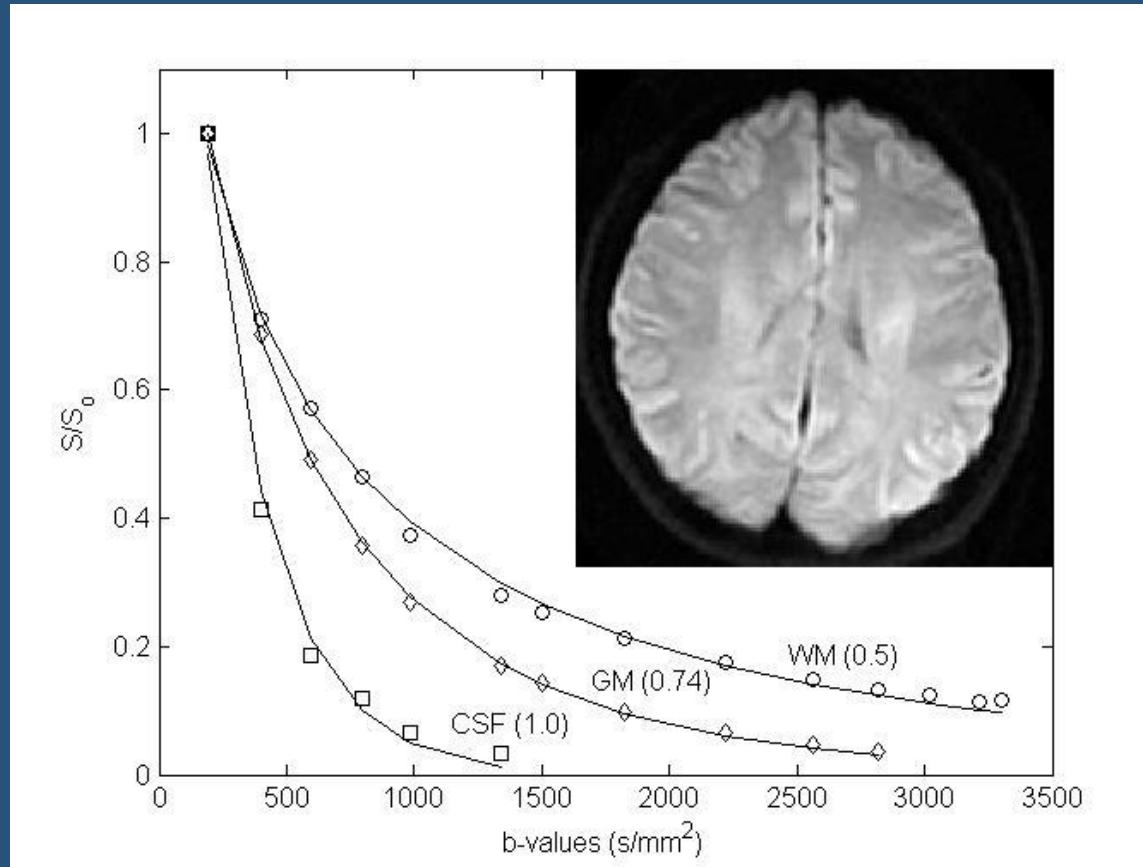




Brain MRI at 3 T

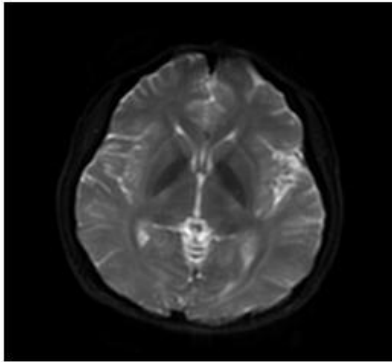


Brain

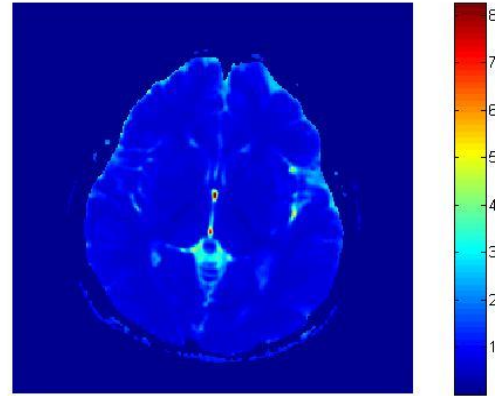


DW-EPI at 3T TR/TE = 4000/97 ms, slice thickness = 3 mm, matrix 256 x 256 and FOV = 22 x 22 cm^2 . Max b-value = 3300 s/mm^2

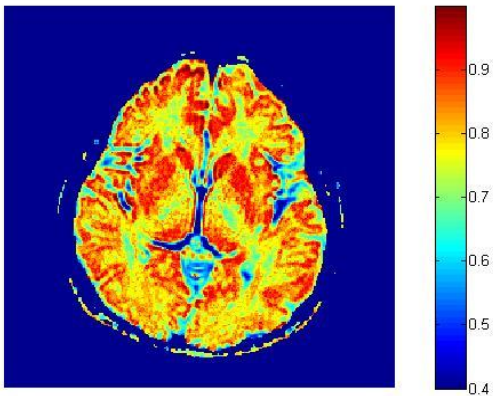
Axial Slice 2



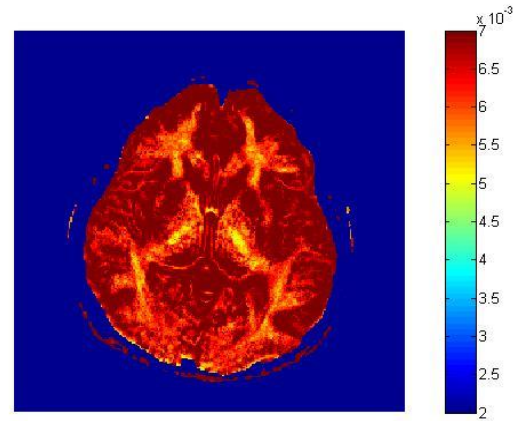
T2



ADC



Beta



Mu

Anomalous Diffusion

Fractional diffusion as a
window into Duchenne
Muscular Dystrophy
pathology

Matt G Hall

*Developmental Imaging and Biophysics
University College, London, UK*

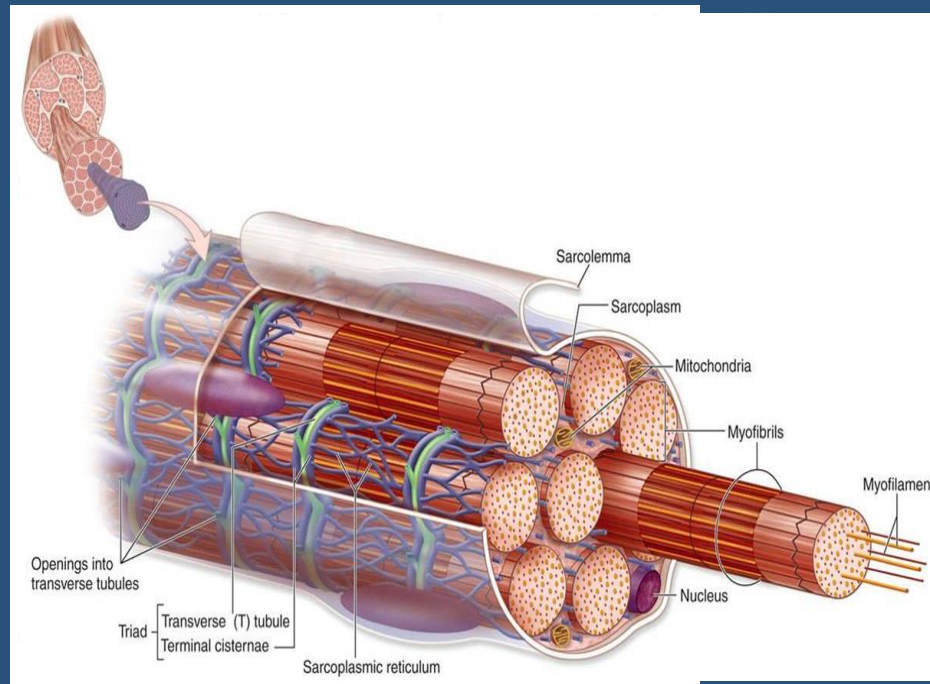


mattghall@gmail.com

Duchenne Muscular Dystrophy (DMD) is a genetic muscle-wasting condition affecting around 1 in 3,600 boys.



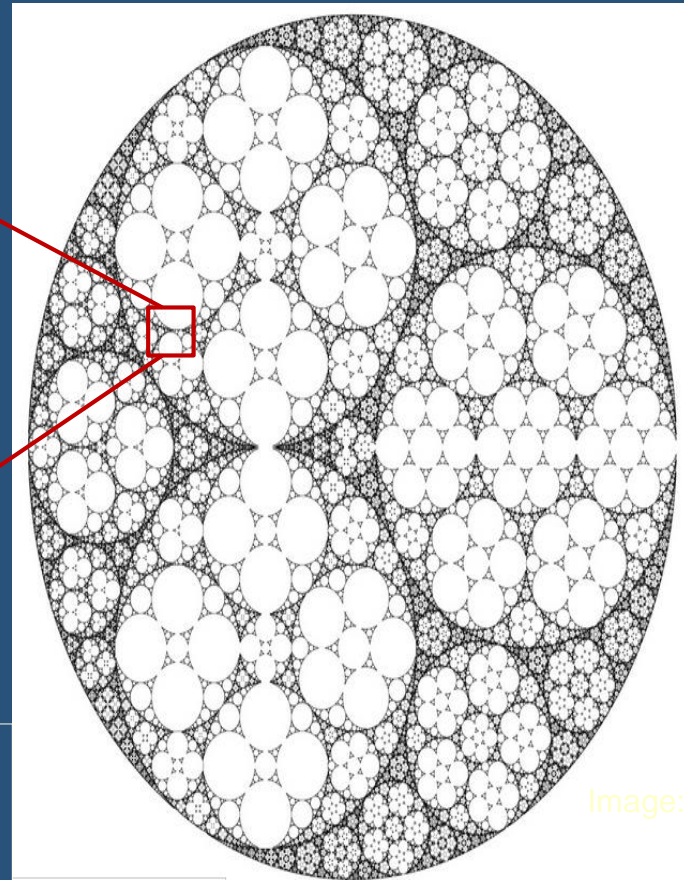
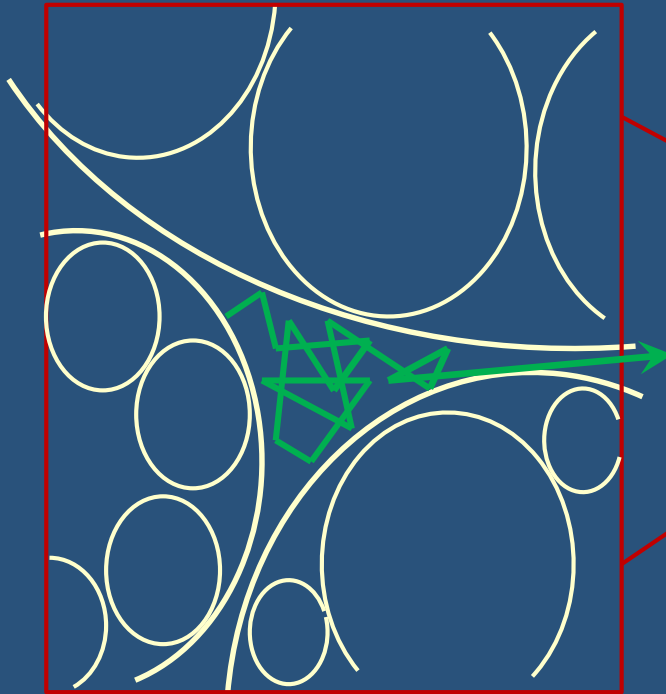
Muscle structure



- Muscle tissue is hierarchical
→ *Myofibres, Myofibrils,*
Myofilaments

Images: Wiley

Diffusion in muscle tissue

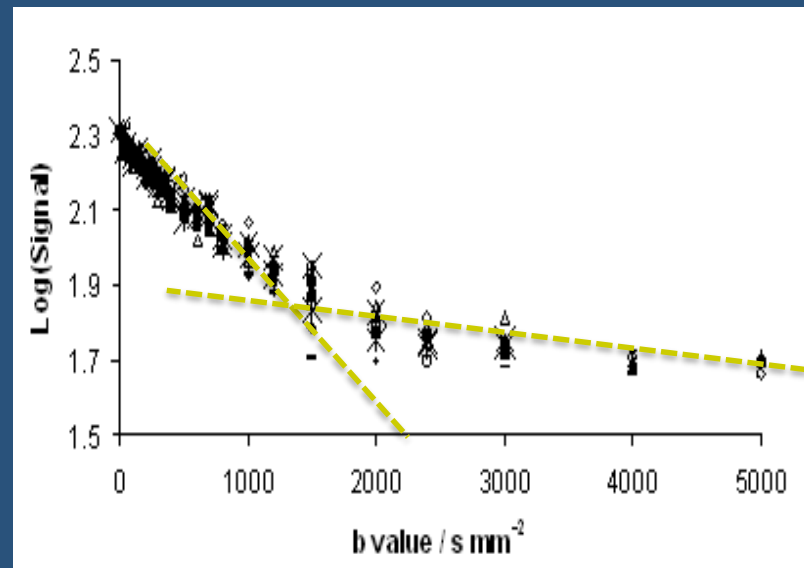


- Most diffusion is confined to small pores, but occasionally spins transition to neighbouring regions
- Changes to muscle structure change the distribution of pores and waiting times between transitions



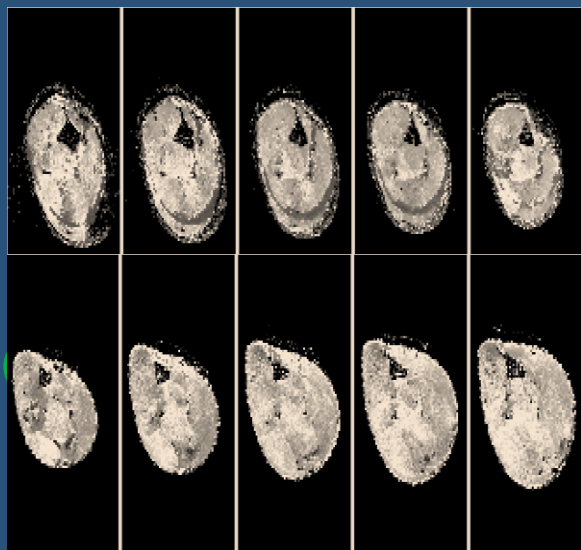
Diffusion MRI

- Regular diffusion imaging (including DTI) assumes that diffusion is averaged out across the sample
- This predicts that the log of the signal vs diffusion weighting will be a straight line
- If we measure this in tissue, however, we get the following, which we fit to the Mittag-Leffler function, $E_{\alpha, \beta}(-D_{\alpha, \beta} q^{\beta} \Delta^{\alpha})$

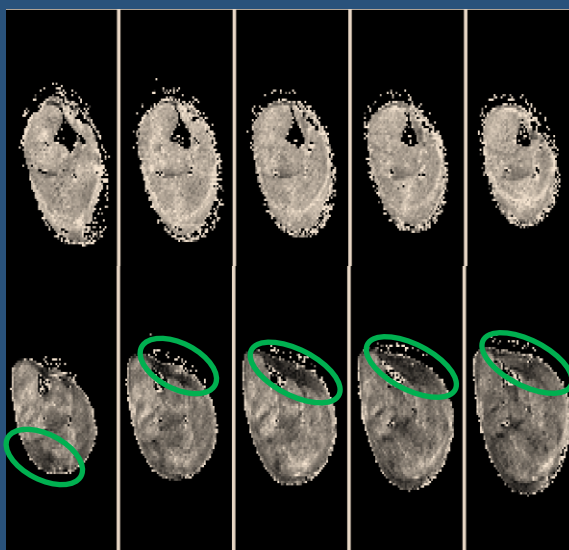




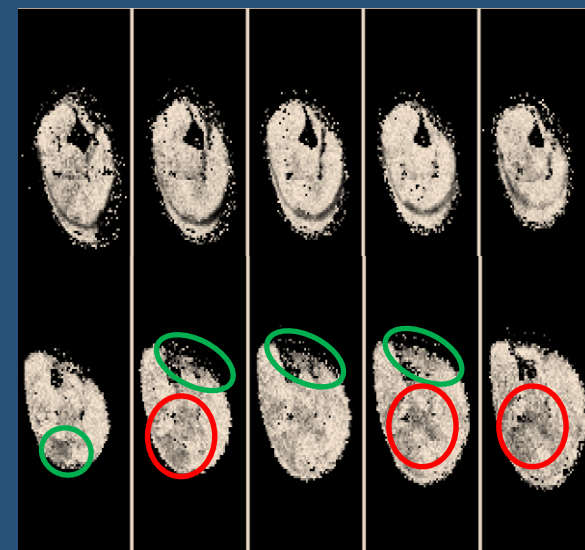
Preclinical results (mice)



$D_{\alpha,\beta}$



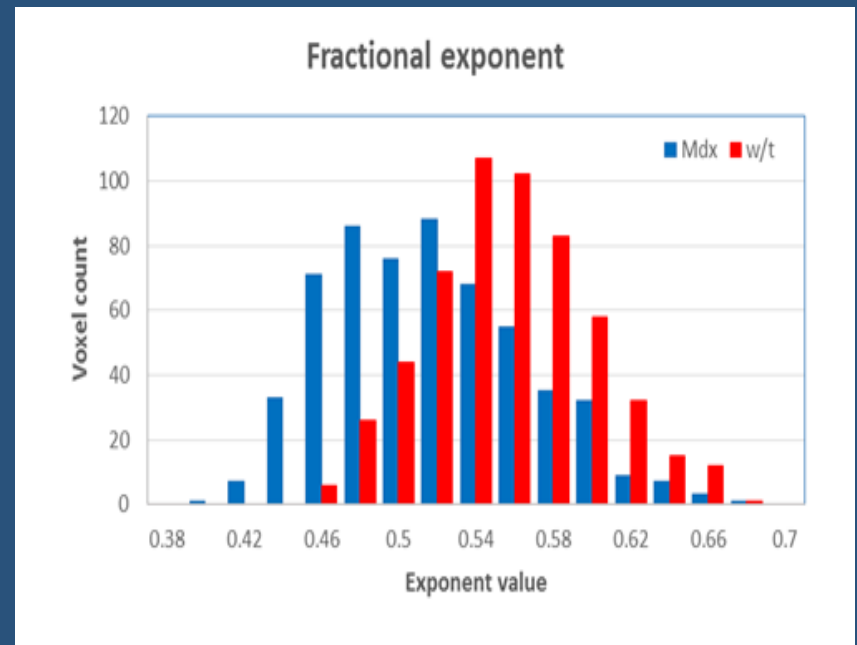
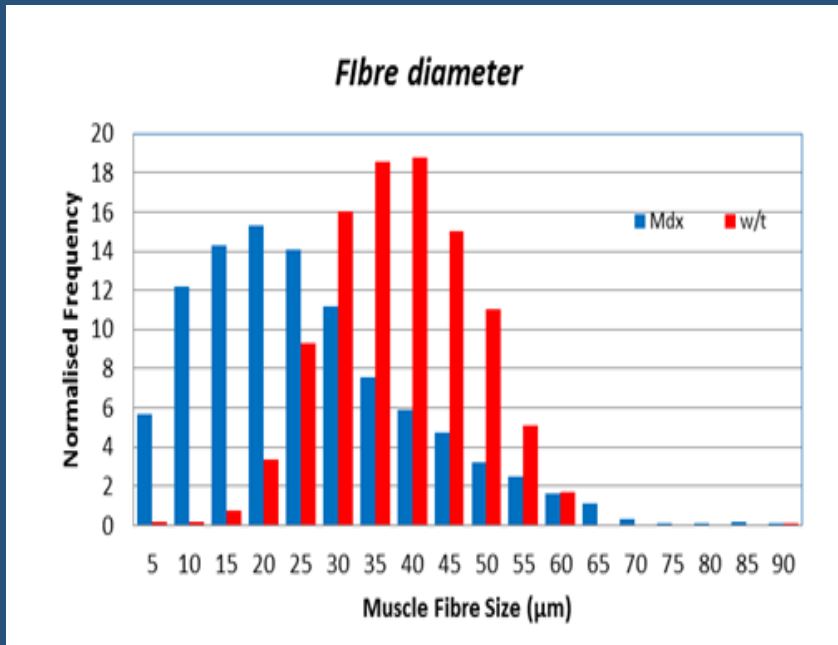
α



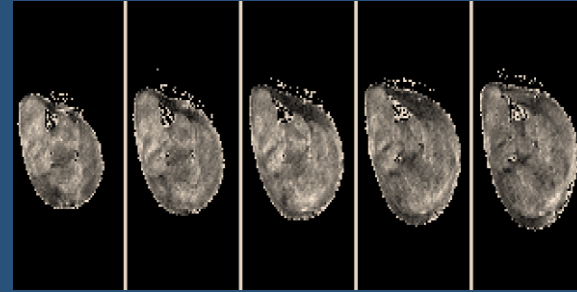
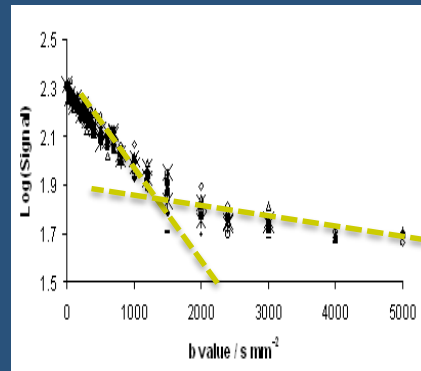
β



Comparison with Histology



Conclusions



The non-monoexponential curve contains information about the tissue hierarchical structure, which provides a model of the decay curve.

Changes in fibre distribution, packing, and permeability change the signal's curvature The Mittag-Leffler function can capture these changes.

Parameter maps for mouse data show darkened regions in Mdx models which are not present in wild type. These regions are observed consistently across N=8 subjects.

Comparison with histology suggests we're seeing changes in fibre size distribution.

Anomalous Diffusion

Fractional Order Calculus (FROC) Model for Pediatric Brain Tumor Differentiation

Muge Karaman

*Department of Radiology
University of Illinois at Chicago*



Brain Tumor Differentiation

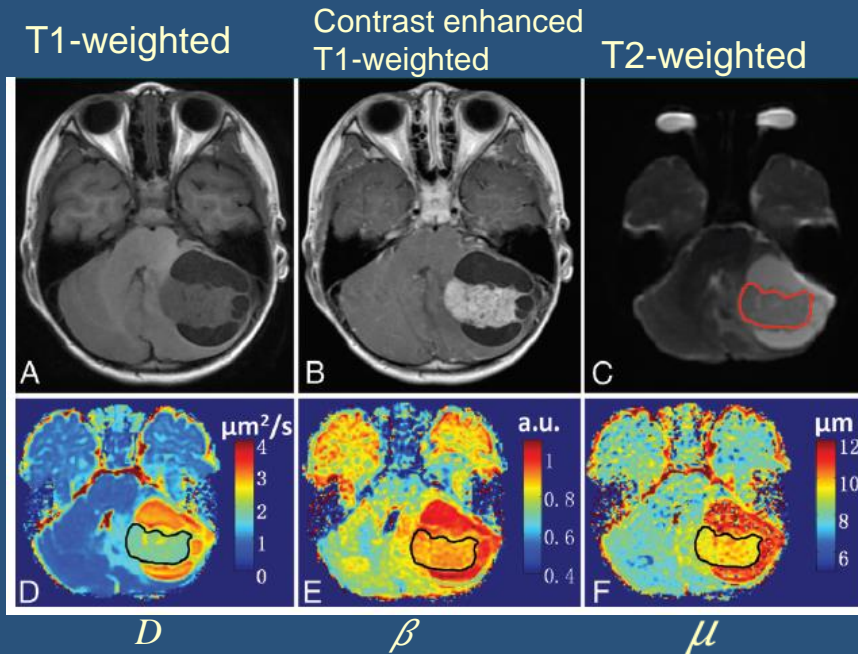


- The diffusion weighted signal attenuation according to the FROC Model

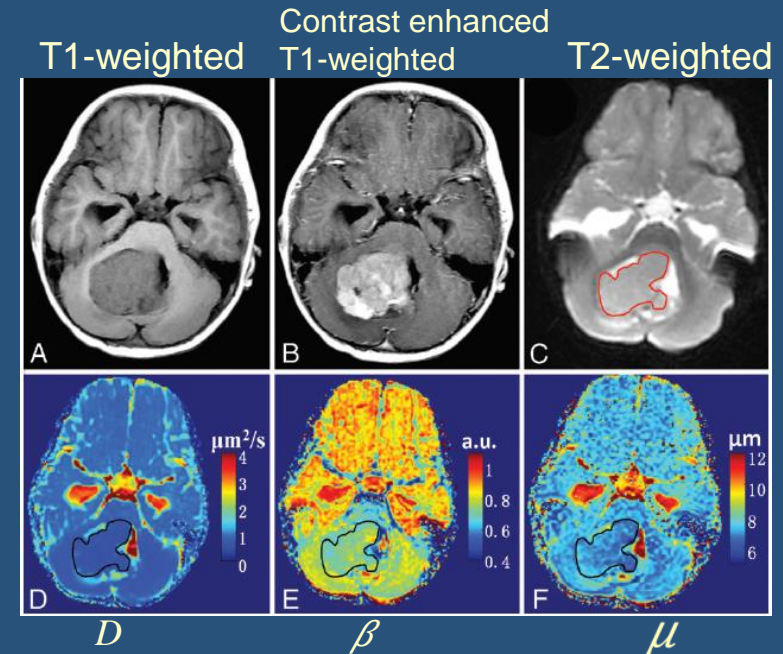
$$S/S_0 = \exp\left(-D\mu^{2(\beta-1)}(\gamma G_d \delta)^{2\beta} \left(\Delta - \frac{2\beta - 1}{2\beta + 1} \delta\right)\right)$$

- Application of the FROC Model to Differentiate Low- and High-grade Pediatric Brain Tumors

Low-grade (WHO II - 4y) Astrocytoma



High-grade (WHO IV - 6y) Medulloblastoma

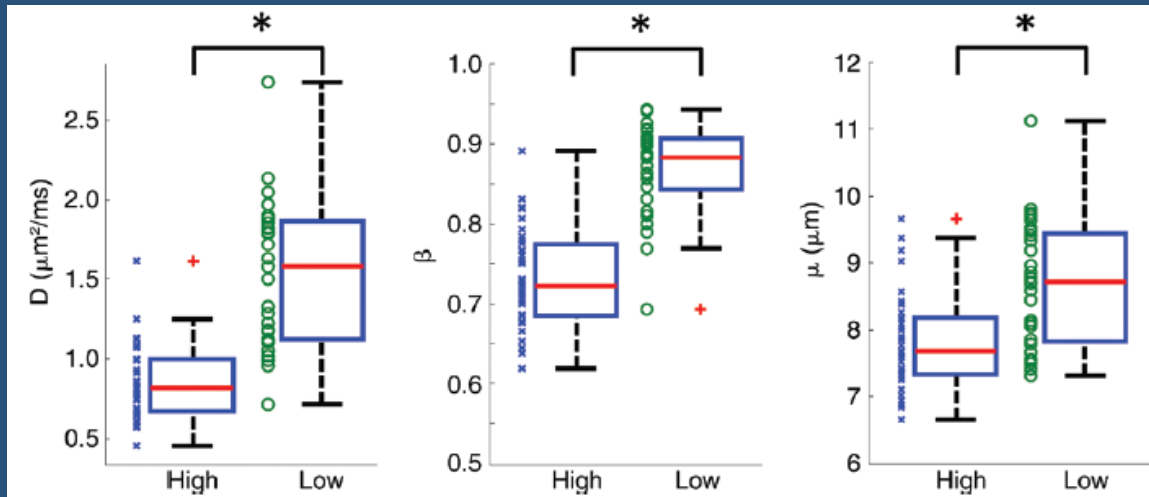


Fractional Order Calculus (FROC) Model for Pediatric Brain Tumor Differentiation

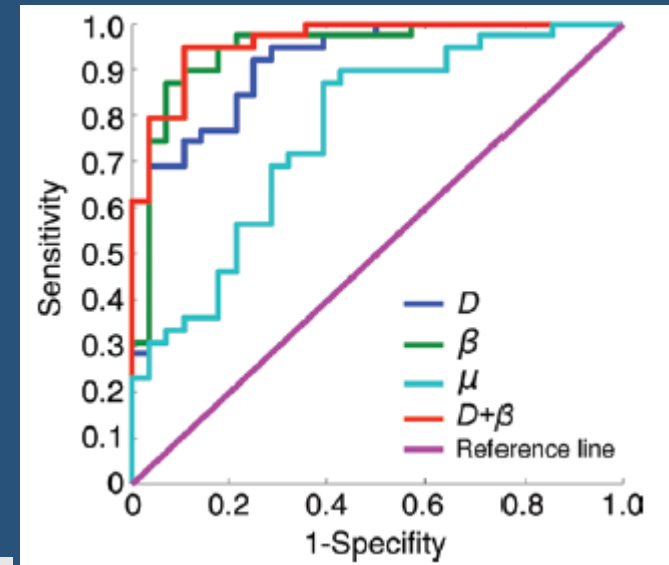


- Group Comparison on the Basis of *the FROC Model*

Scatter diagrams and box plots of the mean values



Receiver operating characteristics (ROC) curves



Area, 95% Confidence Interval, and Asymptotic Significance of ROC Curves by using FROC Parameters for Differentiating Low- and High-grade Pediatric Brain Tumors

Area and Statistics	FROC Parameter			
	D	β	μ	P_0
Area	0.910	0.943	0.763	0.962
95% confidence interval	0.840, 0.981	0.884, 1.0	0.646, 0.879	0.921, 1.0
P value	<.001	<.001	<.001	<.001

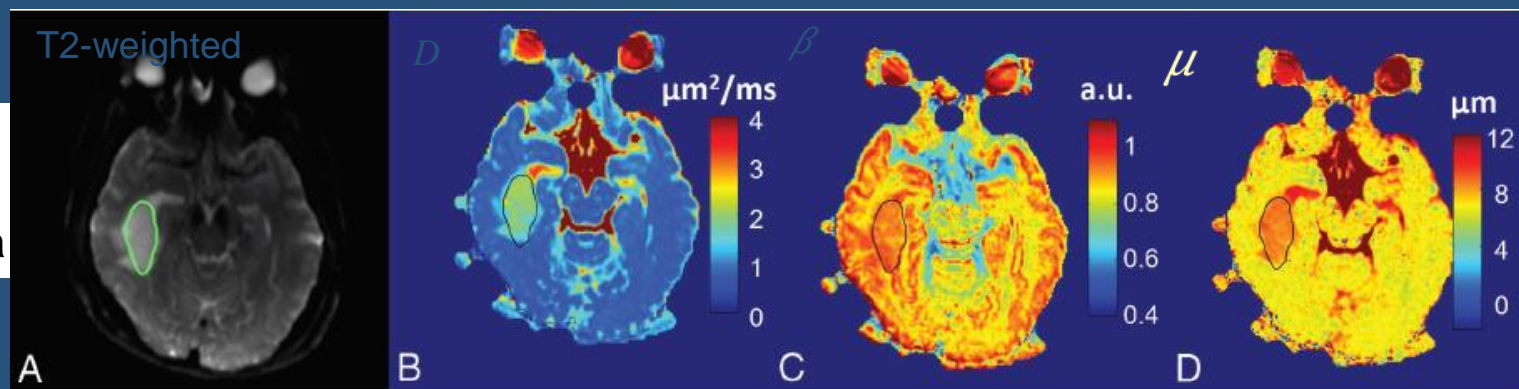
Note.— P_0 = a combination of D and β .

Sui et al., Radiology, 2015.

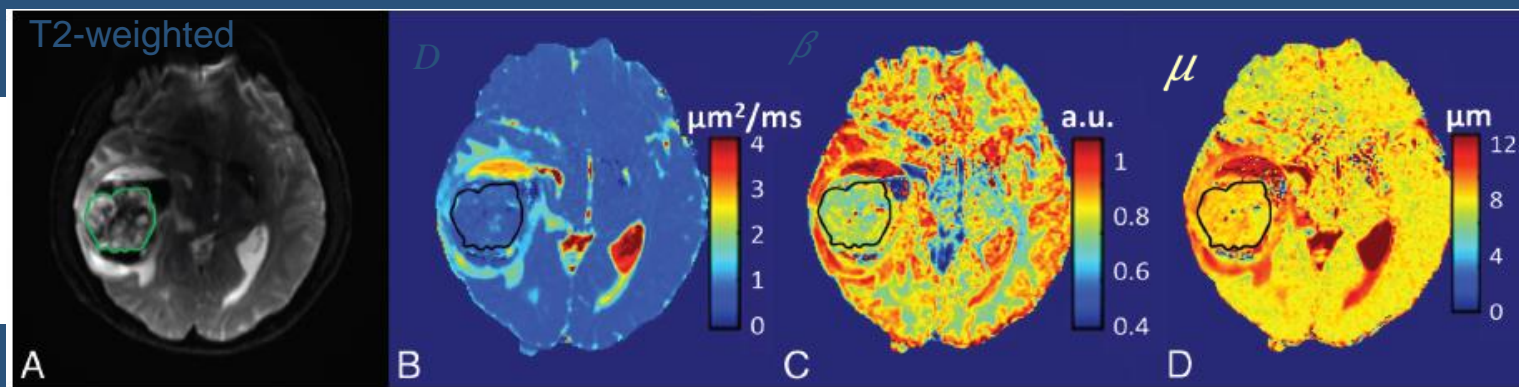


Fractional Order Calculus (FROC) Model for Glioma Differentiation

Low-grade
(WHO I - 41y)
Oligodendroglioma



High-grade
(WHO IV - 38y)
Glioblastoma
Multiforme



Continuous-time Random Walk (CTRW) Model for Brain Tumor Differentiation



- The diffusion weighted signal attenuation according to the CTRW Model

$$S/S_0 = E_{\alpha} \left(-(bD_m)^{\beta} \right)$$

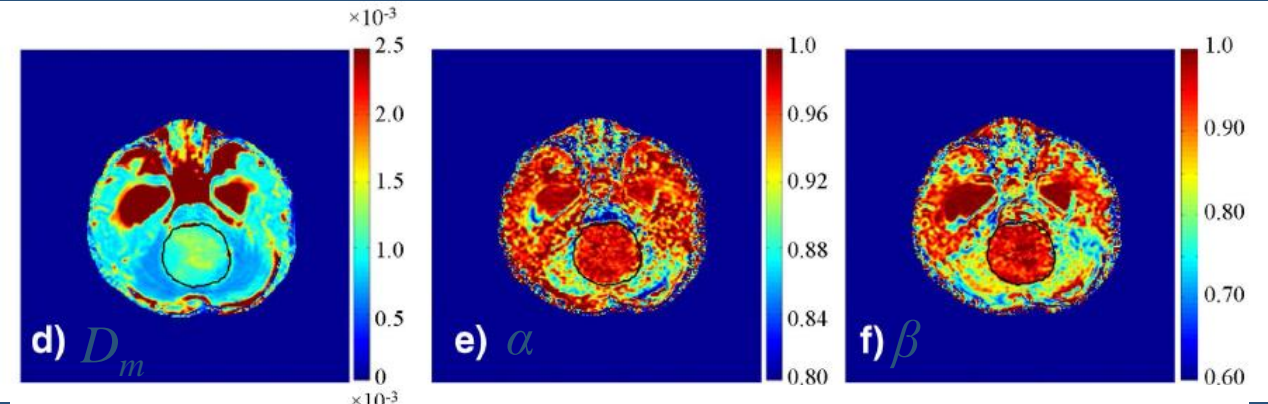
D_m : anomalous diffusion coefficient

α : diffusion waiting time parameter (temporal heterogeneity)

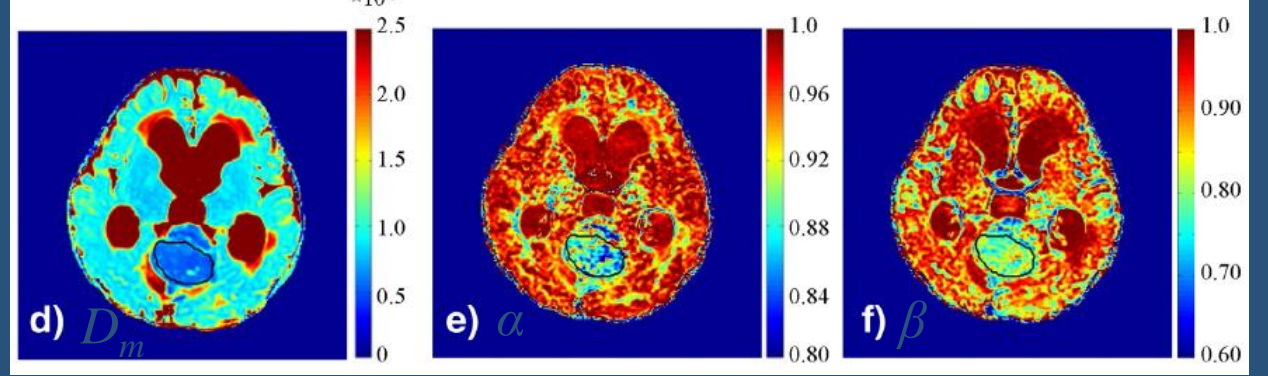
β : diffusion jump length parameter (spatial heterogeneity)

- Application of the CTRW Model to Differentiate Low- and High-grade Pediatric Brain Tumors

Low-grade
(WHO II - 17m)
Ependymoma



High-grade
(WHO IV - 18m)
Medulloblastom
a

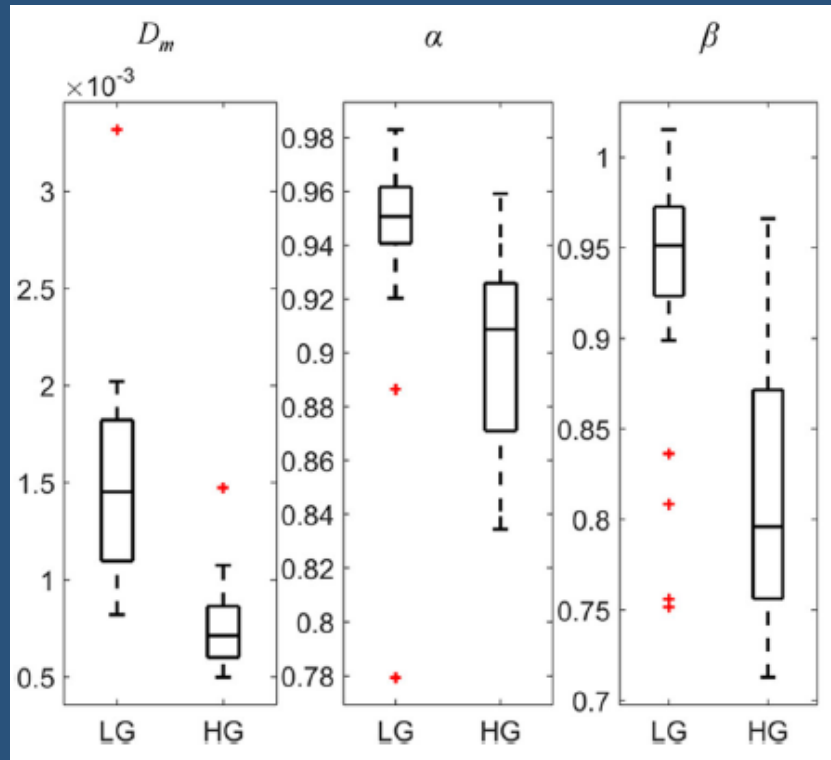


Continuous-time Random Walk (CTRW) Model for Brain Tumor Differentiation

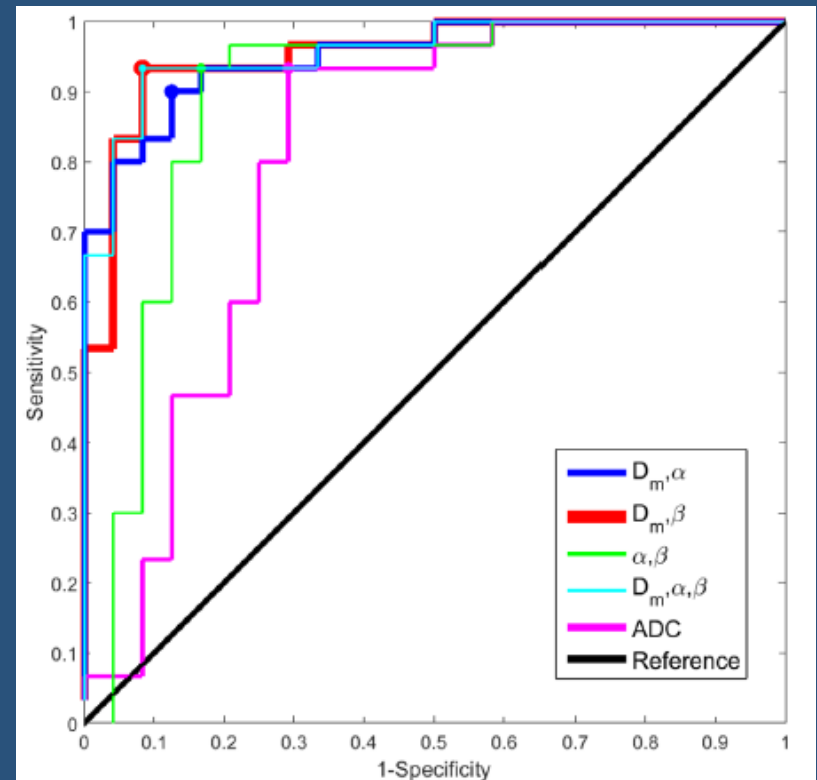


- Group Comparison on the Basis of *the CTRW Model*

Box and whisker plots of the mean values



Receiver operating characteristics (ROC) curves



The area under the curves are **0.951** (D_m, α), **0.952** (D_m, β), **0.898** (α, β), **0.957** (D_m, α, β), and **0.804** (ADC).

	(D_m, α)	(D_m, β)	(α, β)	(D_m, α, β)	ADC
Sensitivity	0.60	0.70	0.86	0.86	0.93
Specificity	0.91	0.83	0.83	0.83	0.54
Accuracy	0.74	0.75	0.85	0.85	0.75



An Alternative Non-Gaussian Diffusion Model: Fractional Motion Model

The diffusion weighted signal attenuation *according to the FM Model**

$$S/S_0 = \exp(-\eta' D_{fm} b^{\varphi/2} \left(\Delta - \frac{\delta}{3}\right)^{-\varphi/2} \Delta^{\varphi+\psi} \delta^{-\varphi})$$

D_{fm} : anomalous diffusion coefficient

φ : parameter that governs the variance of increments

ψ : parameter that governs the correlation properties of

We would like to compare CTRW and FM diffusion models at the level of an *imaging voxel* unlike recent studies performed in *cell culture***.

mkaraman@uic.edu

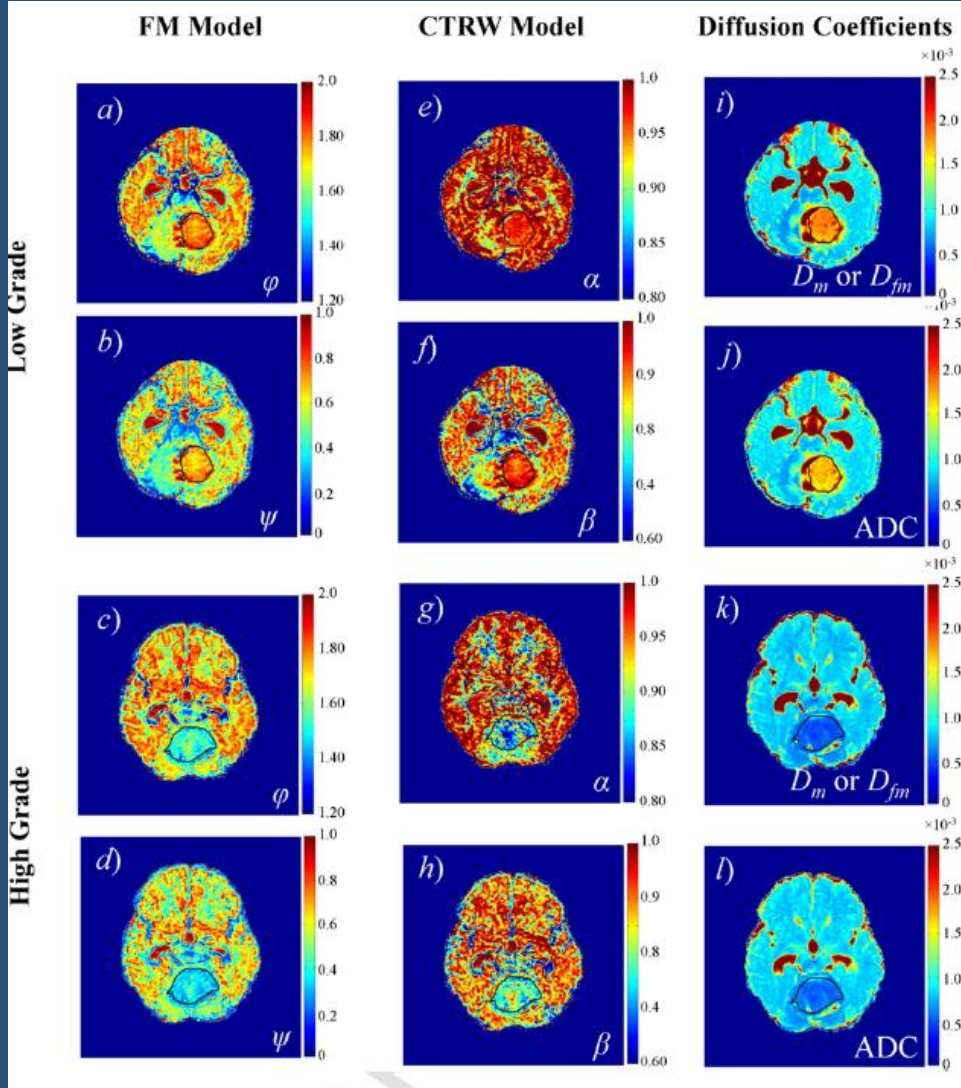
*Y. Fang and J. Gao. Physical Review E 92, 2015.
Karaman et al., NeuroImage: Clinical, *accepted*, 2016.

**Magdziarz et al., Phys. Rev. Lett. 2009;
Szymanski and Weiss, Phys. Rev. Lett. 2009;
Weiss, Phys. Rev. E. 2015; Ernst et al., Soft Matter 2012

An Alternative Non-Gaussian Diffusion Model: Fractional Motion Model



- Comparison of the CTRW and FM Models to Differentiate Low- and High-grade Pediatric Brain Tumors



ROC Results:

Sensitivity, specificity, diagnostic accuracy, and the AUC of the ROC analysis for the different combinations of the FM parameters for tumor differentiation.

	(D_{fm}, φ)	(D_{fm}, ψ)	(φ, ψ)	(D_{fm}, φ, ψ)
Specificity cut-off	0.866	0.866	0.800	0.885
Sensitivity cut-off	0.875	0.875	0.950	0.900
Accuracy	0.871	0.871	0.885	0.885
AUC	0.927	0.933	0.921	0.934

Sensitivity, specificity, diagnostic accuracy, and the AUC of the ROC analysis for the different combinations of the CTRW parameters for tumor differentiation.

	(D_m, α)	(D_m, β)	(α, β)	(D_m, α, β)
Specificity cut-off	0.866	0.866	0.833	0.866
Sensitivity cut-off	0.850	0.850	0.875	0.850
Accuracy	0.857	0.857	0.857	0.857
AUC	0.924	0.921	0.895	0.923

The CTRW and FM models provide similar performance for discriminating malignancy of pediatric brain tumors, which challenges several reports on the drastic difference between the two models observed in cell cultures.

Karaman et al., NeuroImage: Clinical, *accepted*, 2016.

Anomalous Diffusion

Parsimonious continuous time random walk models and **kurtosis** for diffusion in magnetic resonance of biological tissue.

Carson Ingo, Yu Fen Chen, Todd B. Parrish, Andrew G. Webb, and Itamar Ronen

Front. Phys. 3:11.(2015)

C.J. Gorter Center for High Field MRI, Univ. of Leiden, The Netherlands
Northwestern University, Chicago





Gaussian Diffusion

Partial Differential Equation

$$\frac{\partial P(x, t)}{\partial t} = D_{1,2} \frac{\partial^2 P(x, t)}{\partial |x|^2}$$

Fourier Transform Solution

$$p(q, t) = \exp(-D_{1,2}|q|^2 t)$$

Anomalous Subdiffusion

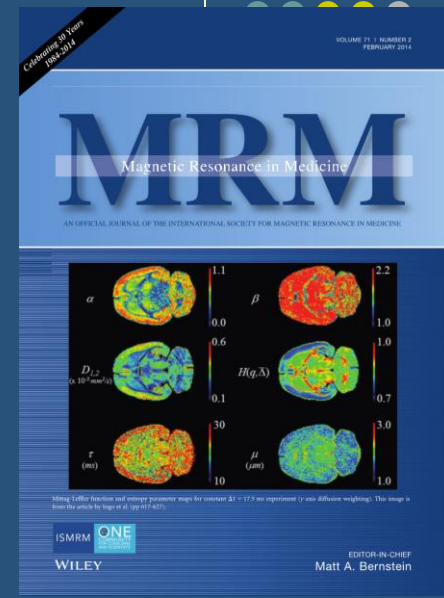
Fractional Partial Differential Equation

$$\frac{\partial^\alpha P(x, t)}{\partial t^\alpha} = D_\alpha \frac{\partial^2 P(x, t)}{\partial |x|^2}$$

Fourier Transform Solution

$$p(q, t) = E_\alpha[-D_\alpha |q|^2 t^\alpha]$$

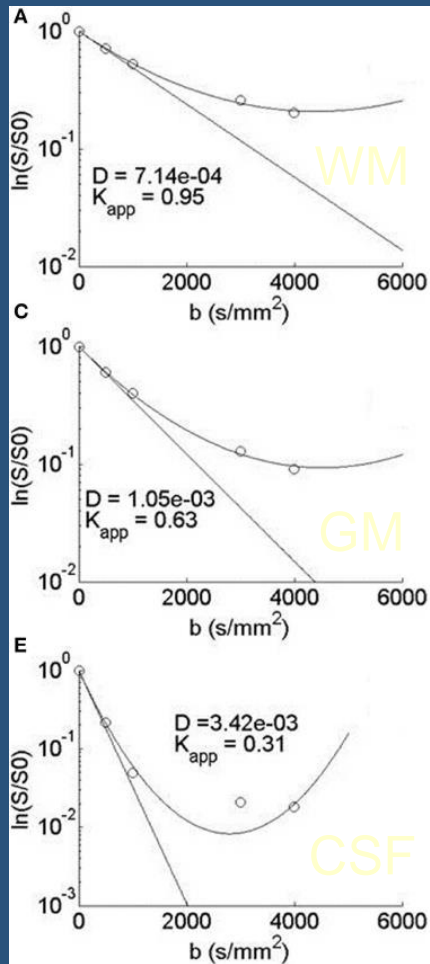
Mittag-Leffler Function (MLF)



Metzler and Klafter, *Phys Rev Lett*, 2000.
Ingo et al., *Magn Reson Med*, 2014.

Ingo C, et al. (2015). *Front. Phys.* 3:11. doi: 10.3389/fphy.2015.00011

Diffusional Kurtosis Imaging (DKI)



$$K \equiv \frac{\langle x^4 \rangle}{\langle x^2 \rangle^2} - 3$$

$$S/S_0 = \exp\left(-bD + \frac{1}{6}b^2D^2K_{app}\right)$$

$$\ln \frac{S(g)}{S(0)} = -\kappa_2 \frac{(\gamma g \delta)^2}{2} + \kappa_4 \frac{(\gamma g \delta)^4}{4!} + \kappa_6 \frac{(\gamma g \delta)^6}{6!} + \dots$$

Ingo C, et al. (2015). *Front. Phys.* 3:11. doi: 10.3389/fphy.2015.00011



Kurtosis in the Mittag-Leffler function

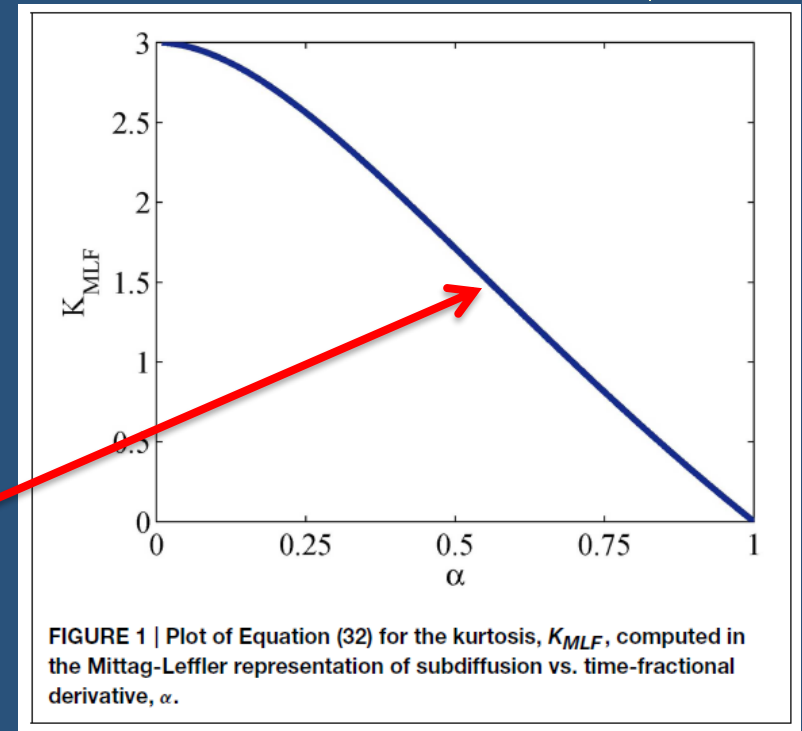
$$K \equiv \frac{\langle x^4 \rangle}{\langle x^2 \rangle^2} - 3$$

$$p(q, t) = E_\alpha[-D_\alpha |q|^2 t^\alpha]$$

$$\langle x^2(t) \rangle = \frac{2D_\alpha}{\Gamma(\alpha + 1)} t^\alpha$$

$$\langle x^4(t) \rangle = \frac{24(D_\alpha)^2}{\Gamma(2\alpha + 1)} t^{2\alpha}$$

$$K_{MLF} = 6 \frac{\Gamma^2(\alpha + 1)}{\Gamma(2\alpha + 1)} - 3$$



Ingo C, et al. (2015). *Front. Phys.* 3:11. doi: 10.3389/fphy.2015.00011



$$\lim_{t \rightarrow \infty} \frac{\langle \delta x^2(t) \rangle}{\langle x(t) \rangle^2} = \frac{2\Gamma^2(\alpha + 1)}{\Gamma(2\alpha + 1)} - 1$$

$$K_{MLF} = 6 \frac{\Gamma^2(\alpha + 1)}{\Gamma(2\alpha + 1)} - 3$$

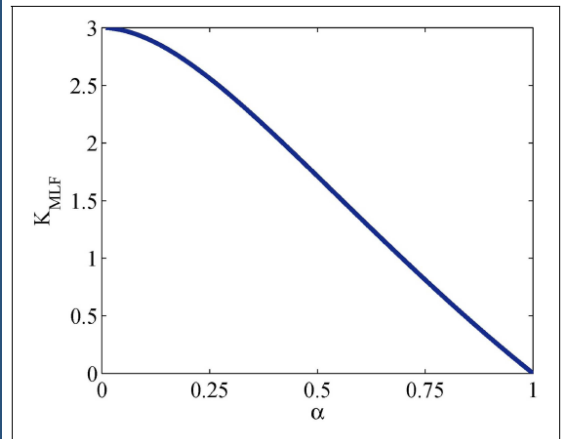
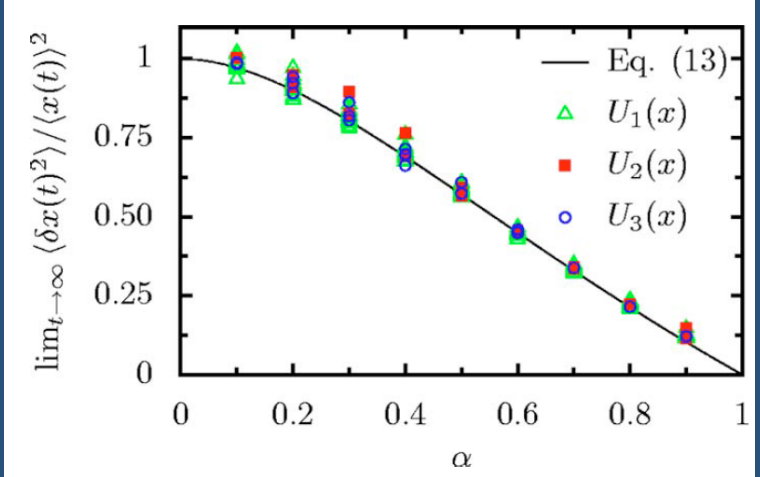


FIG. 2. (Color online) Universal scaling: Asymptotic values of the ratio $\langle \delta x^2(t) \rangle / \langle x(t) \rangle^2$ as a function of the parameter α for anomalous diffusion. All the points corresponding to the same α but different values of F and T match the function given in Eq. (13)

FIGURE 1 | Plot of Equation (32) for the kurtosis, K_{MLF} , computed in the Mittag-Leffler representation of subdiffusion vs. time-fractional derivative, α .

PHYSICAL REVIEW E 73, 020101(R) (2006)

Current and universal scaling in anomalous transport

I. Goychuk,¹ E. Heinsalu,^{1,2,3} M. Patriarca,¹ G. Schmid,¹ and P. Hänggi¹

¹Institut für Physik, Universität Augsburg, Universitätsstrasse 1, D-86135 Augsburg, Germany

²Institute of Theoretical Physics, Tartu University, 4 Tõre Street, 51010 Tartu, Estonia

³Fachbereich Chemie, Philipps-Universität Marburg, 35032 Marburg, Germany

(Received 7 September 2005; published 6 February 2006)

Ingo C, et al. (2015). *Front. Phys.* 3:11. doi: 10.3389/fphy.2015.00011



Methods

- Northwestern University Memorial Hospital
- 1 chronic stroke patient
- 3T Siemens Trio
- Diffusion weighted SE–EPI sequence
- 3 diffusion directions
- b-values: 0, 500, 1000, 3000, 4000 s/mm² with NA = 6
- TE = 102 ms, TR = 6 s, Δ = 41.2 ms, δ = 30.6 ms
- In-plane resolution = 2x2 mm, slice thickness = 4 mm
- 20 slices, scan time ~ 4 min



$$S/S_0 = \exp(-bD + \frac{1}{6}b^2D^2K_{app})$$

$$p(q, t) = E_\alpha[-D_\alpha|q|^2t^\alpha]$$

$$K_{MLF} = 6\frac{\Gamma^2(\alpha + 1)}{\Gamma(2\alpha + 1)} - 3$$

Ingo C, et al. (2015). *Front. Phys.* 3:11. doi: 10.3389/fphy.2015.00011



Results

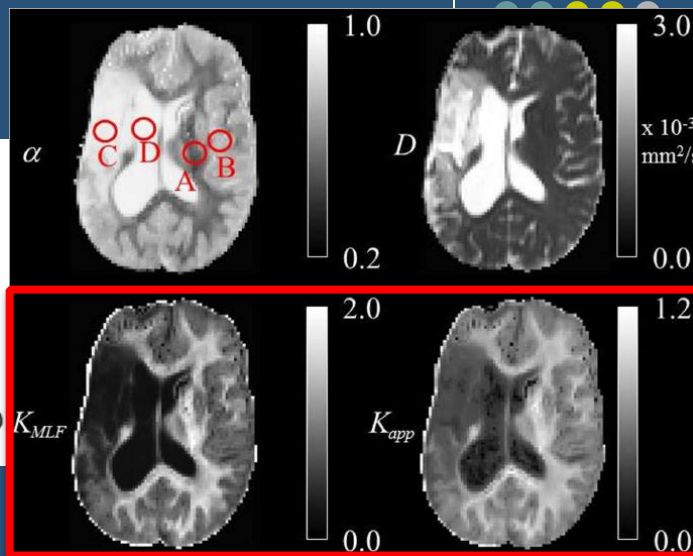
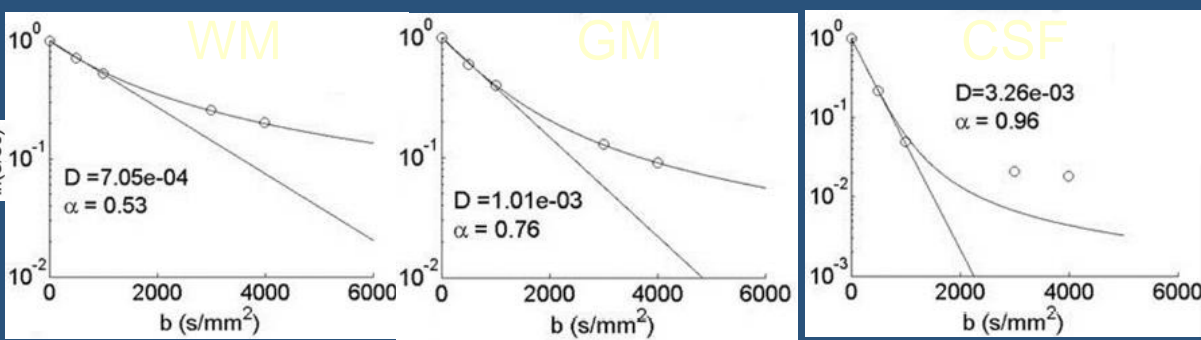
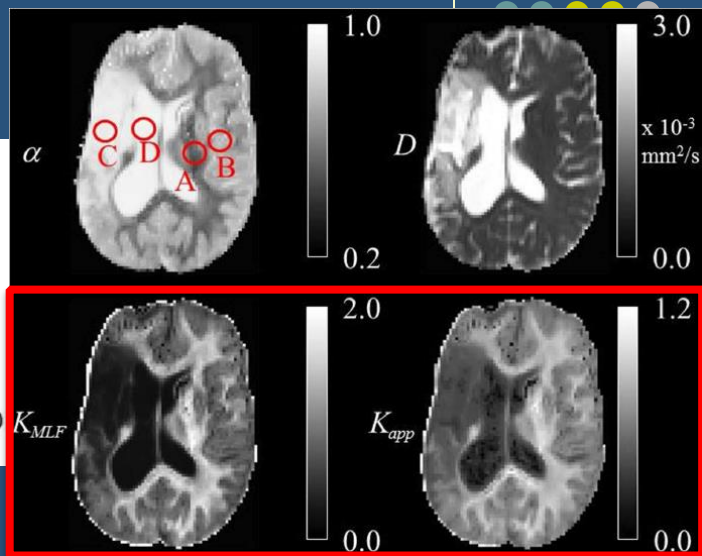
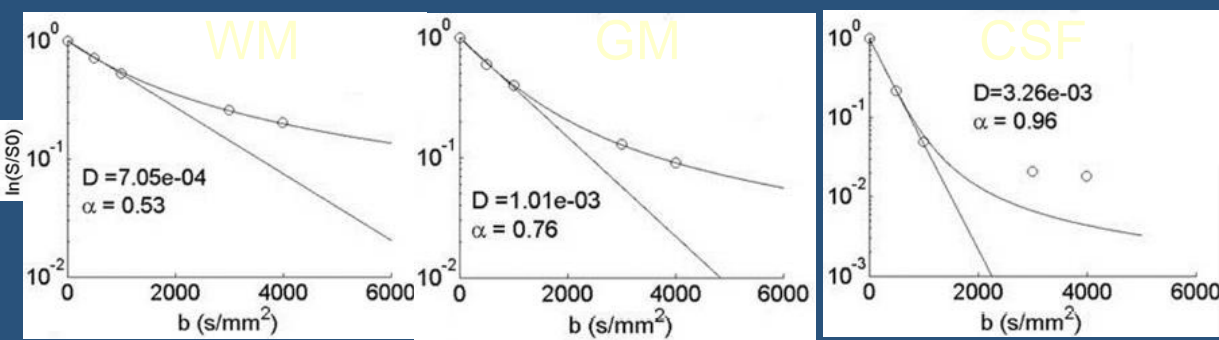


TABLE 1 | Mean and standard deviation of α , K_{MLF} , K_{app} , D_{MLF} , D_K , and ADC values for selected regions of interest (ROI) in the white matter (WM), gray matter (GM), ischemic tissue (IT), and cerebrospinal fluid (CSF) of a chronic ischemic stroke patient's brain.

ROI	α	K_{MLF}	K_{app}	D_{MLF}	D_K	ADC
(A) WM	0.49 ± 0.04	1.75 ± 0.12	0.99 ± 0.07	0.72 ± 0.03	0.75 ± 0.03	0.68 ± 0.02
(B) GM	0.77 ± 0.03	0.75 ± 0.09	0.58 ± 0.05	0.97 ± 0.02	1.02 ± 0.02	0.93 ± 0.01
(C) IT	0.94 ± 0.03	0.18 ± 0.09	0.35 ± 0.03	3.12 ± 0.12	3.26 ± 0.11	2.97 ± 0.10
(D) CSF	0.97 ± 0.01	0.12 ± 0.03	0.29 ± 0.05	3.27 ± 0.11	3.46 ± 0.12	3.12 ± 0.08

The estimated diffusion coefficient values are reported with units $\times 10^{-3}$ mm²/s.



Conclusions and Future Work

- Established mathematical connection between subdiffusion and kurtosis
- No limit on maximum b-value to estimate kurtosis
- K_{MLF} provided improved tissue contrast compared to K_{app}
- Quantify microstructural plasticity with language therapy in chronic stroke patients

Anomalous Diffusion

Tissue microstructure features derived from anomalous diffusion measurements in magnetic resonance imaging.

Yu, Q., Reutens, D., O'Brien, K., & Vegh, V
Human Brain Mapping, accepted 8-Oct-2016.

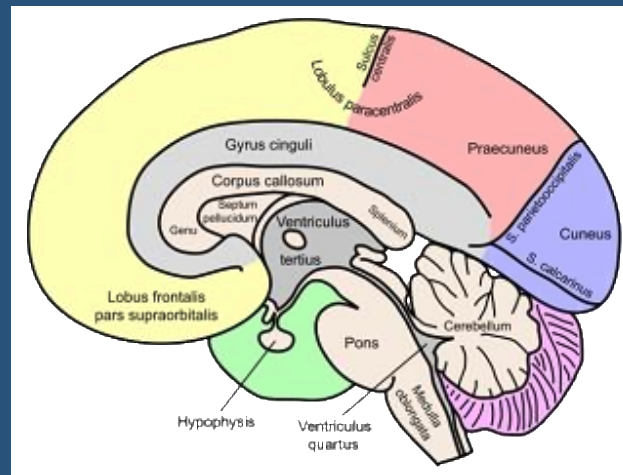
Centre for Advanced Imaging, the University of Queensland, Brisbane, Queensland, Australia



Extract axon radius and volume fraction using tissue model



- Corpus callosum is a white matter structure consisting of highly oriented fibre bundles of varying radii and volume fractions



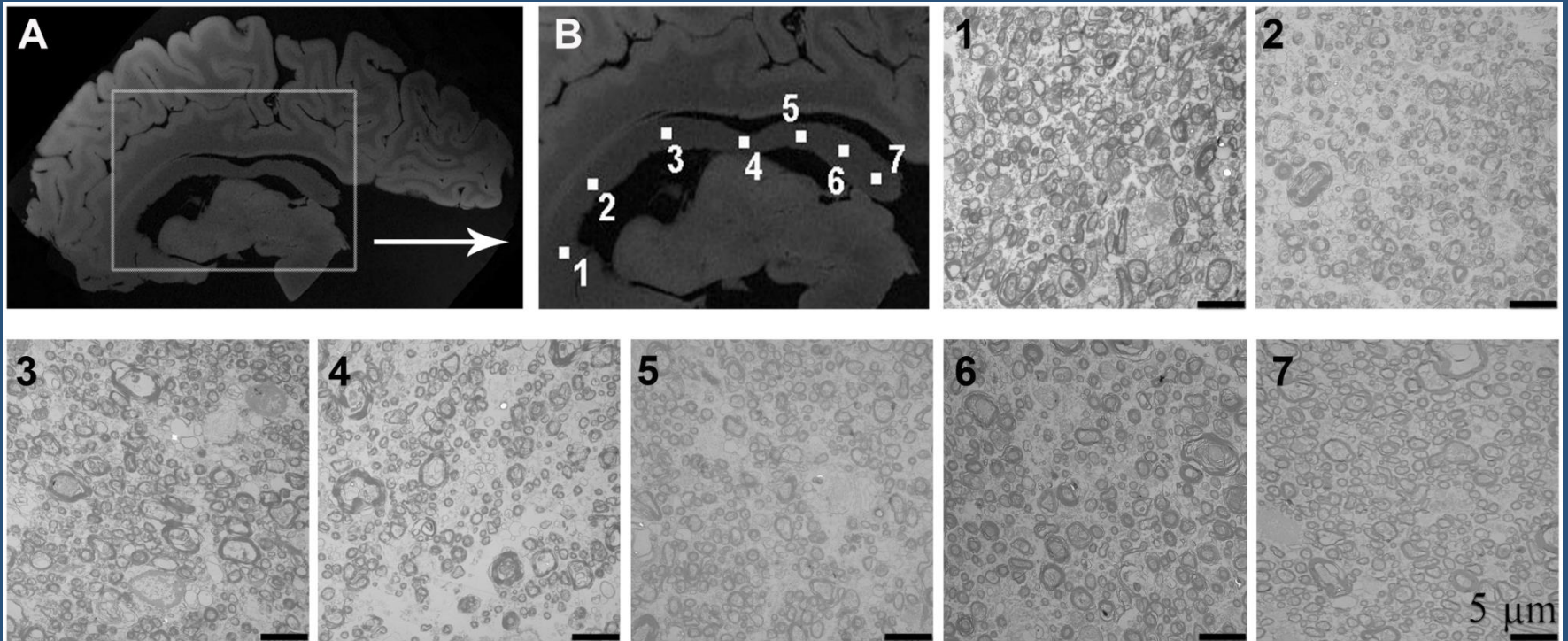
- We aimed to **map axon radii and volume fraction** across the corpus callosum using a tissue model and space fractional anomalous diffusion

Ex vivo experiment



- Subject: A single brain was obtained from the Queensland Brain Bank, Australia (male aged 60).
- EM: Electron microscopy images were used to evaluate axon radius and volume fraction in specific regions-of-interest
- MRI structural data: 7T Siemens Clinscan animal scanner was used to acquire 100 micron³ gradient recalled echo structural data
- MRI diffusion data: 7T Siemens Clinscan animal scanner was used to acquire 300 micron³ diffusion data with b-values from 0 to 5,000s/mm² in steps of 500s/mm², and number of directions increased with b-value to ensure trace of data had consistent SNR across all b-values

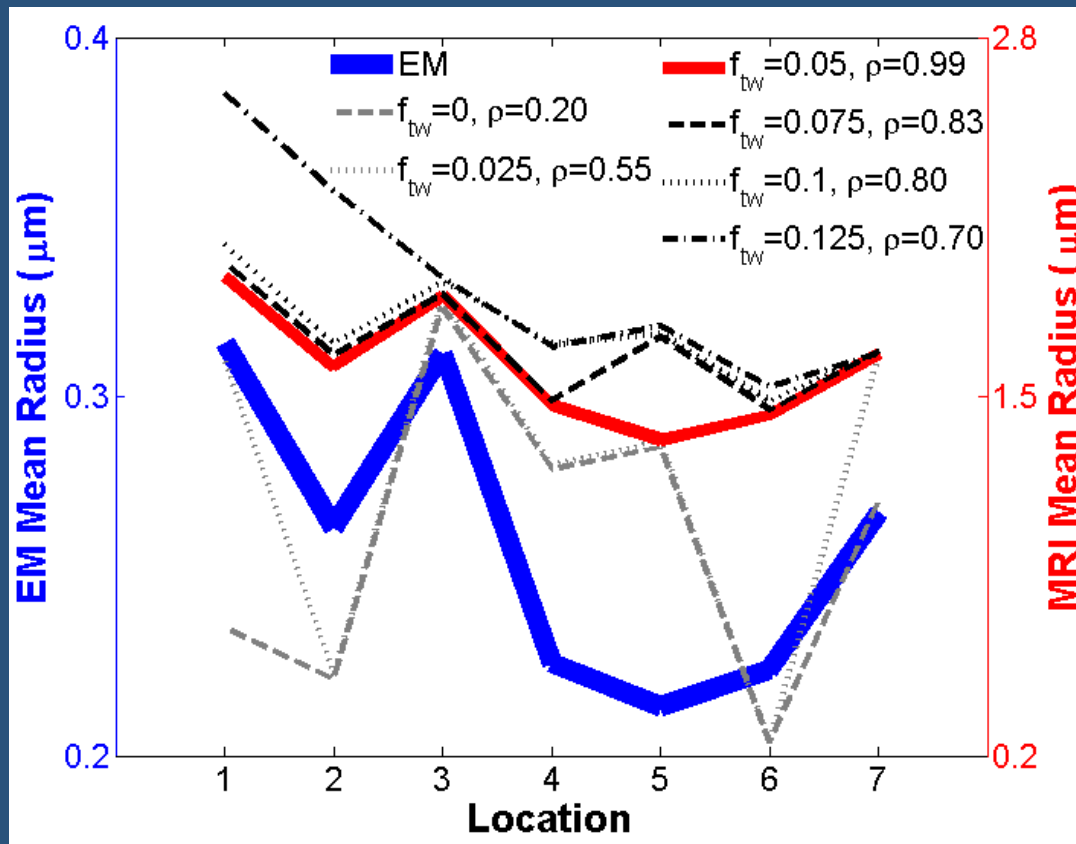
Electron microscopy validation (*ex vivo* experiment)



Results



ex vivo

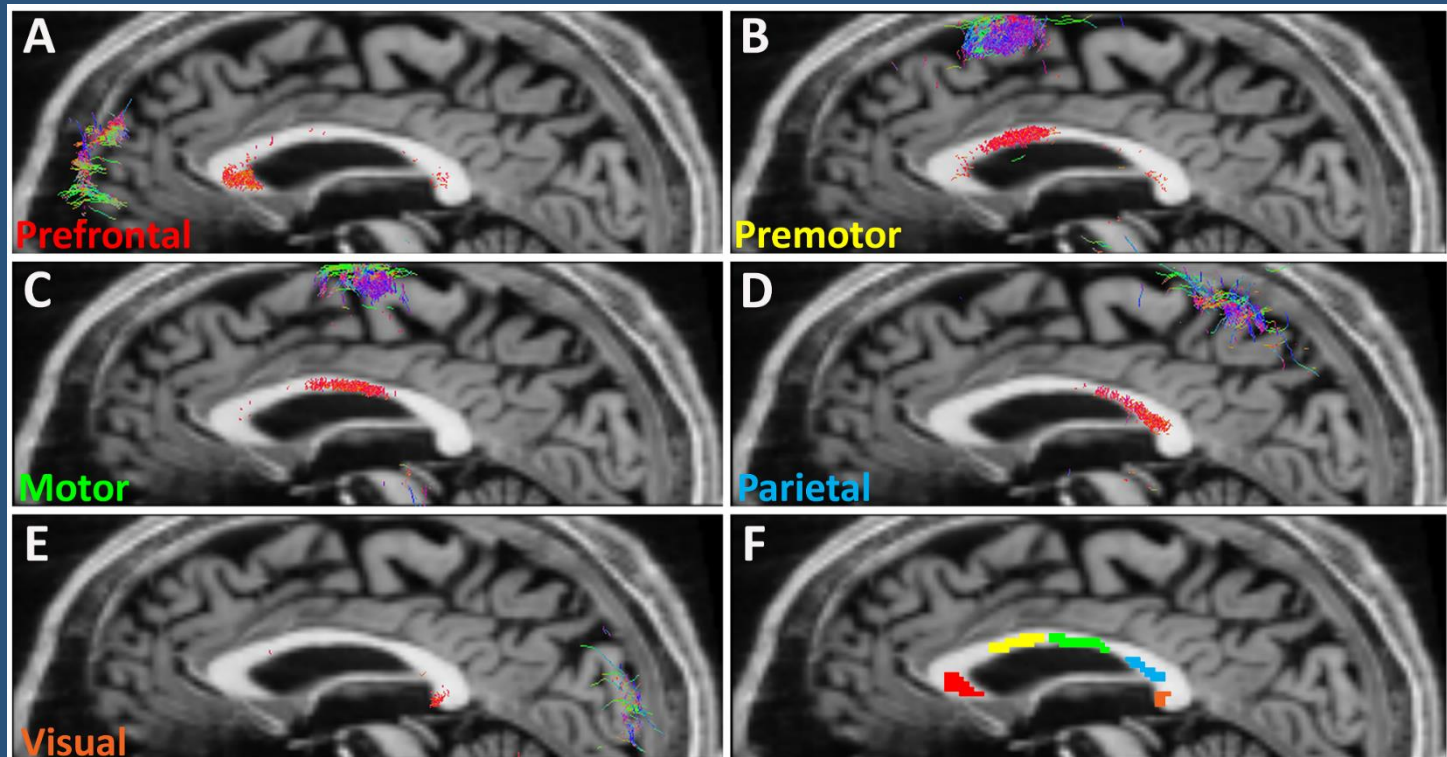


In vivo experiment

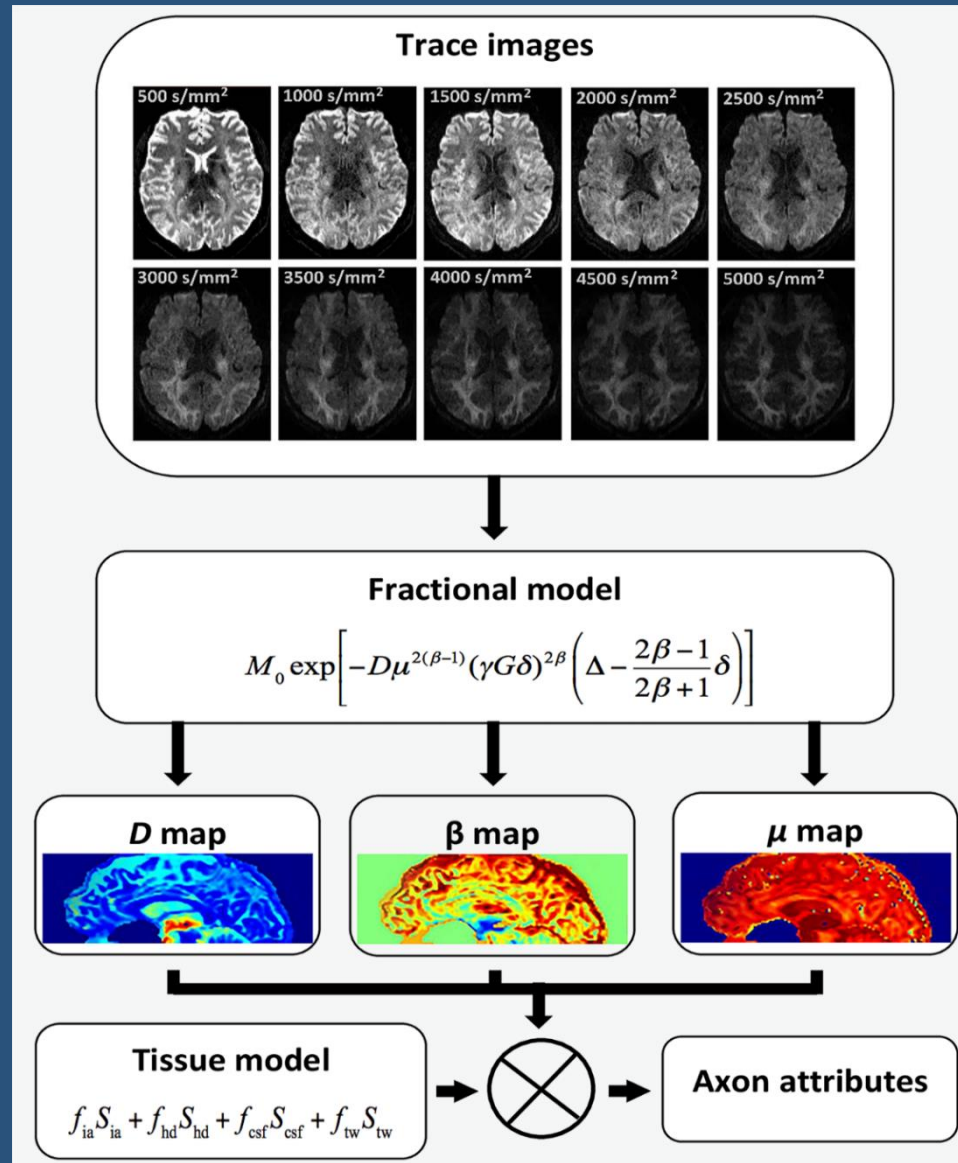


- Subjects: 9 healthy males aged 23-66 years were scanned
- Structural MRI data: 7T MRI gradient recalled echo collected on the Siemens Magnetom Research scanner at 750 micron³ resolution
- Anomalous diffusion data: 1.5mm³ DWI data with b-values from 0 to 5,000s/mm² in steps of 500s/mm², number of directions increased with b-value such that SNR does not degrade
- Tractography data: DWI with b-value = 3,000s/mm² and 64 directions
- Segmentation of the corpus callosum: MRtrix-based probabilistic tractography was performed to segment the corpus callosum into areas projecting into various cortical regions

Segment corpus callosum using tractography (*in vivo* experiment)



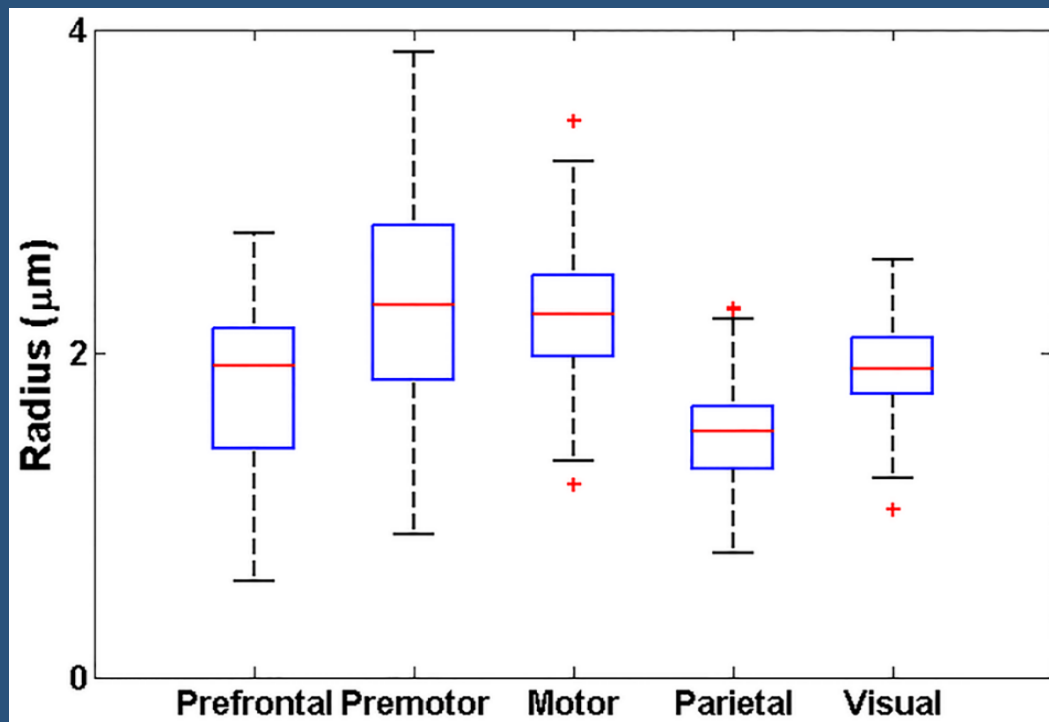
Data Processing



Results



in vivo



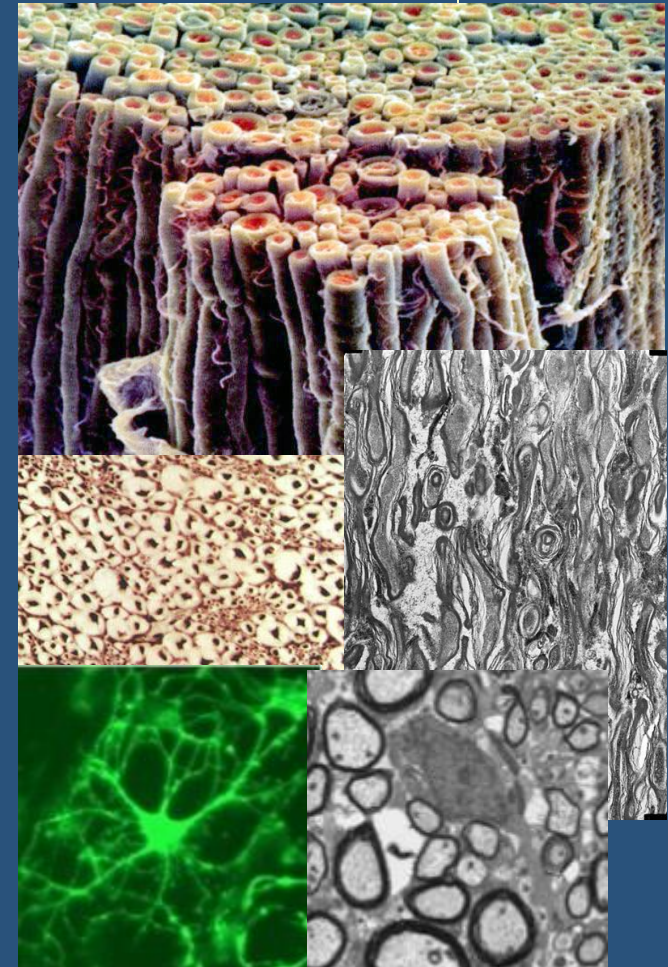
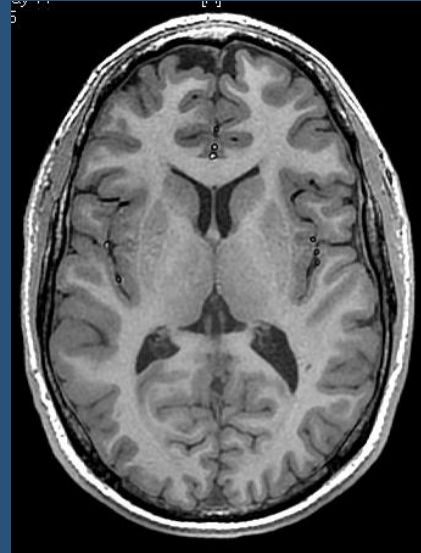
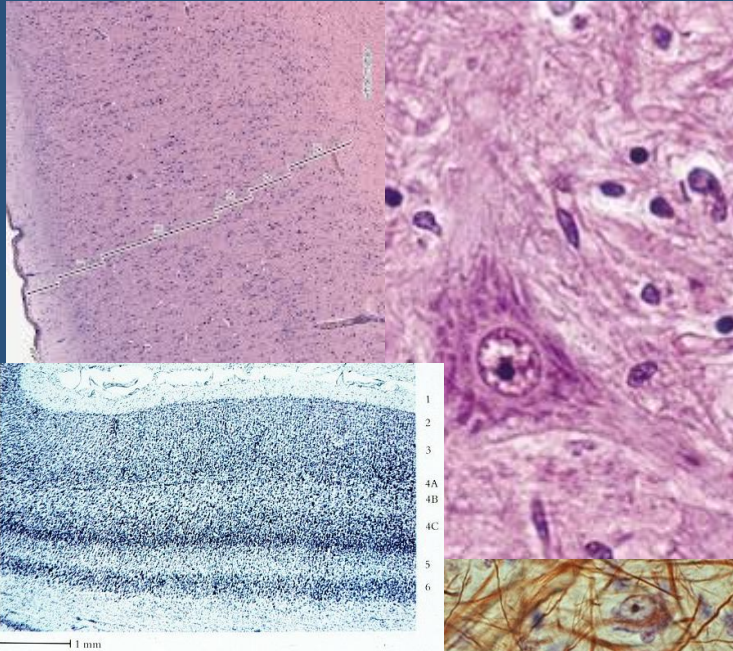
Anomalous Diffusion

Probing Features Of Tissue Microstructure Using The Continuous Time Random Walk Diffusion Model

Dr Thomas. R. Barrick
St. George's, University of London



How Does Microstructure Affect Water Diffusion In Brain Tissue?



Diffusion Time

$$\langle x^2 \rangle = 2Dt$$

Typical length
scale for MRI

1-20 μ m

Image Acquisition



- 3T diffusion-weighted MRI data
 - 2 scanners
 - St George's, University of London (SGUL)
 - Philips Achieva TX clinical system
 - 80 mTm⁻¹ maximum gradient strength
 - Human Connectome Project (HCP)
 - Purpose built enhanced Siemens system
 - 300 mTm⁻¹ maximum gradient strength

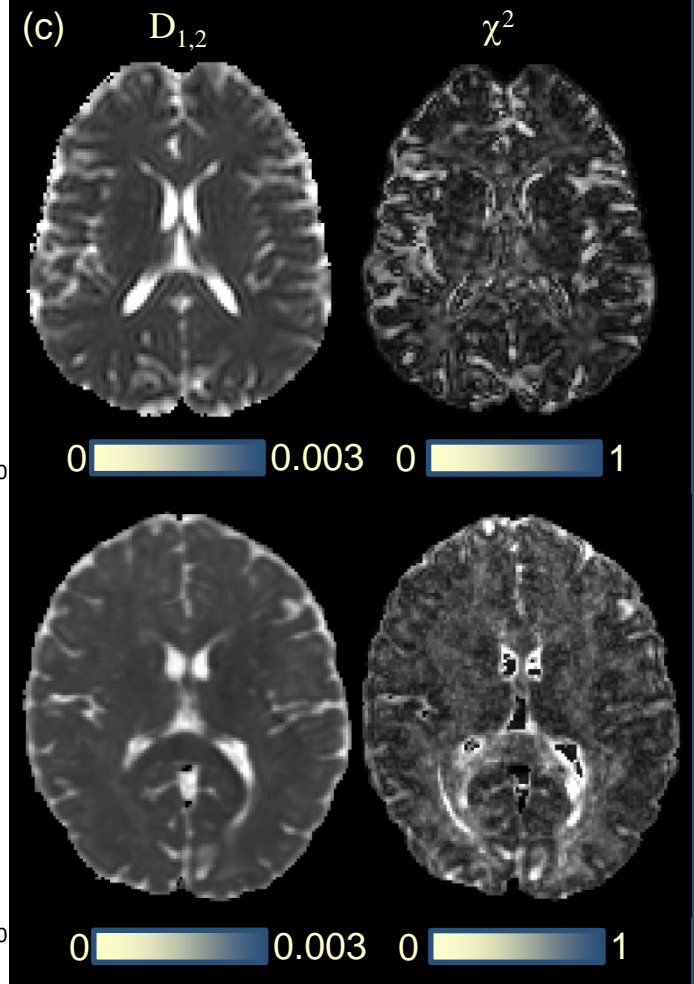
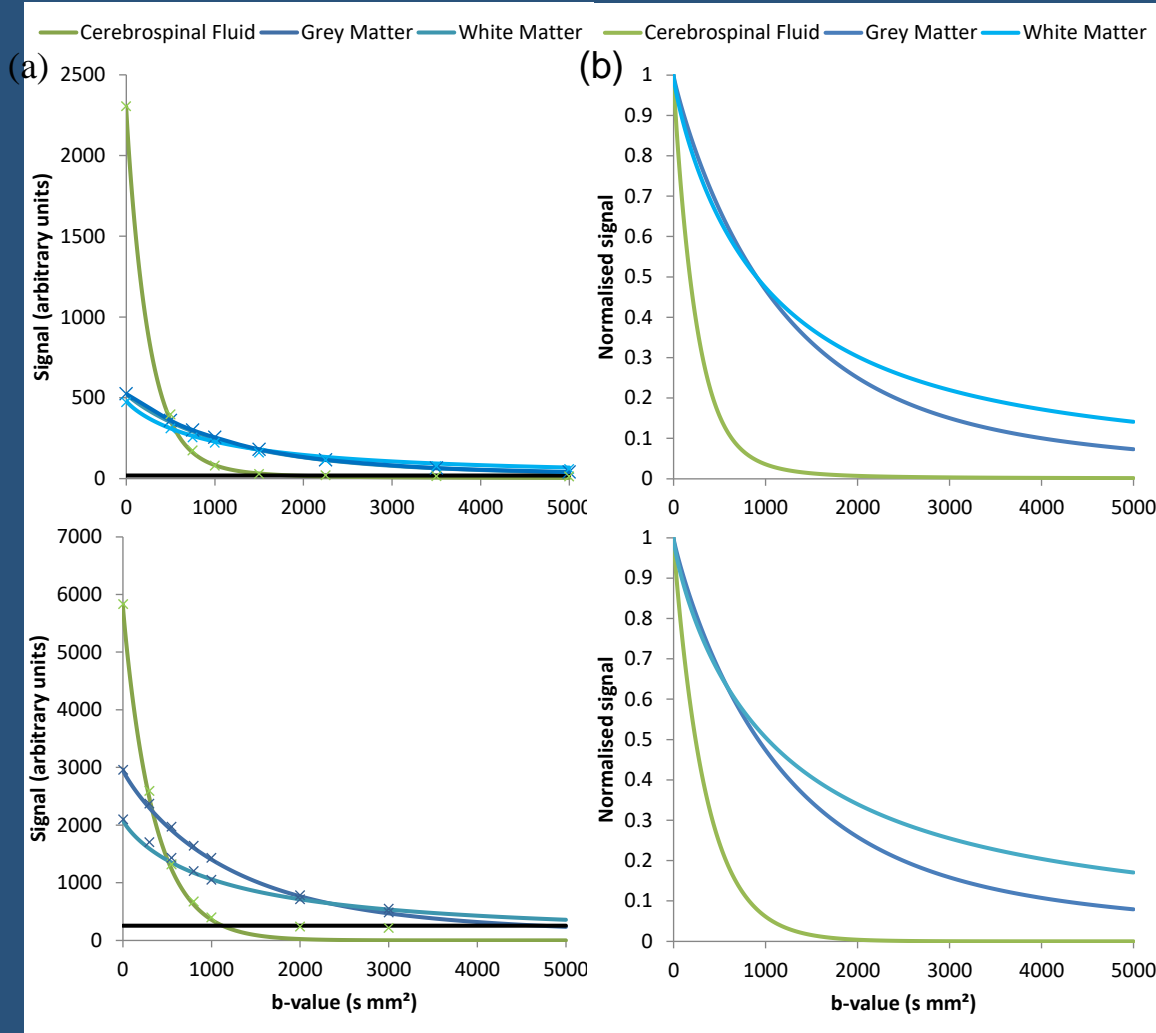


Image Acquisition

- SGUL $\delta=23.5$ ms, $\Delta=43.9$ ms, $\Delta =36.1$ ms
Voxel resolution $2 \times 2 \times 5 \text{mm}^3$
b-values 0, 500, 750, 1000, 1500, 2250, 3500, 5000 s mm^{-2}
3 or 6 diffusion gradient directions,
Acquisition time 6.5 or 13 minutes
- HCP $\delta=10.6$ ms, $\Delta=41.7$ ms, $\Delta =38.2$ ms
Voxel resolution Isotropic 1.25mm^3
b-values 5, 1000, 2000, 3000 s mm^{-2}
180 diffusion gradient directions,
Acquisition time 1 hour

Van Essen et al., 2012

Data Fitting

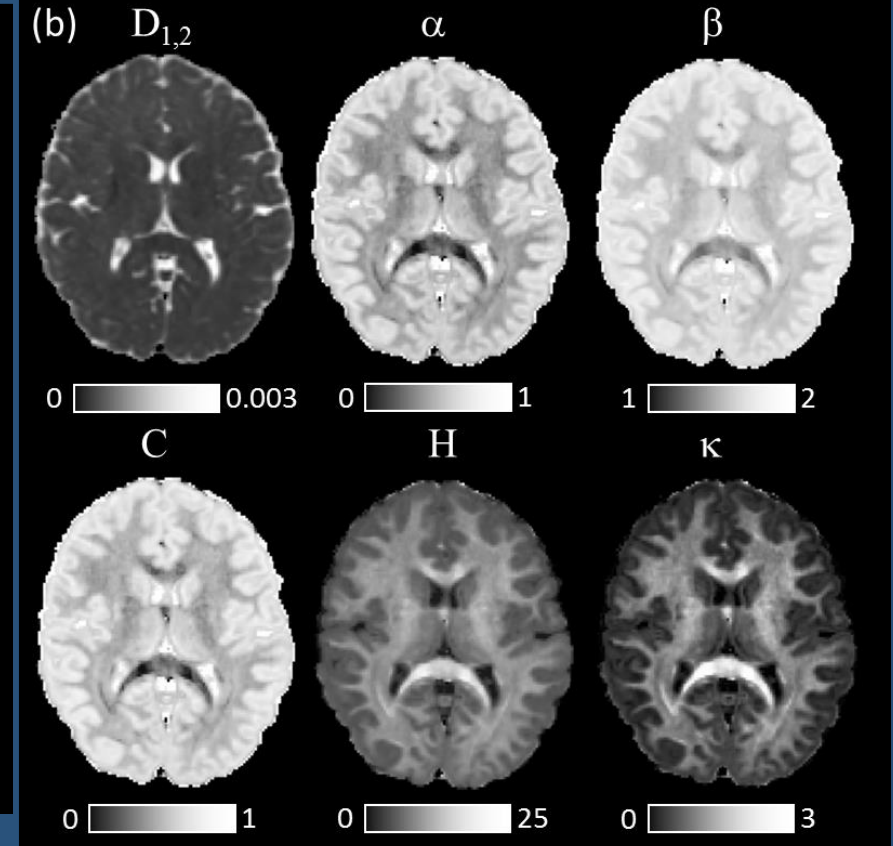
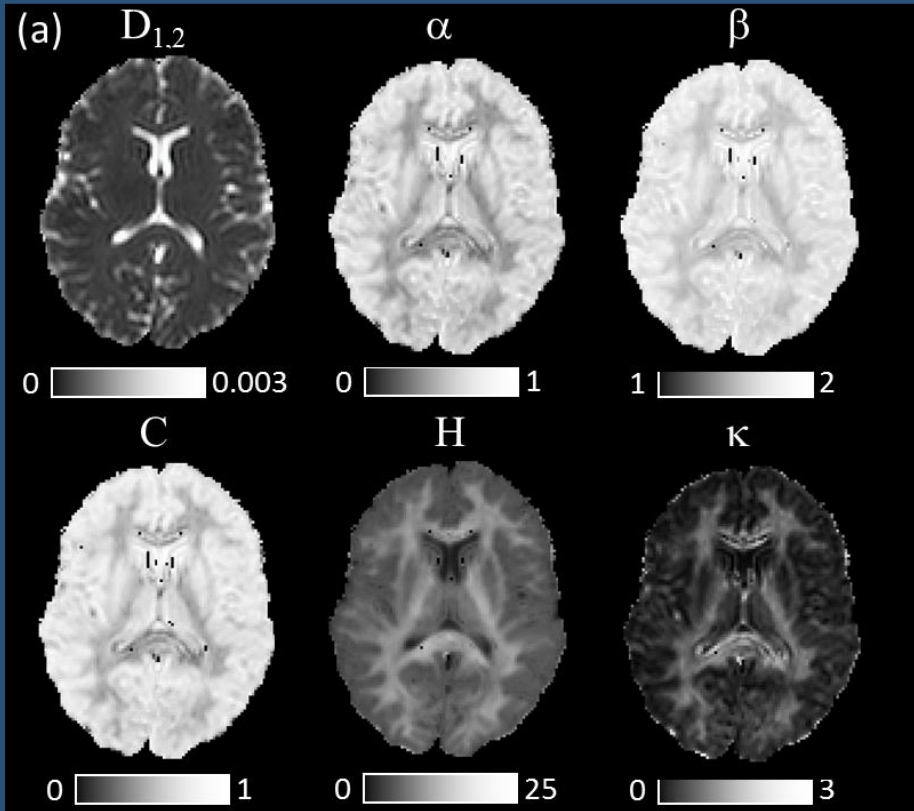


Parameter Maps



St George's Data

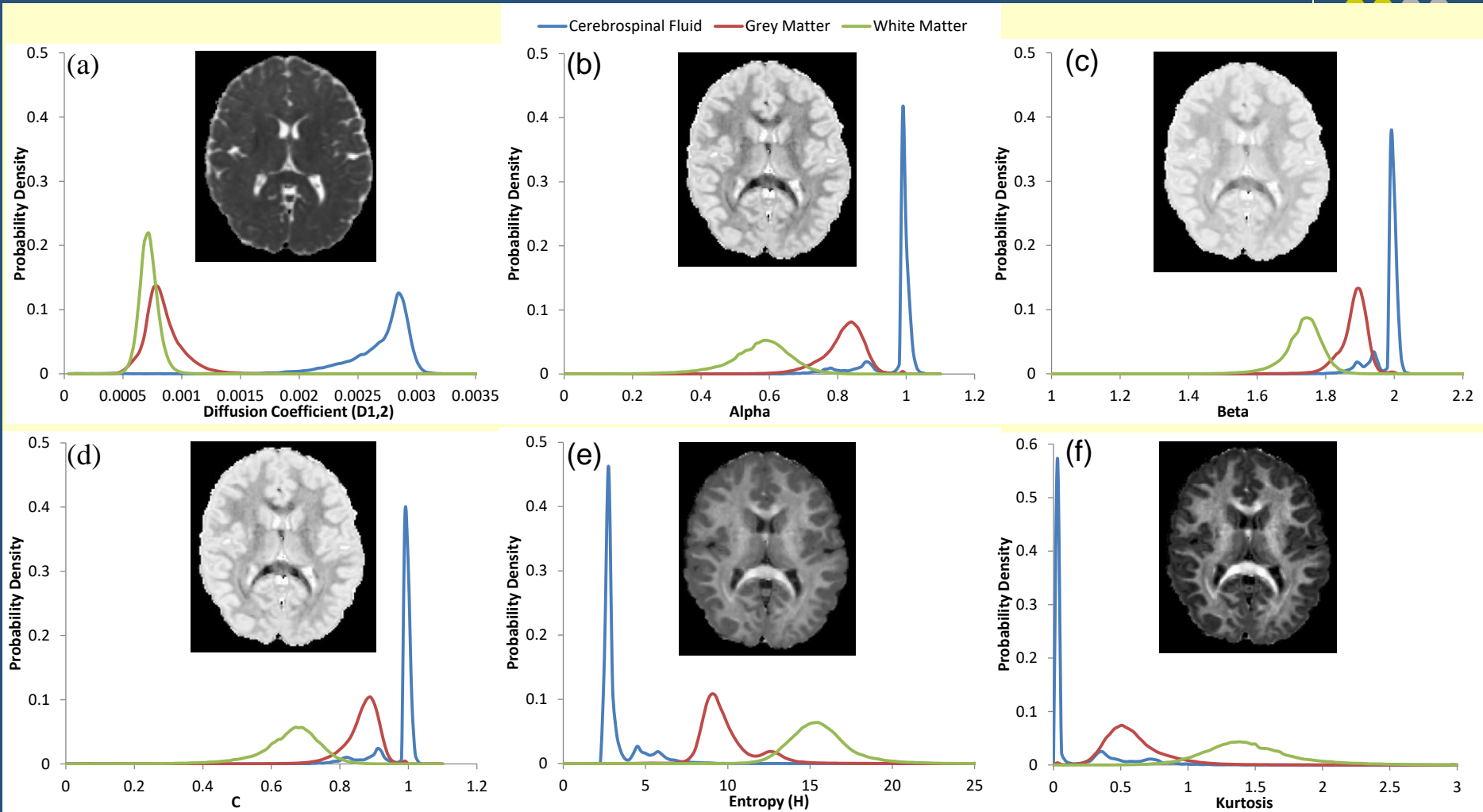
HCP Data



Trace of 6 diffusion gradient directions

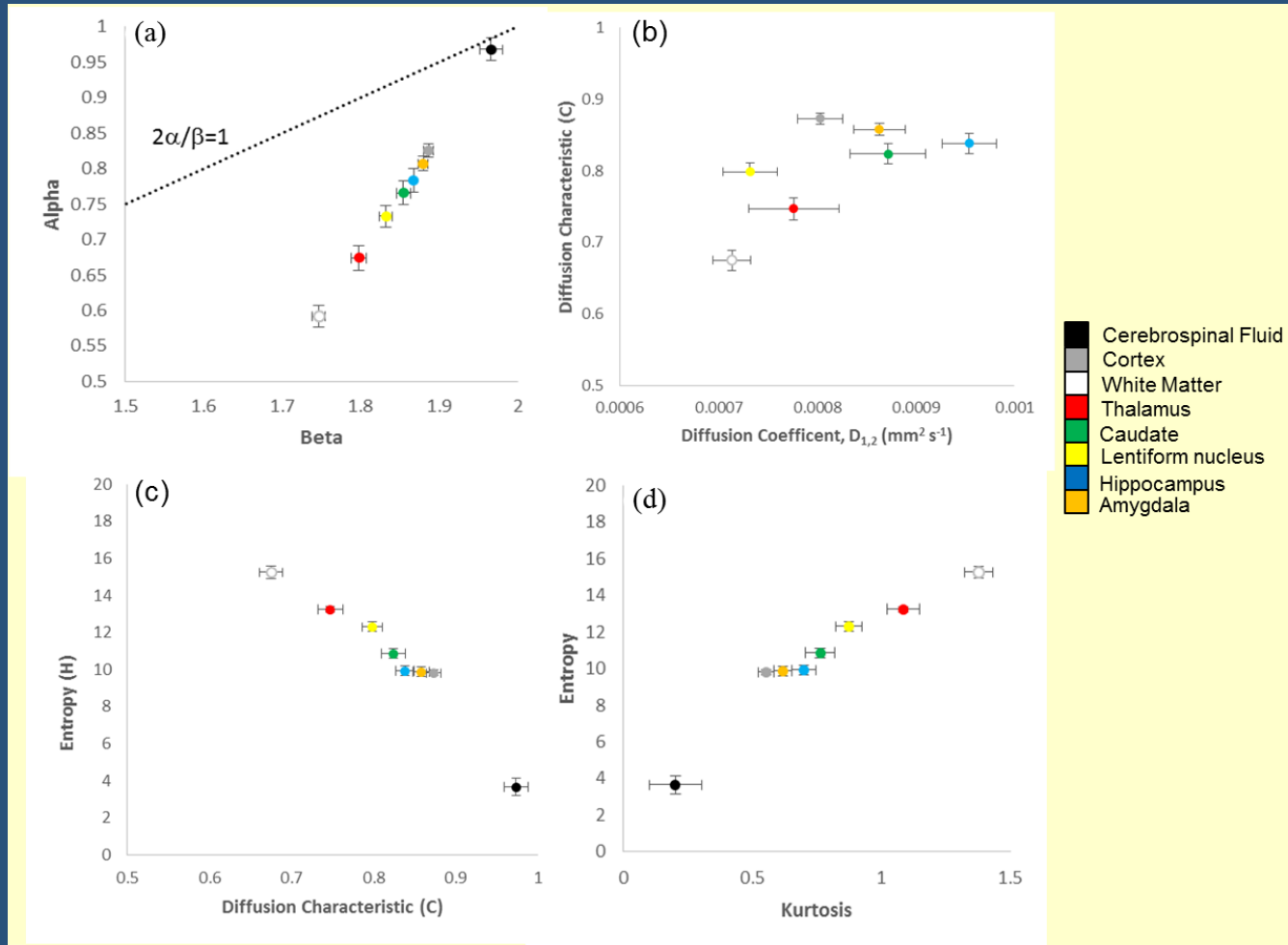
Trace of 180 diffusion gradient directions

Tissue Histograms





Brain Tissue Signatures



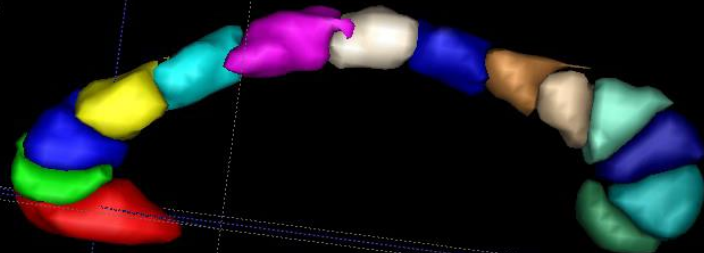
HCP data
(N=10)

$D_{1,2}$ shows
significant
differences
between
acquisitions

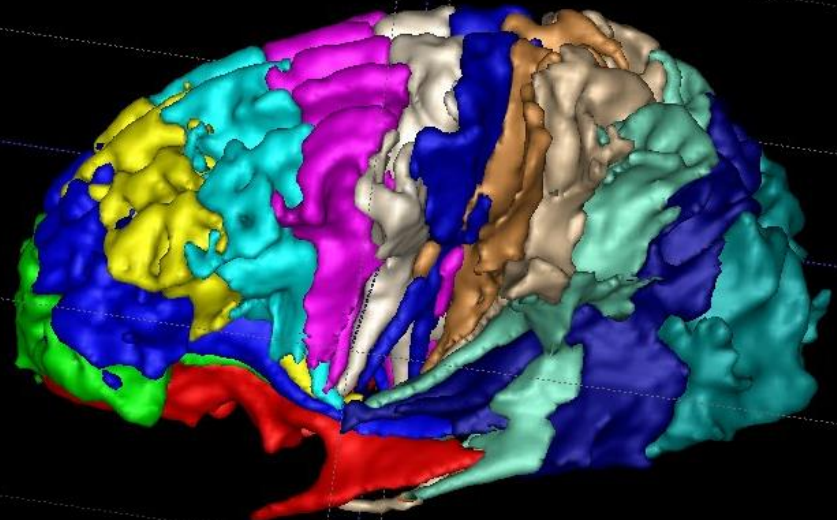
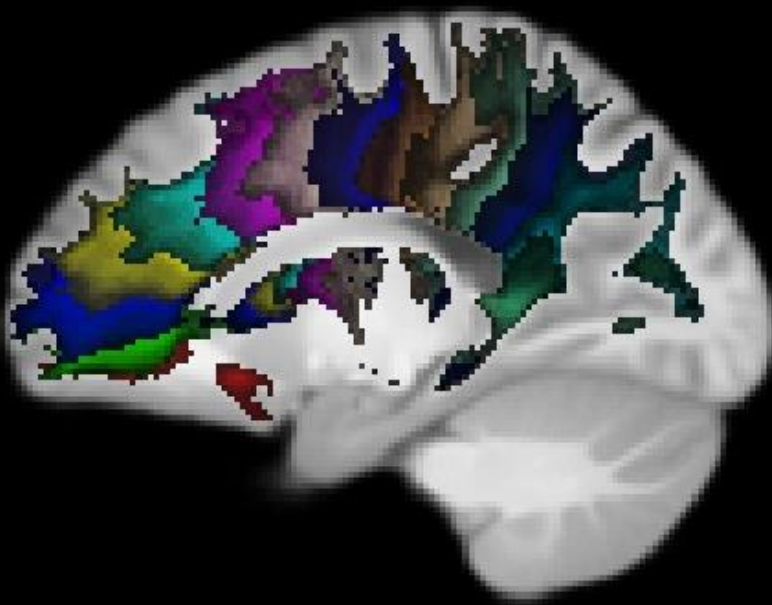
Corpus Callosum



Group Average
Tractography
(N=40)



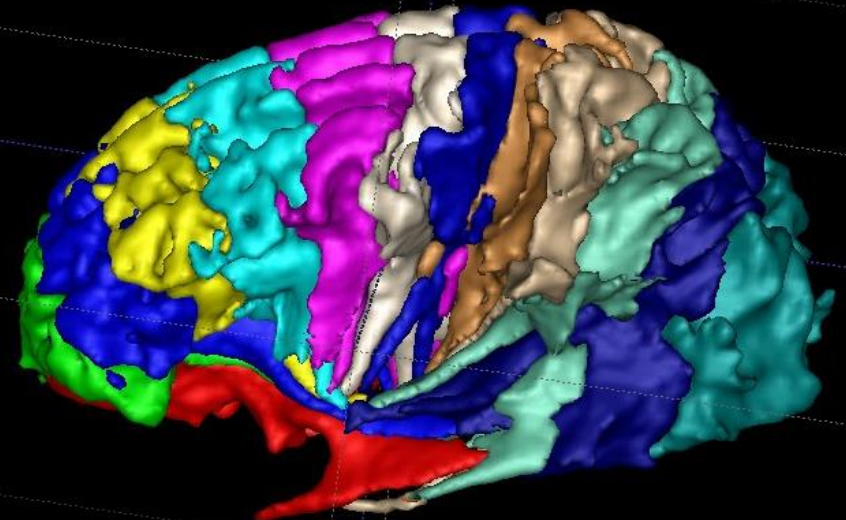
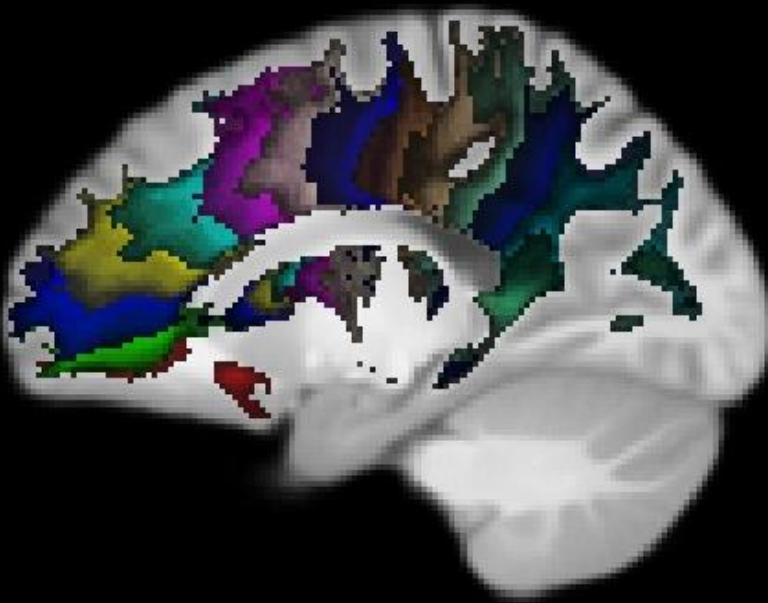
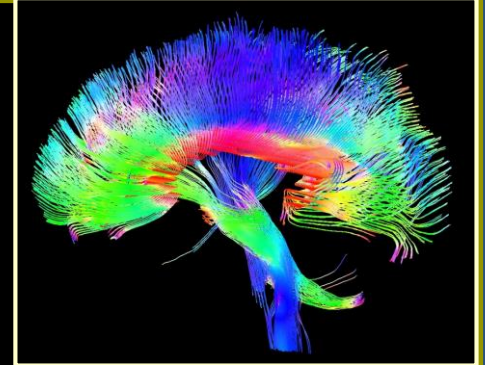
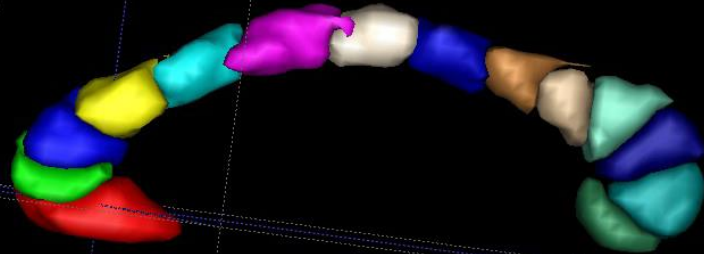
3T HARDI , $\delta=10.6\text{ms}$,
 $\Delta=41.7\text{ms}$
180 diffusion directions,
 $b=0, 1000, 2000,$
 3000 s mm^{-2}
1 hour



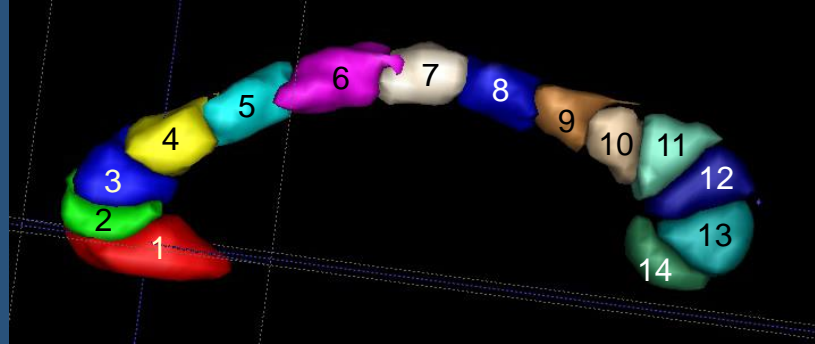
Corpus Callosum



Group Average
Tractography
(N=40)



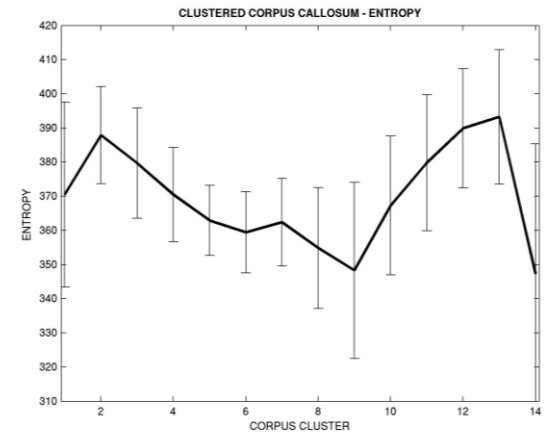
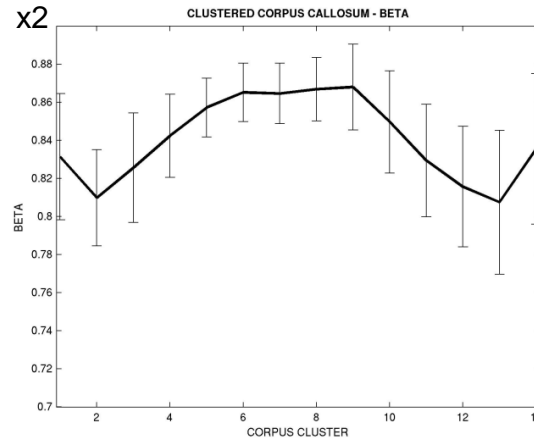
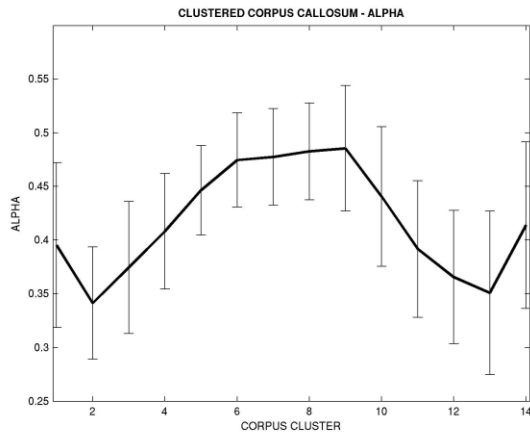
Corpus Callosum



α

β

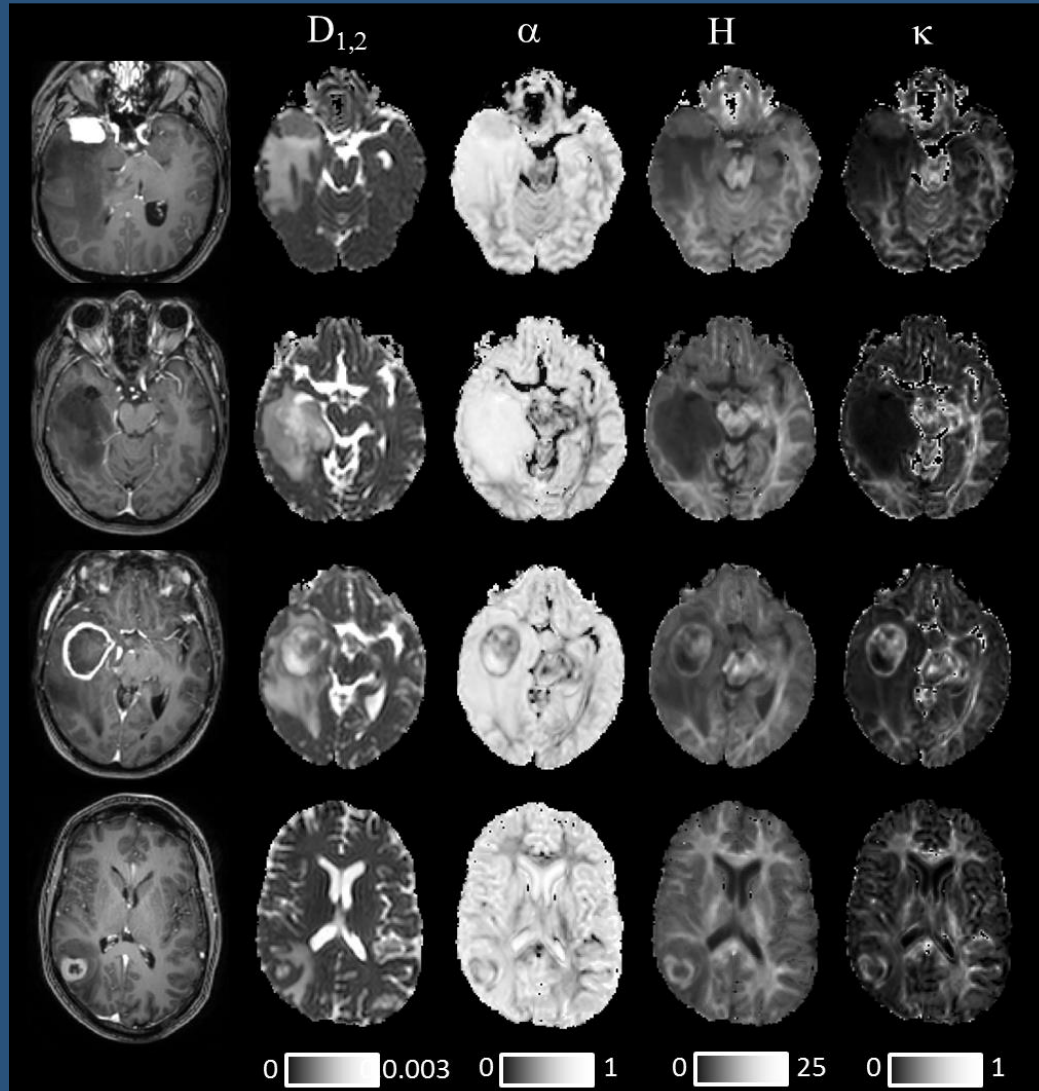
H





Brain Tumour Patients

Grade I Meningioma



Grade II Astrocytoma

Grade I Glioblastoma

Grade IV Metastasis

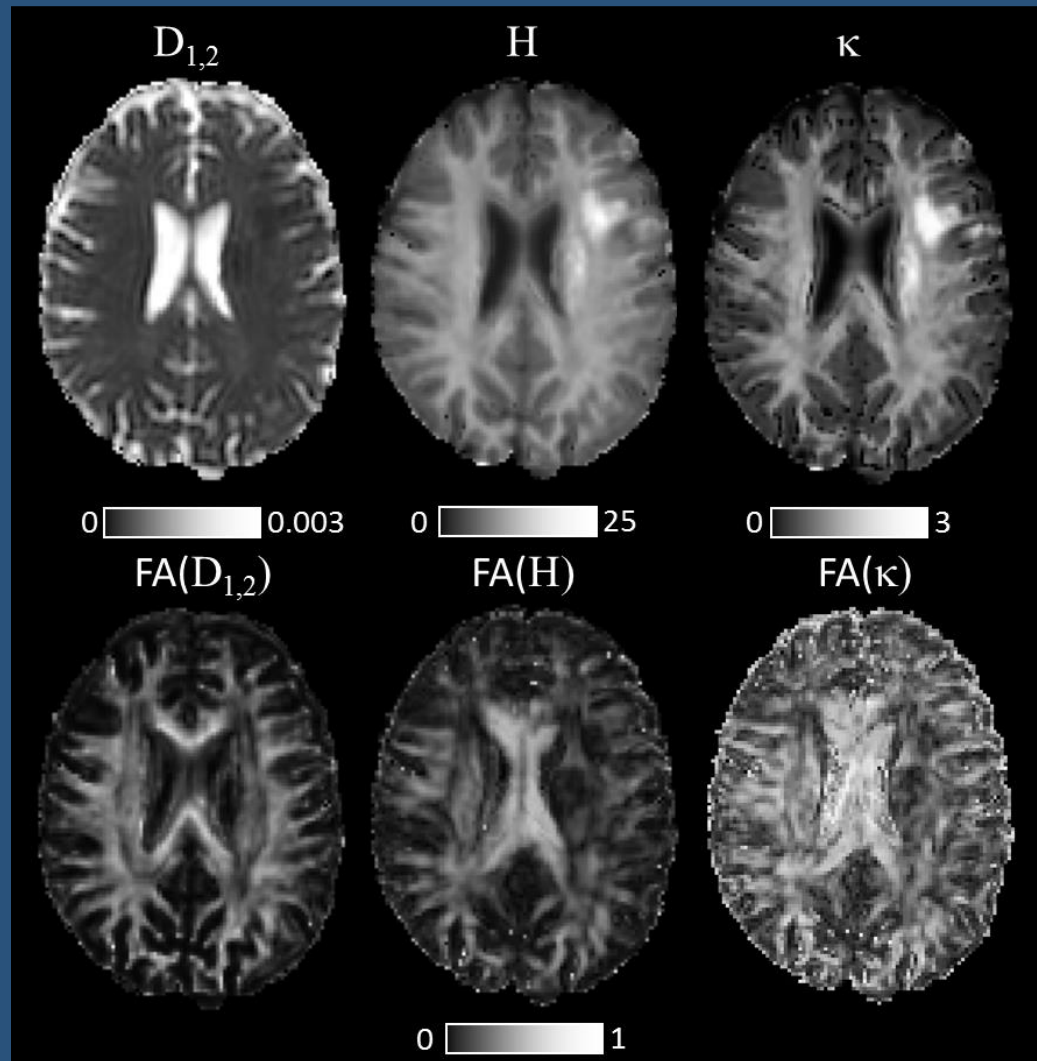
30th June 2015

Dr Thomas. R. Barrick

St. George's, University of London

aDWI, trace of 3 diffusion gradient directions, 6.5 minutes

Acute Stroke Patient



aDTI , 6 diffusion gradient directions, 13 minutes
MLF computed in each direction, tensor fitted to each parameter



Conclusions

- CTRW diffusion model provide parameters that may be interpreted in terms of tissue microstructure
 - Provides tissue contrast
 - Similar parameter values for SGUL and HCP
 - Different effective diffusion times
 - Different voxel sizes
 - Relationship between α and β in tissue?
 - Identifies pathological brain regions
 - Consistent with kurtosis and stretched MLF/exponential results for brain tumour
 - Rodent data for stroke
 - Needs further studies with large patient numbers to identify utility

Kwee et al., 2009

Yi Sui et al., 2015

Grinberg et al., 2014
Rudrapatna et al., 2014

Other Approaches



1. Computing Kurtosis and Spectral Entropy as Anomalous Diffusion Measures

Carson Ingo, Yu Fen Chen, Todd B. Parrish, Andrew G. Webb, and Itamar Ronen

C.J. Gorter Center for High Field MRI, Department of Radiology, Leiden University Medical Center, Leiden, NL, Department of Radiology, Northwestern University, Chicago, IL, United States

2. Fractional and Fractal Derivative Models for the Characterization of Anomalous Diffusion in MRI

Yingjie Liang, Wen Chen, and Richard L. Magin

Hohai University, Nanjing, China and University of Illinois at Chicago, United States

3. Anisotropic Fractional Diffusion Tensor Imaging

Mark M. Meerschaert, Richard L. Magin and Allen Q. Ye

Michigan State University, East Lansing, MI and University of Illinois at Chicago, United States

Acknowledgements



Richard Spencer, NIA, NIH

David Reiter, NIA, NIH

Xiaohong Joe Zhou, UIC MRI Res. Center

Muge Karaman, UIC MRI Res. Center

Yi Sui, UIC, Mayo Clinic

Carson Ingo, UIC, Northwestern

Matt Hall, UCL

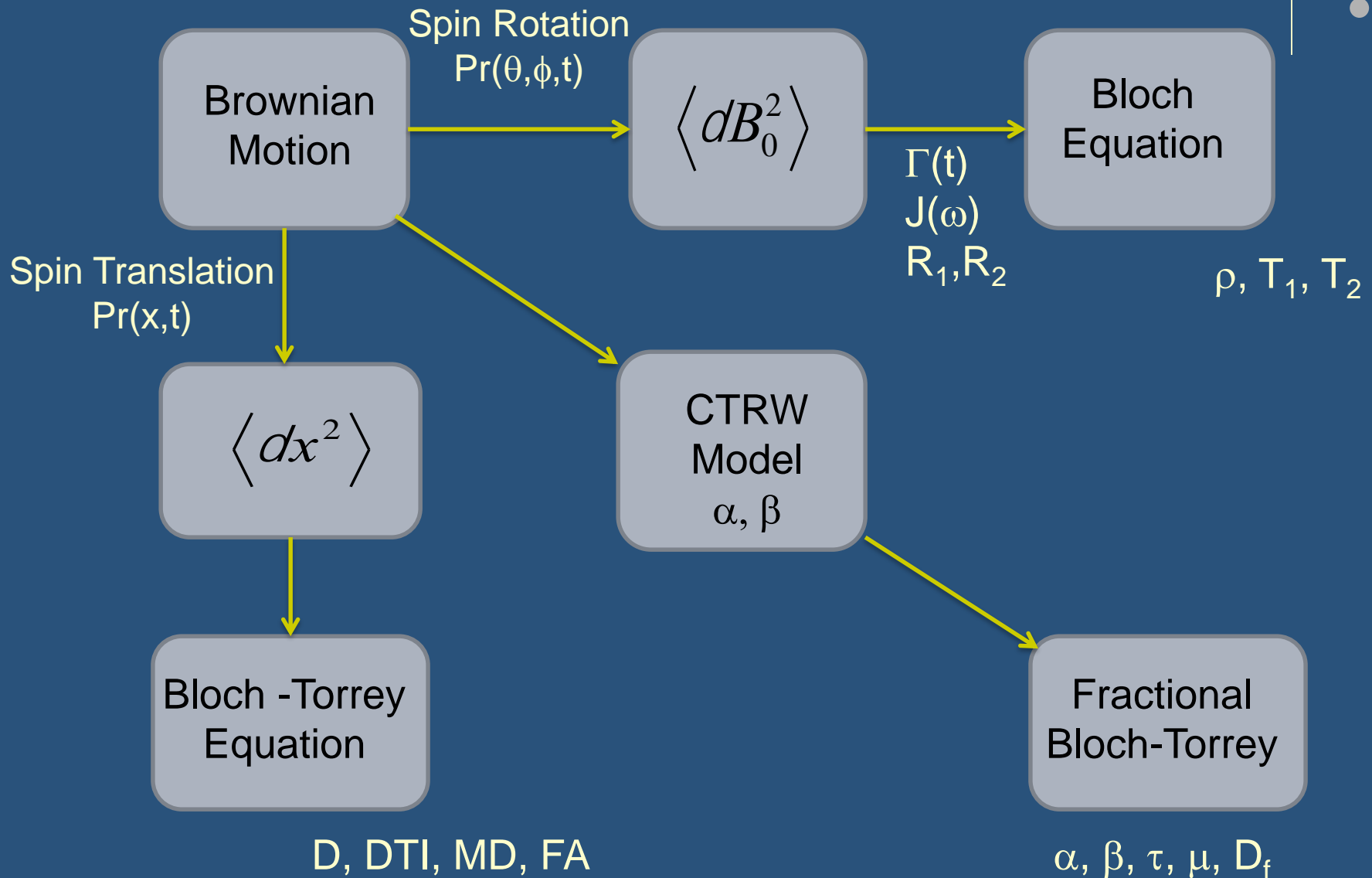
Tom Barrick, St. George's, UL

Viktor Vegh, U Queensland

Qiang Yu, U Queensland



Development of Fractional Magnetic Resonance Models: What next?



Linear and Complex Systems

